

University of Denver

Digital Commons @ DU

---

Electronic Theses and Dissertations

Graduate Studies

---

1-1-2014

## Wireless Sensor Localization: Error Modeling and Analysis for Evaluation and Precision

Omar Ali Zargelin  
University of Denver

Follow this and additional works at: <https://digitalcommons.du.edu/etd>



Part of the [Electrical and Computer Engineering Commons](#)

---

### Recommended Citation

Zargelin, Omar Ali, "Wireless Sensor Localization: Error Modeling and Analysis for Evaluation and Precision" (2014). *Electronic Theses and Dissertations*. 1236.

<https://digitalcommons.du.edu/etd/1236>

This Dissertation is brought to you for free and open access by the Graduate Studies at Digital Commons @ DU. It has been accepted for inclusion in Electronic Theses and Dissertations by an authorized administrator of Digital Commons @ DU. For more information, please contact [jennifer.cox@du.edu](mailto:jennifer.cox@du.edu), [dig-commons@du.edu](mailto:dig-commons@du.edu).

---

# Wireless Sensor Localization: Error Modeling and Analysis for Evaluation and Precision

## Abstract

Wireless sensor networks (WSNs) have shown promise in a broad range of applications. One of the primary challenges in leveraging WSNs lies in gathering accurate position information for the deployed sensors while minimizing power cost. In this research, detailed background research is discussed regarding existing methods and assumptions of modeling methods and processes for estimating sensor positions. Several novel localization methods are developed by applying rigorous mathematical and statistical principles, which exploit constraining properties of the physical problem in order to produce improved location estimates. These methods are suitable for one-, two-, and three-dimensional position estimation in ascending order of difficulty and complexity. Unlike many previously existing methods, the techniques presented in this dissertation utilize practical, realistic assumptions and are progressively designed to mitigate incrementally discovered limitations. The design and results of a developed multiple-layered simulation environment are also presented that model and characterize the developed methods. The approach, developed methodologies, and software infrastructure presented in this dissertation provide a framework for future endeavors within the field of wireless sensor networks.

## Document Type

Dissertation

## Degree Name

Ph.D.

## Department

Electrical Engineering

## First Advisor

Kimon P. Valavanis, Ph.D.

## Second Advisor

Alvaro Arias

## Third Advisor

Jason Zhang

## Keywords

Error analysis, Error modeling, Localization, Wireless sensor network

## Subject Categories

Electrical and Computer Engineering

## Publication Statement

Copyright is held by the author. User is responsible for all copyright compliance.

Wireless Sensor Localization:  
Error Modeling and Analysis for Evaluation and Precision

---

A Dissertation

Presented to

the Faculty of the Daniel Felix Ritchie School of Engineering and Computer Science

University of Denver

---

In Partial Fulfillment

of the Requirements for the Degree

Doctor of Philosophy

---

by

Omar Zargelin

June 2014

Advisor: Prof. Kimon Valavanis

©Copyright by Omar Zargelin 2014

All Rights Reserved

Author: Omar Zargelin  
Title: Wireless Sensor Localization: Error Modeling and Analysis for Evaluation and Precision  
Advisor: Prof. Kimon Valavanis  
Degree Date: June 2014

### **Abstract**

Wireless sensor networks (WSNs) have shown promise in a broad range of applications. One of the primary challenges in leveraging WSNs lies in gathering accurate position information for the deployed sensors while minimizing power cost. In this research, detailed background research is discussed regarding existing methods and assumptions of modeling methods and processes for estimating sensor positions. Several novel localization methods are developed by applying rigorous mathematical and statistical principles, which exploit constraining properties of the physical problem in order to produce improved location estimates. These methods are suitable for one-, two-, and three-dimensional position estimation in ascending order of difficulty and complexity. Unlike many previously existing methods, the techniques presented in this dissertation utilize practical, realistic assumptions and are progressively designed to mitigate incrementally discovered limitations. The design and results of a developed multiple-layered simulation environment are also presented that model and characterize the developed methods. The approach, developed methodologies, and software infrastructure presented in this dissertation provide a framework for future endeavors within the field of wireless sensor networks.

## Table of Contents

Chapter One: Introduction and Rationale .....	1
1.1 Introduction.....	1
1.2 Summary of Contributions.....	4
1.3 Dissertation Outline .....	6
Chapter Two: Background and Literature Review .....	9
2.1 Wireless Sensor Networks .....	9
2.2 Localization.....	10
2.2.1 Nature of Localization .....	11
2.2.2 Related Technologies and Existing Approaches.....	14
2.3 Error-Modeling and Analysis .....	27
2.4 Position Computation.....	28
2.4.1 Triangulation.....	29
2.4.2 Trilateration and Multilateration.....	29
2.4.3 Bounding Box .....	32
2.5 Literature Review.....	33
Chapter Three: Problem Statement.....	39
3.1 Nature of Problem.....	39
Chapter Four: Proposed Methods of Solution .....	42
4.1 Introduction.....	42
4.2 Conventions and Relationships.....	44
4.3 Sensor Localization Using Rough Methods .....	46
4.3.1 One-Dimensional Approach .....	46
4.3.2 Two-Dimensional Approach.....	49
4.3.3 Three-Dimensional Approach outlines .....	54
4.4 Sensor Localization Using Magnitude Bounding Method.....	56
4.4.1 One-Dimensional Approach .....	57
4.4.2 Two-Dimensional Approach.....	58
4.5 Sensor Localization Using Bounded-Error Method .....	59
4.5.1 One-Dimensional Approach .....	61
4.5.2 Two-Dimensional Case.....	68
4.5.3 Three-Dimensional Approach outlines .....	71
4.6 Sensor Localization Using Bounded-Angle Method .....	72
4.6.1 The Relationship between Angles .....	75
4.6.2 Problem Transform From 2-D to 1-D and X Coordinate Estimation .....	79
4.6.3 Problem Retransform From 1-D to 2-D and Y-Coordinate Estimation .....	81
4.6.4 Three-Dimensional Approach Outlines .....	85
4.7 Mobile Beacons Trajectory.....	86

4.8 Measurement-Error Ratio Distribution Assumptions .....	87
Chapter Five: Simulation and results of Sensor Localization.....	89
5.1 Introduction.....	89
5.2 1-D- Methods .....	92
5.2.1 Rough Method .....	93
5.2.2 Magnitude Bounding Method .....	95
5.2.3 Error Bounding Method.....	98
5.3 2-D-Methods.....	99
5.3.1 Finding the Best Beacon Transmission Angle.....	100
5.3.2 Rough Method .....	103
5.3.3 Error Bounding Method.....	107
5.3.4 Angular Bounding Method .....	111
5.4 Methods Comparison .....	117
5.4.1 1-D-Methods Comparison .....	117
5.4.2 2-D-Methods Comparison .....	124
Chapter Six: Conclusion .....	143
References.....	148

## Table of Figures

Figure 2.2-1 Wireless Sensor Network Algorithms.....	16
Figure 2.2-2 Range-Free vs Range-Based .....	17
Figure 2.2-3 Time Difference of Arrival .....	19
Figure 2.2-4 An Antenna Array with N Antenna Elements.....	21
Figure 2.2-5 Static vs Mobile Beacon Classification.....	25
Figure 2.4-1 (a) Triangulation (b) Trilateration (c) Multilateration .....	29
Figure 2.4-2 Building the Bounding Box .....	32
Figure 4.1-1 Flow Chart for Transmission and Receive Beacons and Data a) MB's b) SN's .....	44
Figure 4.3-1 1-D-Basic Rough Method Layout.....	46
Figure 4.3-2 1-D-Multi Sending Case Basic Rough Method Layout .....	48
Figure 4.3-3 2-D Basic Layout .....	51
Figure 4.3-4 2-D- Radial Range for Ratios Uses .....	52
Figure 4.3-5 2-D-Multisending Case Layout.....	53
Figure 4.3-6 3-D-Onesending Case Layout .....	56
Figure 4.4-2 1-D-Adjusted Magnitude Bounding.....	58
Figure 4.4-3 2-D-Magnitude Bounding .....	58
Figure 4.5-1 1-D-Minimum Estimated Error .....	60
Figure 4.5-2 1-D- Estimated Error Bounding .....	62
Figure 4.5-3 1-D- Adjusted Estimated Error Bounding.....	63
Figure 4.5-4 1-D-Part of Estimated Error Cancelation .....	64
Figure 4.5-5 Flow Chart for 1-D- Bounding Algorithm.....	65



Figure 4.5-6 Simplification of the Flow Chart for 1-D- Bounding Algorithm.....	66
Figure 4.5-7 2-D-Estimated Error Bounding Layout.....	68
Figure 4.5-8 2-D-Two Sending Case Estimated Error Bounding Layout .....	69
Figure 4.5-9 2-D-Two Sending Case Estimated Error Bounding using Similar Triangulation.....	71
Figure 4.5-10 3-D-One Sending Case Estimated Error Bounding using Similar Cones ..	72
Figure 4.6-1 Angular Bounding Layout.....	74
Figure 4.6-2 Flow Chart for Angular Bounding Method Algorithm .....	83
Figure 4.6-3 3-DAngular Bounding Method Layout .....	85
Figure 4.7-1 SSL Mobile Trajectory.....	86
Figure 4.7-2 DSL Mobile Trajectory .....	87
Figure 5.2-1 Accuracy of Rough Method vs $\Delta x$ for different $R_{\max}$ 's .....	93
Figure 5.2-2 Accuracy of Ruogh Method vs $\Delta x$ for different D's.....	94
Figure 5.2-3 Accuracy of Magnitude Bounding Method for different $R_{\max}$ 's .....	95
Figure 5.2-4 Accuracy of Magnitude Bounding Method for different D's .....	97
Figure 5.2-5 Accuracy of Error Bounding Method for different $R_{\max}$ 's.....	98
Figure 5.2-6 Accuracy of Error Bounding Method vs DX .....	99
Figure 5.3-1 Sensor Detection for $R_{\max} = 0.1$ .....	100
Figure 5.3-2 Sensor Detection for $R_{\max} = 0.2$ .....	101
Figure 5.3-3 Sensor Detection for $R_{\max} = 0.3$ .....	102
Figure 5.3-4 Sensor Detection for $A = 90$ .....	103
Figure 5.3-5 Localization Results of Rough Method.....	104
Figure 5.3-6 Accuracy of the Rough Method vs. $R_{\max}$ .....	105

Figure 5.3-7 Accuracy of Rough Method vs DX.....	106
Figure 5.3-8 2-D Four Sending Case-Bounded-Error Method.....	107
Figure 5.3-9 Localization Result of Error Bounding Method.....	108
Figure 5.3-10 Accuracy of the Error Bounding Method vs. $R_{\max}$ for different D's .....	109
Figure 5.3-11 Accuracy of the Error Bounding Method vs DX for different D's .....	110
Figure 5.3-12 Localization Result of Angular Bounding Method.....	112
Figure 5.3-13 Angular Bounding Layout.....	114
Figure 5.3-14 Accuracy of the Angular Method vs DX for different $R_{\max}$ 's.....	115
Figure 5.3-15 Accuracy of the Angular Method vs $R_{\max}$ for different D's.....	116
Figure 5.4-1 1-D Methods-Error Comparison for D = 10 .....	118
Figure 5.4-2 1-D Methods-Error Comparison for D = 6 .....	119
Figure 5.4-3 1-D Methods-Error Comparison for D = 2 .....	120
Figure 5.4-4 1-D Methods-Error Comparison for $R_{\max} = 0.3$ .....	121
Figure 5.4-5 1-D Methods-Error Comparison for $R_{\max} = 0.2$ .....	122
Figure 5.4-6 1-D Methods-Error Comparison for $R_{\max} = 0.1$ .....	123
Figure 5.4-7 2-D Methods-Error Comparison for D = 10 .....	125
Figure 5.4-8 2-D Methods-Error Comparison for D = 6 .....	126
Figure 5.4-9 2-D Methods-Error Comparison for D = 2 .....	127
Figure 5.4-10 2-D DSL Methods-Error Comparison for D = 10.....	128
Figure 5.4-11 2-D DSL Methods-Error Comparison for D = 6.....	129
Figure 5.4-12 2-D DSL Methods-Error Comparison for D = 2.....	130
Figure 5.4-13 2-D Methods-Error Comparison for $R_{\max} = 0.3$ .....	131

Figure 5.4-14 2-DMethods-Error Comparison for $R_{\max} = 0.2$ .....	132
Figure 5.4-15 2-DMethods-Error Comparison for $R_{\max} = 0.1$ .....	133
Figure 5.4-16 2-DMethods-Error Comparison for $D = 10$ .....	135
Figure 5.4-17 2-D Methods-Error Comparison for $D = 6$ .....	136
Figure 5.4-18 2-DMethods-Error Comparison for $D = 2$ .....	137
Figure 5.4-19 2-DMethods-Error Comparison for $R_{\max} = 0.3$ .....	139
Figure 5.4-20 2-DMethods-ErrorCcomparison for $R_{\max} = 0.2$ .....	140
Figure 5.4-21 2-DMethods-Error Comparison for $R_{\max} = 0.1$ .....	141

## **Chapter One: Introduction and Rationale**

### **1.1 Introduction**

Wireless sensor networks have become prevalent both in research and applications. These networks, being composed of a large number of cheaply produced, low powered devices, gather small samples of data from different locations, using such data for analysis or to trigger alarm conditions. The devices that comprise the vast majority of the network are known as sensors due to the fact that their primary function is to sense local environmental data. However, the value of this data comes not just from simply analyzing it collectively for statistical purposes, but from analyzing it relative to the location distribution it represents. The data collected from a WSN is at least two-dimensional in that there is always position information associated with the sensed information. While the technology of sensing information has been well-studied, a challenge still remains in accurately and precisely locating the sensors.

Larger, more complex, more powerful devices can utilize technologies like GPS in order to identify locations. In many WSNs, however, the majority of the sensor devices do not have the ‘capacity’ to include such technologies. Thus, it is necessary to use other

means to locate sensors. While many methods are available, few of them produce feasible, reliable, and consistent results worthy of pairing with the gathered data. This problem is more complex than it might initially seem to be. Locating small, somewhat randomly distributed devices containing simple technologies and limited power supplies, requires overcoming many obstacles including communication range, measurement error, cascaded error, and power limitations, just to name a few. The contributions of this research are aimed at addressing these issues and others inherent to localization of WSNs.

The primary contributions focus on methods of analysis and modeling that practically take into account many of the real-world challenges associated with WSN localization. Preliminary distance measurements containing unknown, random quantities of error are derived from beacon signals sent from two mobile beacons based on the received signal strengths (RSS) of the beacons at the sensors. Particular emphasis is given to the bounding, minimization, and even utilization of associated errors in order to provide precise and accurate localization capabilities, while meeting rigid problem constraints. Unlike other methods previously published, this research seeks to avoid making unrealistic assumptions, providing factual, methodical, and mathematically-sound approaches based on long-accepted principles and refined models. One of the core premises of this research is the principle of utilization of all applicable, measurable facets

of the localization problem, including error modeling, through careful modeling. These contributions should provide not only usable methods of localization for problems meeting the assumptions of this research, but a solid foundation on which to build new methods that have different structures and differing assumptions. A series of models and corresponding methods are presented, each building on the previous one and providing increased precision of localization. Both single-dimensional and two-dimensional concepts and models are presented with extension into three dimensions models left as future research. The rough methods presented first provide primitive means of understanding and modeling the localization problem. These methods are simple, fast, and effective, though imprecise. The bounded-magnitude method utilizes known factors and modeling constraints to place the sensor within a certain range of the beacons. The bounded-error method takes an additional step in modeling the error present in the measured readings to further increase the precision in an incremental, algorithmic approach. Last, the bounded-angle method takes a slightly-different approach in recognizing that in multiple dimensions, there are two unknown factors in localization: distance and direction. Each of these methods forms the foundation for modeling and localization to minimize assumptions and increase precision while maintaining accuracy and integrity.

## 1.2 Summary of Contributions

The novel approach in this dissertation relates to utilizing error modeling and analysis to augment the modeling of a localization system. This contributes to new understanding and means of utilizing error prediction as a supplement to system accuracy, rather than tolerated inaccuracy. The methods presented herein attempt to utilize factors that are frequently ignored in other works, aiming at deriving methods and an overall ideology of attempting to transform “negative” factors, such as error, into beneficial and usable results. The RSS-based, anchor-based, mobile beacon approach to localization utilized in this work provides a backdrop of a typical, usable scenario for WSN localization in order to ensure the practical applicability and realism of the proposed methods and subsequent simulation results. These methods presented herein are backed by many simulated trials that illustrate the effectiveness and expected performance of the methods along with detailed error analyses that show how the modeled error is used for bounding sensor locations.

There are three classes of methods presented in this dissertation. The first class is that of rough, approximation methods used to estimate sensor position quickly and simply with a relatively low degree of accuracy and precision. The second class is that of error-bounding methods that utilize knowledge of the estimated error within the system to iteratively increase the precision with which each sensor is localized. The third class is that of angle-bounding methods that build upon the previously-discussed error-bounding methods by extending the concept from componentized, single-dimensional quantities to radial factors.

There are many advantages over existing methods. Many of the existing methods make broad, unrealistic, and unqualified assumptions that do not warrant or allow real application. Often, there is an assumption that the distance between sensor nodes and beacons is known. This is a fallacy as sensor deployment is often imprecise. This leads to questioning the use of static anchors at all as it can be difficult to predict the number and proper placement of such anchors for localization purposes. Another common assumption is related to self-localization methods that assume temporal isolation of error. These methods fail to account for ripples in error caused by inexact or outright erroneous localizations in a way that could affect the usefulness of the entire network. One of the most egregious assumptions is the lack of inclusion of any account for error in localization efforts. These systems make broad and improbable assumptions of perfect measurements. A few works even assume sensor locations and then prove the correctness of those locations using this assumption. This is a type of “catch 22” methodology that is completely inapplicable. The work presented herein proposes methods and uses approaches that attempt to state reasonable assumptions and experimentally determine the effectiveness of true localization scenarios.

The primary foreseen limitations of this research are the lack of substantive, comparative efforts in existing works and the sample error-modeling choices utilized for demonstration of cases-in-point throughout this work. While we believe that there is generalizable potential of the methods and ideology presented within this work along with direct application of the methods herein to the localization problem at hand, it should be noted that unknown and unrealized factors may limit the generalizability of



these methods when more-complex and non-linear models are utilized. The fundamental assumptions of certain error characteristics, such as upper-limit bounding and randomness distribution, may require that further research and testing be performed to ensure applicability and effectiveness in different situations and cases. The overall efficacy and efforts of the methodologies and ideology presented in this work are dependent on the ability to establish relationships between system operational models and error models and utilize as many known and quantifiable factors as possible to augment system predictability. Limitations in the current state-of-the-art RSS modeling methodologies provide both motivations and limitations to this research.

### **1.3 Dissertation Outline**

This dissertation is divided into six progressive sections that fully describe the problem being analyzed, solutions designed, tests considered, results obtained, analyses made, conclusions drawn, and indications of future directions that could be taken to improve and expand upon the efforts undertaken. The first chapter provides an introduction to the topic at hand along with the rationale for its choosing and subsequent approaches. It introduces the research efforts undertaken, recent developments from such research corresponding to the topic, and the reasoning for the design choices and approaches taken and the means of their execution. The second chapter provides an extensive, detailed review of existing efforts and works related to the topic at hand. It provides a thorough discussion of these materials to provide a deep and thorough understanding of the nature of the environment of the topic and the reasoning behind its challenge. This body of information leads to chapter three, which outlines the nature and

concerns of the problem at hand to provide a framework for the solutions to be presented. This chapter focuses upon the specific nature and aspects of the localization problem as it pertains to wireless sensor networks and clearly defines the assumptions and the reasons for their existence within this dissertation along with the potential pitfalls associated with such assumptions and how this dissertation addresses them in a direction uncommon to other existing works. With the problem clearly stated, chapter four proposes the methods of solutions for the problem in increasing dimensional spaces. The described methods were incrementally-designed for this dissertation and are presented in such fashion to illustrate the layered improvements they collectively-demonstrate as each method improves upon its predecessor with the first methods discussed being based on fundamental mathematical and physical concepts and the findings and shortcomings of existing works. With the designed methods fully described, chapter five of this dissertation discusses the simulation that was designed to prove the concepts of the designed methods based upon the problem statement and assumptions previously detailed. It describes the design, operation, and gathered results of the simulation software. This software was specifically designed to exercise and characterize the proposed methods in an even-handed, unbiased manner to provide conclusive, fair measurements as might be made in real-world measurements. Having gathered such measurements, chapter six discusses the detailed analyses and conclusions drawn from the simulation results to fairly and accurately ascertain the viability of the proposed methods and indicate the nature and shortcomings of such methods from a practical perspective of hindsight. The conclusions and directions discussed to conclude this

dissertation should provide indicatively the benefits, applications, and potential areas of expansion of the principles, methods, and designs discussed as a guide to those seeking direct application or future development.

## **Chapter Two: Background and Literature Review**

In order to understand the nature of this research, it is important to review related work. There are three main contextual areas of focus in this research: wireless sensor networks, localization, and error-modeling. While the primary focus of the research is in the area of localization, important consideration needs to be given to the other two areas.

### **2.1 Wireless Sensor Networks**

Wireless sensor networks (WSNs) are a type of ad-hoc network in which small devices containing environment-sensing hardware and wireless communication devices are the primary structural component [1]. These sensors are deployed over a relatively large area in hopes of gathering a topological collection of information containing many small samples. There are many important applications for WSNs, including geological data gathering, construction, and military applications [2]. The sensors are commonly referred to as nodes, or regular nodes, and may be as many as a million in number or more. Because these sensors are incredibly small, light-weight, low-powered, and cheaply-produced, their useful life spans and operational flexibilities are incredibly limited [3]. Their communication ranges and battery lives are amongst their most primary limitations [4]. As such, data gathering efforts, quantities of communication, and on-board processing must be carefully planned and budgeted.

Wireless sensor networks often have unbalanced assignments of processing and data-gathering responsibilities [5]. Because the sensors have limited capability and are focused

on very specific data gathering activities, it is necessary to provide support for the massive number of sensors in terms of data recovery and eventual processing. This involves providing data recovery mechanisms that can be positioned within the communication range of the sensors, which is a challenging task given the large number of sensors and the potentially massive deployment area over which the sensors are deployed. Many schemes have been derived for accomplishment of this task, including deployment of higher-powered support nodes, sometimes called cluster heads, and complex algorithmic approaches involving dynamic sensor behavior and delegation of responsibilities. The method of solving the communication problem often leads to classifying a particular network based on its communication organization and infrastructure.

The classification of WSNs as ad-hoc networks comes from the fact that nodes are often deployed from a long range with little control over the precision of their eventual deployment locations. Due to their small size and simplicity, the sensors have no controllable mobility. The means of deployment, lack of mobility control, and incredibly-limited communication range of the sensors provide a challenge of locating the sensors once they have been deployed, a process known as localization, which is discussed in detail in the next section [2, 6, 7].

## **2.2 Localization**

Once a collection of sensors has been deployed, the primary challenge being faced is the ability to locate those sensors. Knowing the location of the sensors is important for two critical reasons. At first, the location at which a sensor's data is

gathered is one of the primary pieces of information desired for data analysis purposes. Indeed, a collection of sensor network data without location information would be nearly worthless. This is because the geographic topology of the information is as important as the individual pieces of information themselves [6].

The second critical reason involves the fact that in order to have any data to analyze at all, it is necessary to ‘recover’ the data from the sensors. This involves transmission of data from individual sensors, a costly and complex effort based on the sensors' limited battery lives, limited communication ranges, and large deployment area. It might be necessary to position a data recovery device within less than a few meters of any given sensor in order to recover its gathered data! Due to the small size of the sensor devices, automated means of locating the sensors via detailed imaging or simple estimation have been proven difficult. This is especially true when sensors are obstructed by other objects or contained within other objects. When it is important to know where a sensor is located to a precision of a few centimeters or less, the precision of the means of locating sensors becomes quite important. In this section, we will first discuss the nature of localization, including its structure and challenges. This will be followed by a discussion of some of the technological approaches towards localization with particular emphasis on those utilized by this research [6, 8, 9].

### **2.2.1 Nature of Localization**

Localization is the process of given locality to a physical entity. In any discussion of location, it is important to note the universal fact that the location of something is an entirely relative matter. It is fundamentally impossible to give location to anything

without reference to the location of something else! This makes location a problem of relationship. Often, it is the likelihood of two subjects in some characteristic that places them “locally” with one another relative to other subjects that are not as like in characteristic. For purposes of geographic location, the primary reference object is that of the Earth itself. The characteristic of concern is that of a physical point on the Earth's surface, making the relationship of concern one of physical distance from that point. Thus, localization here involves the use of known points and translation of distance to match those points.

The surface of the Earth, while having distinguishing characteristics, does not provide regular, predictable points from which to reference, especially when the scale of reference needs to be rather small, as is the case with sensor nodes. Furthermore, in order to locate a sensor, either the sensor's position must be already known or the distance from a point of known location must be found. Adding to this challenge is that it is often necessary to receive some type of wireless communication from a sensor in order to attempt any kind of distance measurement. For reasons discussed earlier, simply detecting light from a sensor, a process known as imaging, often lacks the precision and suitability needed for many applications. Thus, an invisible detection method is necessary.

The simplest and most fundamental approach to this method is that of asking a sensor to respond to a simple query in order to know of its presence and attempt to determine its location based on the properties of the communication medium. The query is often known as a beacon with the transmitter of such a beacon being known as an

anchor. This is similar to the popular children's game “Marco Polo” in which the medium of sound wave traversal through air is the means of communication and the loudness and directional information contained within received sounds is used to locate other players. When one player shouts “Marco!”, the other players respond with “Polo!”. This is a classic example of beacon/response localization.

Given a beacon system in a particular medium, the processes of locating a sensor node requires mathematically processing the communication information within the medium in order to accurately and precisely locate the sensor. This mathematical processing is often known as trilateration; involving the solution of several related equations based on multiple known locations (usually three) and distance measurements from those known locations to the unknown sensor location. The accuracy of the localization is proportional to the number of known points with a certain minimum number of known points being necessary to obtain any results at all. The primary reason for using three points is to overcome the reflective problem of using only two where it may be impossible to know on which side of the shared axis of the two points a sensor may be located. Trilateration in three dimensions adds another degree of freedom of location than in two dimensions, though the principle and approach still remains the same. Later in this research, many aspects of the mathematics involved with trilateration and its close relative, triangulation, will be discussed in great detail.

Even with an established medium and calculation method for distance measurement, the challenge of the breadth of possible localization must be addressed. Due to the small size and capabilities of a sensor, the proximate distance of a known



point from the sensor is proportional to the scale in which the sensor operates, which is likely only a few meters. Thus, even if adequate known points were available as distributed throughout the field of deployment, the deployment and management of such known-point devices would create a problem on the scale of the sensor localization problem itself. Unless a complex and potentially-fragile hierarchical location scheme is desired in which locating a sensor involves multiple distance-measurement “hops” from lower-powered devices to higher-powered devices, it might be suggested that a mobile system be utilized to perform beacon transmission and response gathering. Indeed, such a mobile beacon system is utilized in the methods of this research. To understand such systems, further discussion of the technological aspects of approaching the localization problem is discussed.

### **2.2.2 Related Technologies and Existing Approaches**

There are many existing technologies and a variety of approaches in the field of WSNs regarding localization [6, 9, 10, 11, 12, 13, 14, 15]. This Section outlines some of the distinctions in approaches and classifications of the different technologies and conceptual approaches and discusses the purposes and some of the limitations concerning them. It should be noted that the application of many of the technologies and approaches herein is heavily dependent upon the specific application requirements and nature of the environment of deployment [2]. It would be imprudent to classify any approach or particular technology as strictly advantageous, though it can be noted that a clear understanding of system usage, parameters, and goals will likely indicate certain means more readily than others.

### ***2.2.2.1 Global Positioning Systems (GPSs)***

Of the many approaches to localization, by far one of the most accurate and ubiquitous is the GPS. These systems utilize geo-stationary satellites in order to accurately trilaterate the position of a GPS-enabled device [16]. They are so central to most localization schemes that even if they are not utilized at the lower levels of a localization scheme, such as the nodes in a WSN, they are often utilized at the highest level, such as locating the network as-a-whole relative to the global coordinate system. GPS satellites provide the de facto points of reference for most localization hierarchies [17].

### ***2.2.2.2 Algorithms***

There are many classifications of algorithmic approaches as shown in Figure 2.1. These often depend on the specific structure and configuration of the WSN being localized. Furthermore, a single algorithm can be related to more than one classification [6, 18].

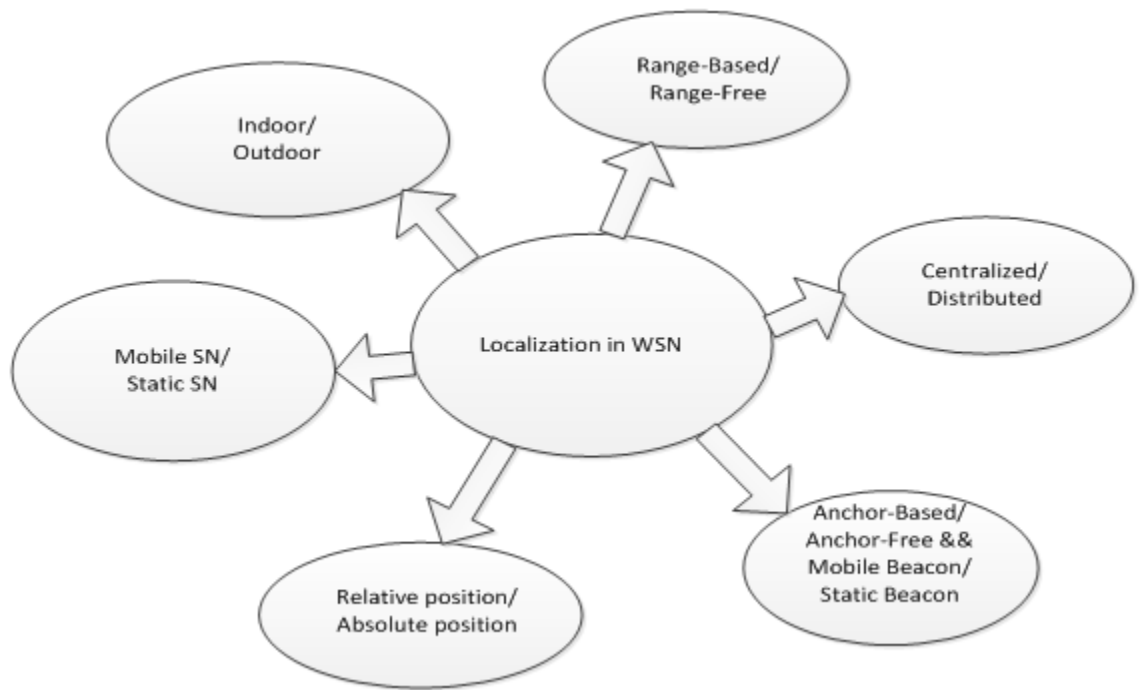


Figure 2.2-1 Wireless Sensor Network Algorithms

#### ***2.2.2.2.1 Range-Based/Range-Free***

Range-based algorithms [6, 19, 20, 21, 22, 23, 24, 25] are based on the assumption that the absolute distance between a sensor nodes and an anchor can be measured using distance and/or angle information related to the beacon. Some of these types of information include: time of arrival (ToA), time difference of arrival (TDoA), received signal strength (RSS), and angle of arrival (AOA). This information is usually paired with one more computation methods, such as maximum likelihood, trilateration, multi-trilateration, or triangulation, to determine the position of each sensor node. One advantage of this type

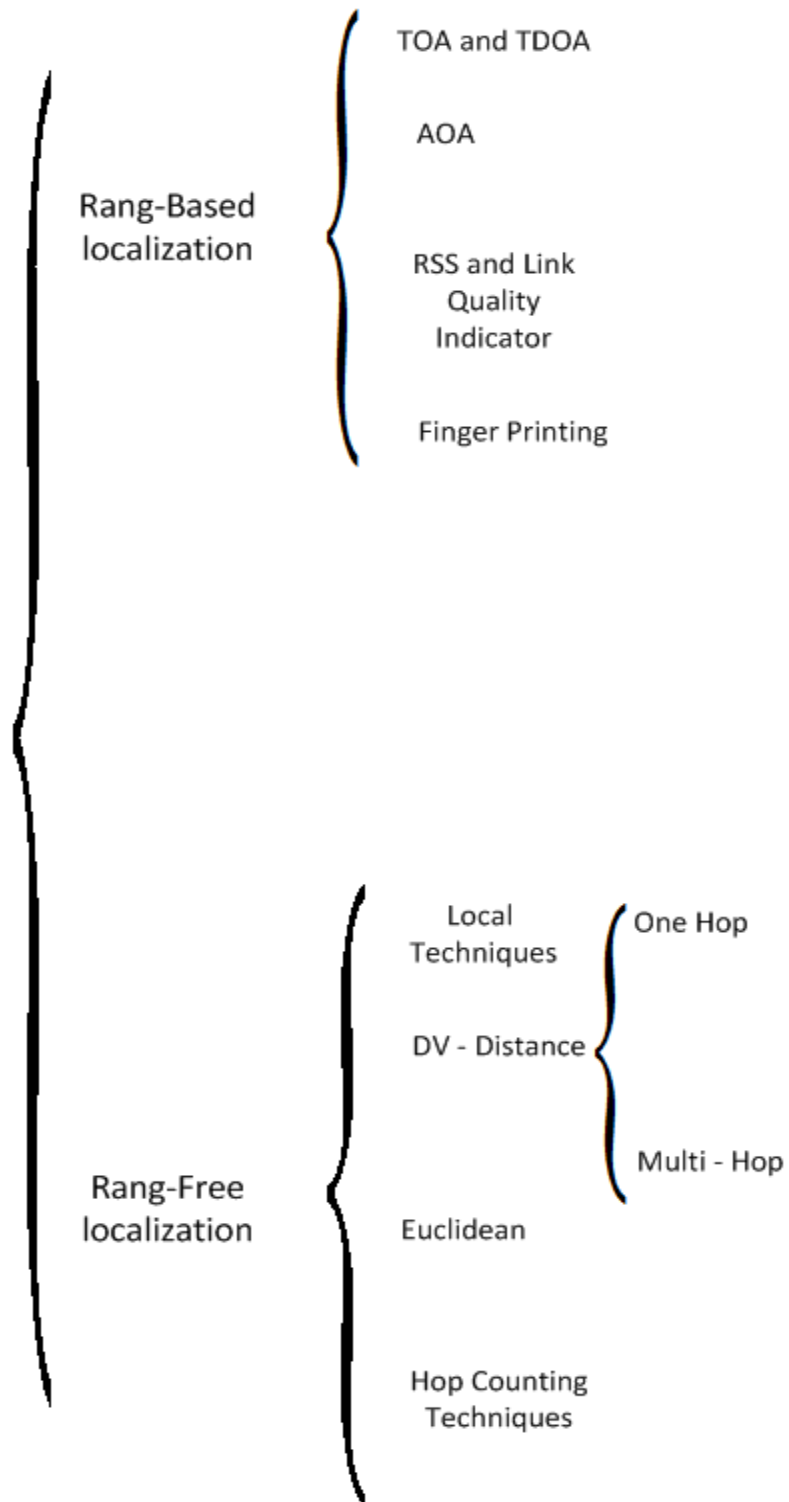


Figure 2.2-2 Range-Free vs Range-Based

of localization algorithm is its high precision and accuracy while utilizing relatively few anchors. One disadvantage is the added cost of additional hardware needing to each sensor for ranging purposes. Another clear disadvantage is the sensitivity of results to noise and obstruction of line of sight (LoS).

Time-of-arrival (ToA) and time difference of arrival (TDoA) utilize the fact that the distance between a sensor node and an anchor can be determined by the time of flight (ToF) of communication signals (e.g. RF or acoustic signals) [6, 26]. These two pieces of information are amongst the most accurate for range-based approaches in regards to distance-estimation, being formulated as  $d = V_p * \text{ToF}$  where  $V_p$  is the propagation speed of the communication signal in the current medium. The most common and familiar approach is ToA, which is used by GPS systems. This approach can be further classified into two approaches: using a one-way signal, which requires synchronization between anchors sensor nodes, and using a two-way signal, which does not require any synchronization though at the cost of network delay. TDoA approaches require that nodes transmit two different types of signals that travel at different speeds, such as RF and acoustic [6, 18, 19, 20]. This eliminates the necessity of knowing the absolute transmission times. In the case of using a radio and an acoustic signal, the destination node receives the radio signal first due to its faster propagation speed when compared with the acoustic signal as shown in Figure 2.2.3. The receipt times of the two types of signals are recorded in order to calculate the time-difference to estimate distance. This approach is extremely accurate so long as LoS and appropriate environmental conditions

are met, which can be difficult inside of buildings or in mountainous terrains. Additionally, the speed of the acoustic

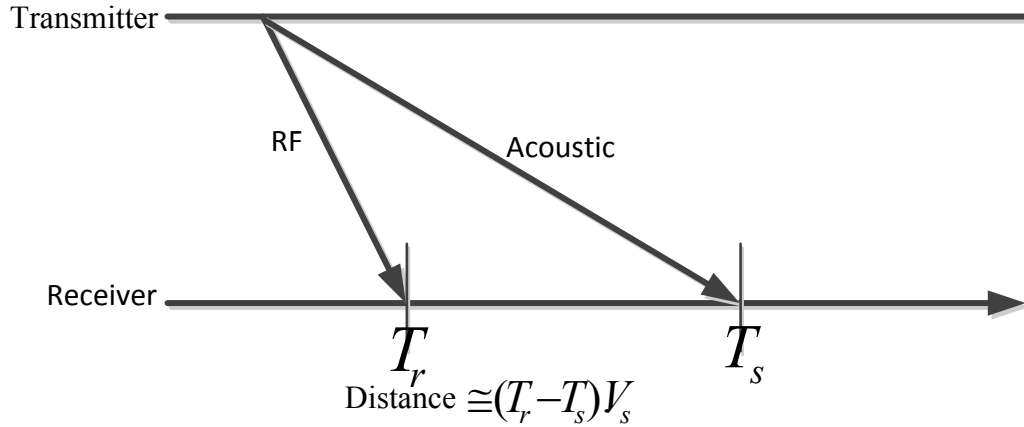


Figure.2.2-3 Time Difference of Arrival

signals depends heavily on environmental factors, such as temperature [6].

Received signal strength (RSS) approaches are popular because they do not require any special hardware and most sensor nodes on the market can perform power measurements [6, 27, 28, 29, 30, 31]. These approaches use a quantified received signal strength indicator (RSSI) based on the fact that beacon signals lose power (suffer attenuation) during propagation, a factor known as path loss. Although RSSI approaches are inexpensive and easy to implement, they face specific challenges, such as multi-path fading, channel noise effects, and background interference, making distance estimations based on these approaches inaccurate compared with other types of approaches. The received power of these techniques can be formulated by

$$P_r = P_t \cdot G_t \cdot G_r \cdot \left(\frac{\lambda}{4\pi d}\right)^2 \quad (2.1)$$

where  $P_t$  and  $P_r$  are the transmitted and received power,  $G_t$  and  $G_r$  are the transmitter and receiver antenna gains,  $\lambda$  is the wavelength, and  $d$  is a calibrated distance constant [6, 23, 24, 31, 32]. This research makes heavy use of the RSS approach and attempts to address and gain advantage from its shortcomings.

Angle of Arrival (AoA) approaches rely on observing phase or time differences between signals arriving at different antennas within an antenna array in order to determine the direction of an anchor. AoA approaches achieve high levels of accuracy to within a few degrees at the cost of needed multiple antennae [6, 19, 27]. The size of sensor nodes affects the spatial separation possible between antennae, which in turn affect the usefulness of these types of approaches. Additionally, multipath reflections, directivities of antennae, and shadowing can affect measurements. The following figure illustrates  $n$  arrays for the antenna.

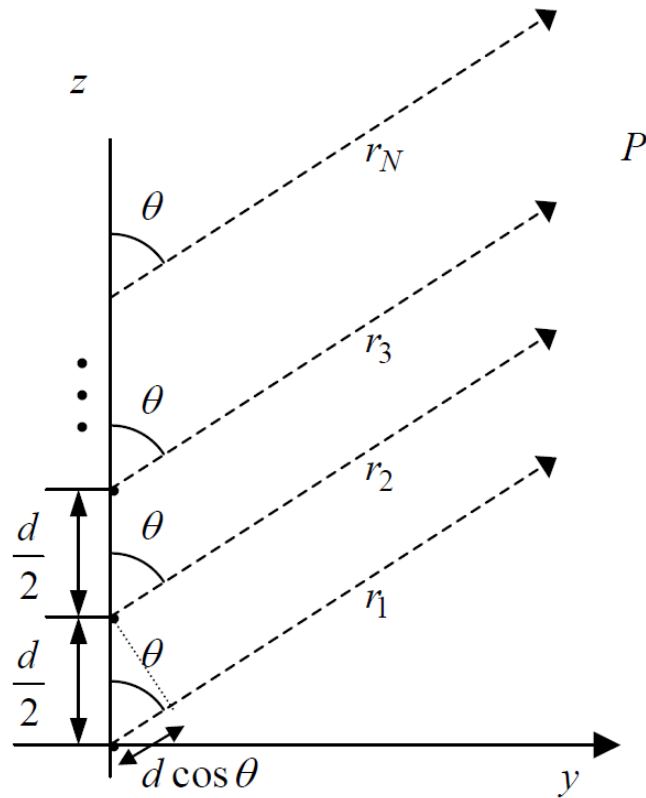


Figure 2.2-4 An Antenna Array with N Antenna Elements

Range- Free approaches do not rely on any of these range-based pieces of information [6, 33, 34, 35, 36, 37, 38]. These approaches are connectivity-based and include hop-based (one-hop or multi-hop) and Euclidean approaches. They utilize an awareness of who is connected to whom to estimate locations of sensor nodes. The principle of these algorithms is that if two nodes can communicate with each other, the distance between them must be within the maximum communication range of the sensor nodes being utilized, which is typically quite short. An advantage of these approaches is the simplicity and relatively low-cost of sensor nodes due to not needed special hardware. Disadvantages include the need for large numbers of anchor nodes, a relatively large



radio range, and specific deployments to obtain satisfactory accuracy [6, 39]. There are some researches making balance between range based and range free [40].

Hop-based approaches calculate a distance vector (DV) based on flooding beacons sent by anchors to all reachable nodes within the WSN. The number of hops taken by each flooded message from one node to the next allows sensor nodes to become aware of their relative distances to each anchor. When an anchor receives a message from another anchor, it estimates the average distance of one hop using the locations of both anchors and the hop-count, which is then sent back to the sensor network as a correction factor. Using this correction factor, sensor nodes are able to estimate their distances to anchors based on some type of computation method, such as trilateration.

#### ***2.2.2.2.1 Anchor-Based/Anchor-Free***

This algorithm classification is based on whether or not an algorithm needs the use of anchors. Certain range-free algorithms utilize an anchor-free approach to simply estimate locality. Anchor-based approaches use anchor nodes to rotate, transform, and sometimes scale a relative coordinate system to an absolute coordinate system. For two-dimensional spaces, at least three non-collinear anchor nodes are required. This increases to four non-planar nodes for three-dimensional spaces. The final coordinate assignments of a sensor nodes are valid with respect to a global coordinate system or any other coordinate system being used. A drawback to anchor-based algorithms is that another positioning system is required to determine anchor node positions. Another drawback to anchor-based algorithms is that anchor nodes are relatively expensive as they usually require a GPS receiver to be mounted on them. Location information can also be hard-

coded into each anchor node, a quite expensive task requiring careful deployment of anchor nodes as required. Anchor-free approaches [6, 41] do not require anchor nodes and provide only relative node localization of sensor nodes in regard to other sensor nodes. For some applications, such relative coordinates are sufficient. Geographic routing protocols need select the next forwarding node based on that node being closer to the destination, a relative metric.

#### ***2.2.2.2.3 Mobile-Beacon/Static-Beacon***

Static beacons are fixed in location and must be placed in specific locations within the WSN. A minimum number of anchor nodes are required for adequate results with determination of optimal placing [6], two factors that are drawbacks to static placement. Mobile beacons have certain distinct advantages, such as heavy reuse requiring considerably fewer beacons and reduced communication costs between beacon nodes and sensor nodes. Mobile anchors can be mounted to carriers such as traditional vehicles that can traverse the deployment area. The main problem with using mobile beacons is in finding the optimal trajectory path to ensure that the distance between anchors and sensor nodes is within communication range of the sensor nodes. This adds an additional coordination and timing factor to approaches using mobile beacons. Indeed, there is a sub-field of study in regards to mobile beacon trajectories with different approaches suggested, such as Random Waypoint (RWP) [6, 42, 43, 44]. This work makes heavy use of mobile beacons and discusses the use of trajectory planning and its effects on localization.

The following figure, figure 2.2.5, summarizes the different aspects of mobile and static beacons. The majority of previous researches used just one Mobile Beacon [45, 46, 47, 48, 49, 50, 51], but there are some others that used more than one mobile anchors [52, 53, 54]. The Sparse-Straight-Line (SSL) and Dense-Straight-Line (DSL) [55, 56] approaches to mobile beacon trajectory will be further explained in Section 4.7. For our simulation purposes, both approaches were made possible and considered. The Random Waypoint and Spiral approaches are also feasible and have been considered as future work for the purposes of this dissertation. The layered-scan model, applicable to three-dimensional localization, is considered in this dissertation as a possibility for future consideration of expanded efforts in three dimensions.

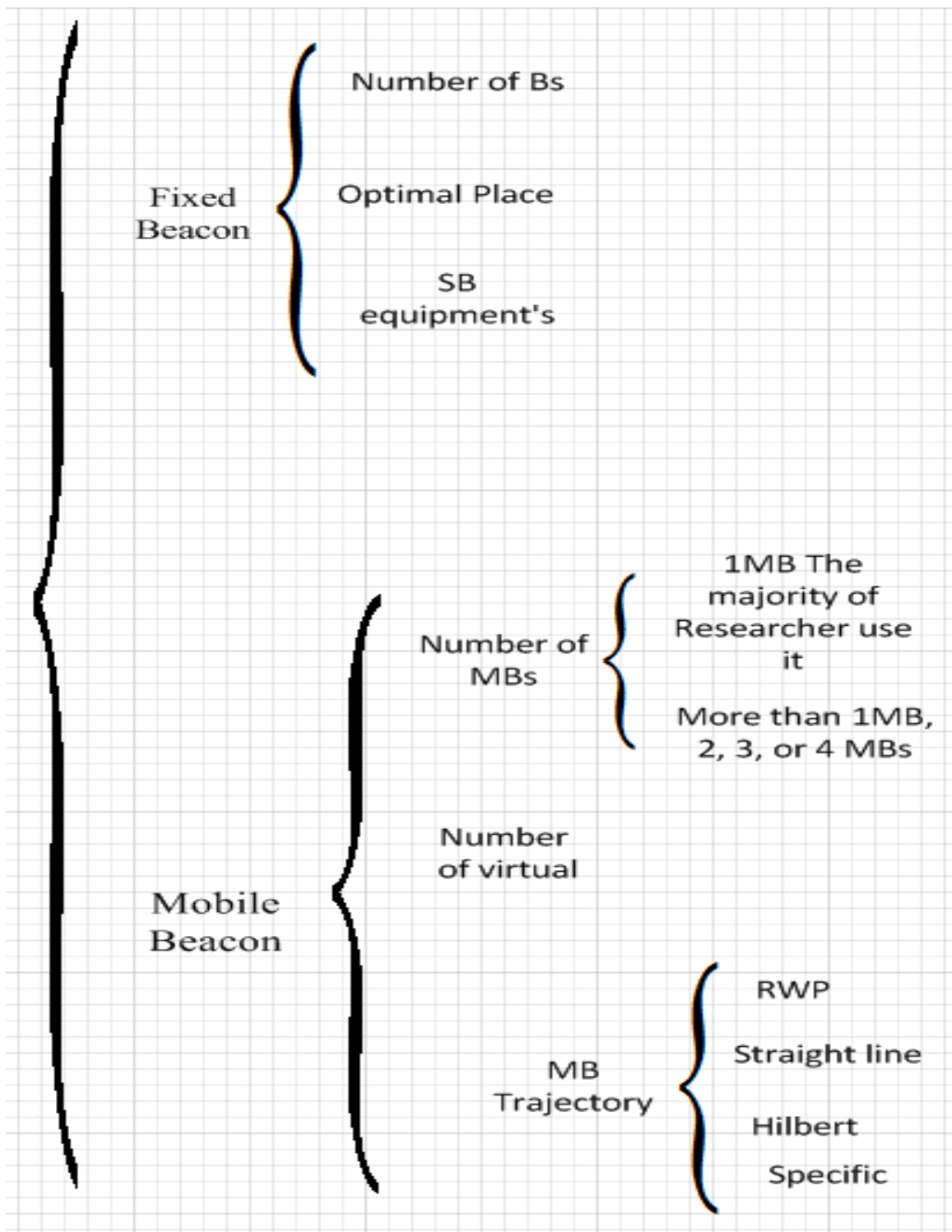


Figure 2.2-5 Static vs Mobile Beacon Classification

#### ***2.2.2.2.2 Relative-Position/Absolute-Position***

This classification relates to whether localization is to give position information relative to a global coordinate system or simply identify neighbors and approximate distances. As was previously mentioned, certain applications focus only on proximate distance and do not need absolute location information [6].

#### ***2.2.2.2.3 Mobile-Sensor/Static-Sensor***

Similarly to the concept of mobile or static beacons, sensors can be made to be mobile or static. For purposes of this research, we primarily concern ourselves with statically-positioned sensor nodes, though mobile sensor node localization could be seen as a potential extension [6].

#### ***2.2.2.2.6 Indoor/Outdoor***

This is a relatively simple classification, but one worthy of note as indoor and outdoor applications often have very different needs and challenges [57]. Factors such as line of sight (LoS) and material effects often characterize indoor applications [58]. Outdoor applications typically have a much larger deployment area [59]. This research primarily focuses on outdoor applications, though indoor applications could also be considered [6,36].

#### ***2.2.2.2.7 Centralized / Distributed***

This type of algorithm classification defines the infrastructure and function of a WSN. A centralized algorithm operates to collect data from remote sensor nodes to increasingly-centralized points [6, 60, 61, 62]. A distributed algorithm decentralizes the nature of this task amongst the masses of sensor nodes [2, 6, 61, 63]. This research

focuses on a “flat” decentralized approach by having ultimate data recovery come directly from the nodes themselves on an individual basis.

### **2.3 Error-Modeling and Analysis**

The principle of error-modeling is the qualification and quantification of errors present within a system. This is of critical importance to ensure accuracy and qualify precision. In the distance-based localization scheme that is the primary focus of this research, the means and approach to modeling error present both advantages and limitations to the methods discussed. Error-modeling is similar to solution modeling in that the nature of the physical problem at hand and the mathematical representation of the problem dictate the effectiveness of the method. One of the primary distinctions when working with error is relating incurred error to the operational model of the system itself. Often, the two models take similar forms and have related structures and properties. Each controls the other in some way and yet error can be seen as an independent factor because its elimination would seemingly be possible if the operational model of the system were able to do so. Thus, error-modeling can be seen as a means of classifying the shortcomings of the operational model itself, qualifying and quantifying factors that are otherwise ignored or marginalized in the operational model. While modeling and quantifying error is useful for statement of the precision of system outcomes, analysis is often needed to make full use of the observed error [64, 65, 66, 67, 68, 69, 70].

When analyzing error, it is sometimes possible to augment the original system model to allow the error incurred to become a part of the system definition rather than an unwanted factor to be considered separately. Because error is often systematically-related

to system operation, it is also often governed by the operational and structure of the system itself. As there are relationships amongst varying operations and instances of operations of a system, so there are also relationships amongst the error incurred during these operations. It is these relationships and the analysis and transformation of them that are central to this work. Supplementing error analyses to system models creates a type of feedback mechanism that can lead to better understanding and possible improvement-upon results garnered from typical system operations. As all system modeling is a type of prediction of behaviors, so error-modeling can itself provide additional sets of predictable behavior upon which improved analyses and better decisions can be made.

#### **2.4 Position Computation**

After blind nodes estimate the distances between themselves and neighboring anchors, using one or more distance estimation methods, they need to compute their locations in the case of self-localization or they should send the gathered data with extra ID information to a central system, which will compute the sensor node locations. Many methods exist for position computation, including trilateration, multilateration, triangulation, bounding box estimation, probabilistic estimation, central positioning, and others [6, 53, 62, 63]. A localization system's performance depends on the availability of information and environmental constraints, which can affect the choice of a method. Not all methods are appropriate for all applications. Figure 2.3.1 shows some of well-known methods.

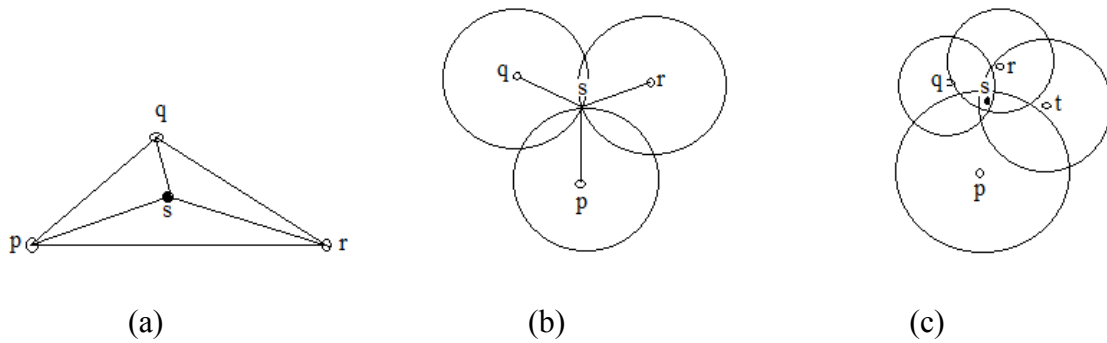


Figure 2.4-1 (a) Triangulation (b) Trilateration (c) Multilateration

### 2.4.1 Triangulation

Triangulation involves the use of angular relationships rather than distance relationships. The node itself may determine its position, which is common in WSNs, or this can be done remotely. As is shown in the figure above, a minimum of three reference nodes are necessary for unknown nodes to be able to estimate their positions based on the trigonometric relationships of their angles in relation to the reference nodes [6, 71].

### 2.4.2 Trilateration and Multilateration

Trilateration is the most common localization computation method used to determine absolute or relative locations of unknown nodes. This is accomplished based on geometric distance relationships of circles, spheres, and triangles. In addition to its practical applications in wireless sensor networks, trilateration has other uses in surveying and navigation, including use in global positioning systems (GPSs). In contrast to triangulation, trilateration does not involve the measurement of angles. It uses the range information from each anchor node as distance measurements upon which to



perform computations. For two dimensions, at least three anchor nodes are necessary. For three dimensions, at least four anchor nodes are necessary [6, 61].

Let  $(x_i, y_i)$  be the known position of anchor <sub>$i$</sub> , then let  $d_i$  be the estimated distance from that anchor to an unknown sensor node, which lies in  $(x, y)$  position. We can consider the distance between the anchor- and sensor position as a radius, then the system of equations can be described as:

$$\begin{aligned} (x_1 - x)^2 + (y_1 - y)^2 &= d_1^2 \\ &\vdots \\ &\vdots \\ (x_n - x)^2 + (y_n - y)^2 &= d_n^2 \end{aligned}$$

By rearranging the terms, a proper system of linear equations can be obtained in the form  $Ax = b$ , where

$$A = \begin{bmatrix} 2(x_1 - x_n) & 2(y_1 - y_n) \\ \vdots & \vdots \\ 2(x_{n-1} - x_n) & 2(y_{n-1} - y_n) \end{bmatrix}$$

$$b = \begin{bmatrix} x_1^2 - x_n^2 + y_1^2 - y_n^2 + d_1^2 - d_n^2 \\ \vdots \\ x_{n-1}^2 - x_n^2 + y_{n-1}^2 - y_n^2 + d_{n-1}^2 - d_n^2 \end{bmatrix}$$

This system of equations can be solved using a standard least-squares method as follow:

$$\hat{x} = (A^T A)^{-1}$$

Trilateration fails rare cases if there is no inverse to A. However, in most cases, a highly accurate sensor location estimation can be found.

An additional check can be done by computing the residue between the given distance ( $d_i$ ) and the estimated location [6]:

$$residue = \frac{\sum_{i=1}^n [(x_i - \hat{x})^2 + (y_i - \hat{y})^2]^{1/2} - d_i}{n}$$

If the residue is large, the system of equations is inconsistent. The estimated location will be rejected if the residue length exceeds the radio range [6].

Trilateration assumes perfect range measurements between the target nodes and three fixed anchors. If these measurements contain errors, solving the linear systems will yield incorrect positions. In multilateration this problem can be solved by using more than three anchors. In solving the linear system, the measurements' mean-square errors are minimized thus producing better results than trilateration.

Given measured and estimated distance values, multilateration is used to maximize the likely estimation of node positions by computing a minimum least-square estimation of the error, which is defined as the difference between the measured and estimated values.

When no range information is available, trilateration and multilateration are ineffective, calling for the use of the proximity technique. It determines whether or not a node is in range or near a reference point by having the reference transmit periodic beacon signals and determine if the node is able to receive at least a certain number of the beacon signals, which is set as a threshold. In a period of time, if a node receives a

number of beacon signals greater than the set threshold, it is determined to be in proximity of the reference point.

### 2.4.3 Bounding Box

The bounding box method uses squares to bound the possible positions of each unknown sensor node. A bounding box is defined for each reference, beacon, node  $i$  as a square with its center at the position of the node  $(x_i, y_i)$  as presented in figure 2.3.2. So, if the estimated distance is  $d_i$ , the sides of the square will be of size  $2 * d_i$ , making the corner coordinates  $(x_i - d_i, y_i - d_i)$ ,  $(x_i - d_i, y_i + d_i)$ ,  $(x_i + d_i, y_i + d_i)$ , and  $(x_i + d_i, y_i - d_i)$ .

Without any need for floating point operations, the intersection of all bounding boxes can be easily computed by finding the minimum of the high coordinates and the maximum of the low coordinates. This is depicted in the figure below with the shaded rectangle, the center of which is the estimated position of the unknown node [6, 63, 70].

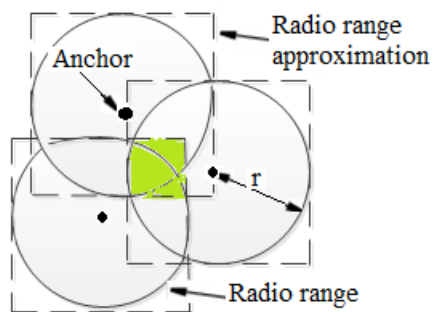


Figure 2.4-2 Building the Bounding Box

The main disadvantage of this method is that the error is greater than that produced by the trilateration method. The main advantage is that finding the intersection of squares uses few processor resources compared with finding the intersection of circles.

## 2.5 Literature Review

Han [8] proposed a Localization Mobile Anchor algorithm that was based on Trilateration (LMAT) in WSNs. He studied five different traveling trajectories, namely LMAT, SPIRAL, SCAN, DOUBLE SCAN and HILBERT algorithms to optimize the mobile beacon trajectory. Liu [25] presented a random-direction mobility model for mobile beacons to cover the sensor area and compares his results with Ssu's and Yu's algorithms. Teng proposed in [29] a distributed MRC localization scheme with a specific trajectory in static WSNs. Furthermore, Teng developed with his group two improved approaches (MRC\_Nearst and MRC\_Centroid) for applications that operate within noisy environments. The results show that MRC\_Centroid is the best method for noisy environments. In [42], Park studied the mobile trajectory path and its effect on localization accuracy using the slope of the trend line and the closest point to the static sensor node on the trajectory of the mobile beacon. He, then, compared the method of Ssu et al., with his proposed methods, which included methods with and without filtering.

A directional antenna was used as equipped hardware in mobile beacons to obtain a high-level of received power by unknown nodes. Ou [27] proposed a range-free localization scheme with four directional antennas for each mobile anchor. Another type of directional antenna, rotary, was used to periodically send messages in a determined azimuth within the ADAL (Azimuthally Defined Area Localization) [58] scheme by Guerrero. In this method, the centroid of the intersection area of several beacon messages is used by unknown nodes to determine their positions. In [59], Zhang developed a single beam directional antenna and varied the mobile beacon velocity to obtain more accuracy.

In some research papers, more than one directional antenna was applied for each MB to enhance accuracy and reduce power consumption.

Guo [57] proposed a mobile-assisted localization scheme, called perpendicular Intersection, which use a delicate tradeoff balance between range-free and range-based approaches instead of RSSI directly mapping value. Chen [39] proposed another type of intersection method called BLI (Border Line Intersection Localization) method where the first and last MB messages were recorded by unknown sensors to determine the border with which to compute their locations.

The weighted-centroid localization method, which uses three mobile beacons, was proposed in [54]. In addition, Cui [52] proposed another weighted centroid localization method using four mobile beacons with two different trajectory “RWP and Layered-Scan” of mobile beacon. In [37], the authors compared TRL, FMB (Four Mobile Beacons), and TMB for RWP (Random Waypoint) model and straight-line moving trajectories.

In [45], Kim proposed a novel range-based localization scheme which involves a movement strategy with a low computational complexity of mobile anchor, called mobile beacon-assisted localization (MBAL). Bahi et al. [46] developed a range-based localization scheme that uses a Hilbert space-filling curve as the trajectory for the mobile beacon. A GMAN (Group of Mobile Anchor Nodes) was proposed in a range-based localization scheme by Zhang et al. [50] to move through the network area allowing unknown sensor nodes to estimate their positions according to the beacon point set determined based on RSSI.

Zhao [47] presented a combined node clustering scheme, which increment localization and mobile beacon assistance together, Mobile Beacon Assisted Localization based on Network Density Clustering (MBL(ndc))

Lee et al. [48] presented a mobile assisted, which moves straight line, localization scheme based on geometric constraints utilizing three reference points. Ssu et al. [38] presented a localization scheme by which the unknown nodes estimate their locations based on geometry conjecture (perpendicular bisector of a chord).

Xu and his group [41] proposed an Anchor-Free Mobile Geographic Distribution Localization (MGDL) algorithm to monitor and detect the movement of sensor nodes. After the movement is detected, the moved node will trigger a series of mobile localization procedures to recomputed the new locations. MGDL was applied for static and mobile nodes and then compared with the elastic localization algorithm (ELA) and MCL. Chia – Ho Ou [51] presented a range-free localization scheme based on standard geometric corollaries using flying anchors for 3D. The same scheme was developed with four mobile beacons with RWP and layered scan moving trajectory by Cui [32].

[36] Reviewed and classified localization schemes using different numbers of criteria for indoor and outdoor environments. Kushwah developed a passive method in [28]. Since only a few acoustic mobile beacons emit acoustic signals, the unknown nodes just receive these and RF signals to estimate their locations. In [43], Localization method on the virtual force and anty colon algorithm was proposed and then compared to Hilbert method by Geng. Fu [30] proposed a three dimensional space based localization scheme called SMAL, the average localization error is very low (0.04%).

Doherty [65] used a rectangular bounding method to bound possible positions for all the unknown nodes in the network and minimize the bounded area with any additional constraints. In [68], parametric channel mode is presented and localization error is reduced by Tarrio. Karagiannis [69] presented four error models and used the points of intersection to form circles with estimated distances from each other. This was done in order to apply different methods to form clusters. Ragio [70] used a bounding box method to minimize the error of localization for mobile WSN constraining the received samples. Ying and his group [73] developed a new algorithm called Ecolocation (error controlling localization technique) based on RF sequences to minimize the localization error. In [64], Qiao proposed two gradient descent algorithms to obtain excellent localization accuracy. The same idea was used with the combination of pruning inconsistent measurements to higher the localization accuracy which was presented by Garg [67]. Sirakumar. S [66] developed a genetic algorithm for Error minimization in WSN. Demirbas [71] presented a robust and light weight solution to use the ratio of RSS which is from a light weight receiver to overcome a signal received power fluctuation. In [72], Baro presented a practical swarm potentialization (osp) algorithm to bound the area where the sensor can be located, and minimize error.

Although static and mobile beacons are both feasible options for a WSN, current, modern approach to localization are typically based on the use of mobile beacons due to their flexibility of application and lower cost. The table below summarizes a number of the aspects and parameters of current works that utilize mobile beacons in order to provide a broad cross-section of the efforts within the area of localization.

Table 1 Mobile Beacons assisted localization solutions comparison

Ref	# of Ns/ # of MBs	2D/3D Area	Com m. Range	Para m.	MB path Trajectory / Speed	Error	Notes
27	1000/1 or more	2D	30m	RSS	RWP/ $\leq R/2$	0.1-0.75	NA
16	300/1%:1:5%	3D/ 100*100*100	Random way	RSSI	Random	- NA	NA
25	100/1	2D/ 150*150	NA	RSSI	NA	NA	NA
28	50	3D/ 100*100*20	$R \leq 30$ m		NA	0.8962 – 4.5119	At least half of Ns on ground
29	NA/1	2D/ 500*500	100u	RSS & MRC	specific	0.1-0.185 depends on parameter Except time 0.1-2	MRC centroid is the best method
30	50 / 1	3D/ 500*500*500	NA -	RSS	Front back and left and right 20m Up down 10m	0.03 – 0.14 depends on average distance	NA
34	200 / 1	2D/ 500*500	NA	NA	Straight line 10:10:50m/s	0.8 to 5.34 depends on MAs & alg. type	Single beam direction antenna
35	100/8	2D/ 100*100	20m	RSS	RWP	0.38 – 1m depends on changing Param.	each MB has 4 Directional Antennas
37	100/1	2D/ 100*100	15m & 30m	RSS	RWP 10m/s	11.68-14.98%	MB has M levels trans. power
22	300 / 1	2D/ 100*100	20m	NA	Straight	0.5 – 10 m depends on b	NA



					line, 10m/s	in localization error of MB	
41	400/4	NA	15m	RSS I	NA	5 to14% for St. Ns 20to29% for M. Ns	MGDL & ELA methods for static and mobile Ns
42	1/1	2D	NA	RSS I	Several different directions	12-23.5	With and without filter
43	200/1	2D/ 100*100	10m for MB &Ns	RSS I	Virtual	Can be reduce with increasing the # of virtual beacons	Equal distance 3 layer
45	120 & 300 / 1	2D/ 200*200		RSS I	Random	MB-R = 40, SR = 20m	NA
46	10 to 200	2D/ 65*65	MB-R=15	RSS I & ToA	Hilbert	Average error 1.3m	NA
47	415	2D/ 280*280			Hilbert	R =21m	The entire network divided to 18 clusters
48	500 / 1	2D/ 100*100	NA	NA	NA	4 – 30 m depends on the number of virtual beacons	NA
38	319 / 1	2D/ 100*100	10 – 25m	NA	RWP	NA	centroid
51	300/4	3D/ 100*100 * 100	NA	NA	RWP	1 – 1.5	NA
52	100/4	3D/ 100*100 *100	10 & 20m	RSS	RWP & layered scan	10%	11b
53	5 / 1	2D/ 500*890	NA	NA	NA	NA	NA

54	200 / 3	2D/ 173*100	5, 10, 20, and 25 m for both	RSS	RWP & Straight lines	14.97 -25.99 RWP 18.72- 20.26% Straight lines	NA
55	300/1	2D/ 500*500	6m	RSS	SSI, DSL, and random	0.063 – 0.0491 for DSL 0.171 – 0.964 for SSL	NA
56	100 / 1	2D/ 200*200	30m	RSS I	Straight line fixed speed	3 – 15 m	UKF-Filter
57	100/ 1	2D/ 324*324	-	RSS I	Random	0.31 – 3.97	Different experiment s

### Chapter Three: Problem Statement

#### 3.1 Nature of Problem

This research addresses the problem of localization of sensor nodes within a WSN. The sensor nodes are assumed to be randomly, statically-positioned throughout a relatively-large deployment area. Mobile anchors with directional transmission capabilities are assumed to be mounted on a vehicle capable of accurately traversing the deployment area, recovering the sensor data, and performing all necessary in-operation processing tasks. The use of RSS information and direct data recovery from sensor nodes provides the base structure and challenge of the work. The limited communication range and capabilities of sensor nodes and the frequently erroneous feedback provided by RSS

information present challenges that have not been adequately addressed or overcome in existing work in the literature.

The intended outcomes of this work are to present a detailed understanding of the use of error-modeling in augmenting distance measurements, model the RSS localization system presented, generate methods to characterize the error present in the system, and simulate the resulting models and methods to validate the improvements in localization achieved by the conceived methods. Final analysis of the simulation results will provide a means of drawing conclusions as to the practical behaviors of the localization system and the true effectiveness of the methods presented. Current efforts in this work indicate that additional algorithmic enhancements may be possible once preliminary simulation results are analyzed.

This research is intended to be both a proof of concept of the usage of error-modeling and analysis in localization as well as a platform for further research into additional methods and concepts of “holistic” modeling in which potentially-undesirable system behaviors, such as incorrect measurements, can be exploited to the benefit of improved system output.

The sections that follow indicate the proposed methods of solution to the localization problem and illustrate the simulation that was designed based on these methods along with results and analyses based on this simulation. The proposed range from a space of a single dimension to that of three dimensions, which is the most likely application space for future localization efforts. The proposed solutions build upon one another progressing from a single dimension to three dimensions, which follows the

nature of the localization problem in that each dimension effectively constitutes a separate localization problem with certain mathematical and physical relationships correlating the dimensional solutions. Based upon these solutions, the designed simulation tests the functionality, limits, and nature of the solutions further.

The simulation environment was designed to follow the specific nature of the localization problem in that the simulated environment, dimensional measurements, and physical characteristics modeled within the simulation are based directly from what might be expected in a real-world application. This ensures certain quality in the results gathered and the subsequent analyses in that they follow from a modeled environment intended to match the real environment closely-enough to provide what we believe to be conclusively-coherent results. Before discussing such results though, the next section provides the necessary details of the mathematical and physical modeling of the proposed solutions methods.

## **Chapter Four: Proposed Methods of Solution**

### **4.1 Introduction**

Assume that there exist two mobile beacons located before and after a sensor in terms of direction of travel of the beacons and that no other location information regarding the sensor's location is known. This entails envisioning three axes through the beacons: the first being the axis of travel passing through both beacons, the second passing perpendicularly through the first at the "after" beacon that points in the direction of travel, and the third passing perpendicularly through the first at the "before" beacon that is behind in the direction of travel. Thus, it can be seen that these three axes, when viewed from above in two dimensions, divide the space into six regions. If we define the direction of travel to be to the right, we find that three regions exist above the axis of travel and three exist below. Two of those regions exist before, or to the left of, the "before" axis. Another two of those regions exist between the "before" and "after" axes. The remaining two of those regions exist after, or to the right of, the "after" axis.

As the beacons move in the direction of travel, some of the space in the center two regions shifts to become part of the left two regions, while some of the space of the right two regions shifts to become part of the center two regions. The beacons are assumed to be directional with a 180 degree range of transmission and reception. Additionally, if a reading at a point in time is missing from one beacon, the corresponding reading from the other beacon is discarded. From this, it becomes clear

that the “before” beacon, facing to the right, and the “after” beacon, facing to the left, can only communicate with a sensor that lies between the two vertical axes they create. It should also be clear that communications between the two beacons and the sensor can be considered related based on time of communication, allowing us to pair the information gathered at the two beacons for any given point in time. This is due to the fact that at the time the communications were made, the sensor was in the same fixed location relative to both beacons. If both sets of communications are intended to determine the position of the sensor, they should both clearly indicate the same position. As the beacons move, new pairs of information are attained at fixed steps in movement. Because the sensor itself does not move, any new position indications should identify the same location of the sensor as any previous position indications. This is fundamentally equivalent to placing a multitude of paired, directional beacons at fixed intervals. The complete procedure for Mobile Beacons (MB’s) and Sensor Nodes (SN’s) are given in the following flow chart [6, 71, 72, 73, 74].

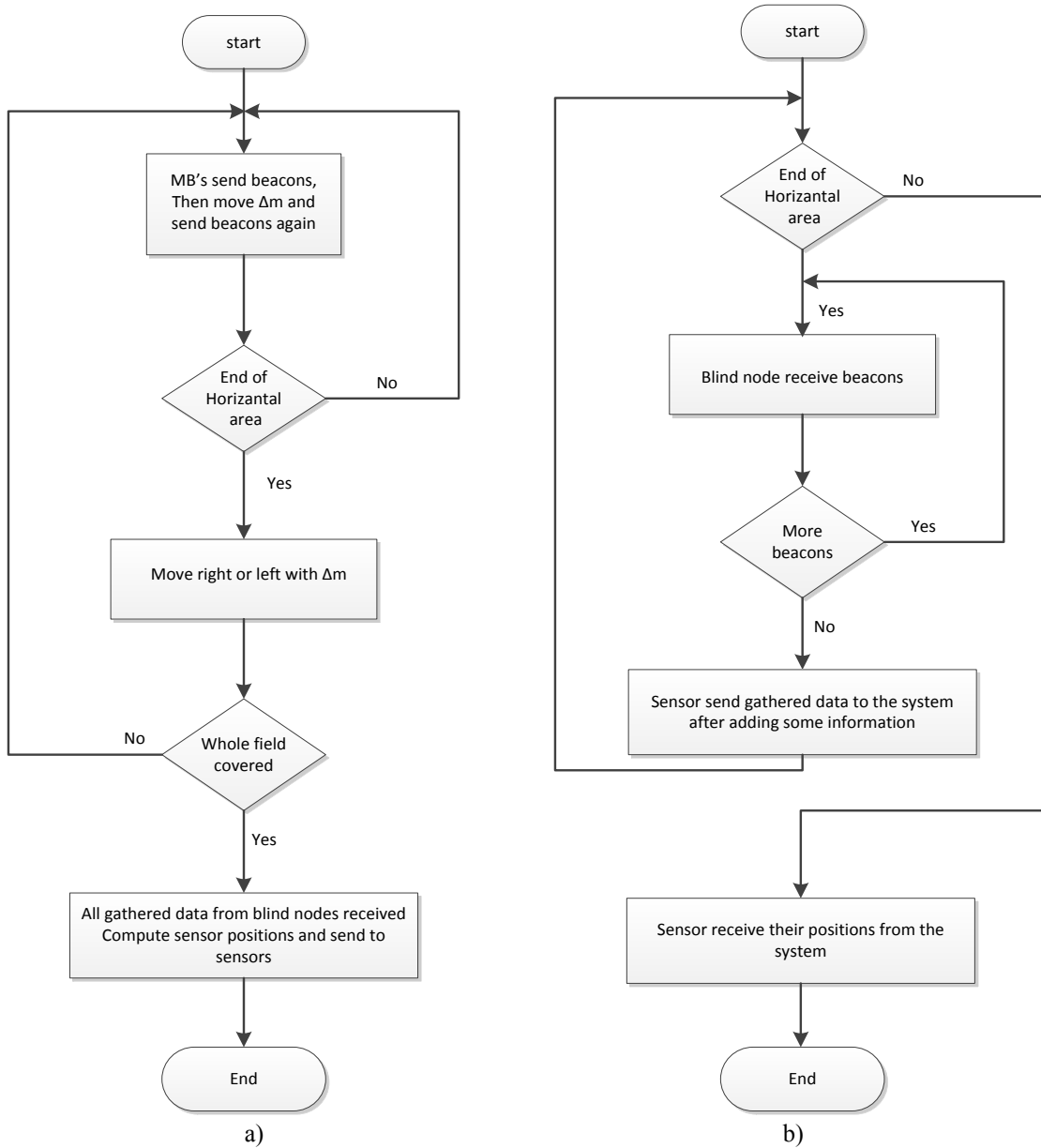


Figure 4.1-1 Flow Chart for Transmission and Receive Beacons and Data a) MB's b) SN's

## 4.2 Conventions and Relationships

A “b” in subscript denotes a relationship to a beacon “before” a sensor.

An “a” in subscript denotes a relationship to a beacon “after” a sensor.

An “i” or “j” in subscript denotes a sample taken at a particular point by a beacon before or after the sensor, respectively.

Variables with a “ $\hat{\phantom{x}}$ ” above them indicate estimates of their plain counterparts.

The following conventions are used throughout this document:

S = sensor location (unknown)

B = beacon location (known)

$\Delta m$  = movement step distance of beacons (chosen constant)

D = distance between paired “before” and “after” beacons (chosen constant integral multiple of  $\Delta m$ )

d = distance between a beacon and a sensor

r = uniformly-distributed random power loss ratio in beacon transmission (unknown)

e = error in distance measurement d, seen as a shortage resulting from r (unknown)

$d_r$  = measured d based upon power reading of beacon transmission (known)

The following relationships hold throughout this document:

$$S = B_b + d_b = B_a - d_a \quad (4.1)$$

$$B(i+1) = B_i + \Delta m \quad (4.2)$$

$$D = d_b + d_a = |B_a - B_b| \quad (4.3)$$

$$d_b = d r_b + e_b \quad (4.4)$$

$$0 \leq r \leq 0.3 \text{ (assumption), } e = d \cdot r \text{ (assumption)}$$

$$d_a = d r_a + e_a \quad (4.5)$$

$$d_r = d - e = d \cdot (1 - r) \quad (4.6)$$

$$d r_b \leq d_b \quad (4.7)$$



$$dr_a \leq d_a. \quad (4.8)$$

### 4.3 Sensor Localization Using Rough Methods

Clearly determining  $d_b$  or  $d_a$  in one dimensional case and determining both in two dimensional cases will yield the unknown location of a sensor. Because only estimates of  $d_b$  and  $d_a$  ( $dr_b$  and  $dr_a$ ) can be obtained via calculation based on the signal strength of the beacons sent from A and B, it is necessary to use appropriate methodologies to reduce the errors in distance measurement ( $eb$  and  $ea$ ) inherent in  $d_{rb}$  and  $d_{ra}$ . The methods discussed in this section, categorized by dimensionality, provide crude means of estimating the location of a sensor and form the foundational precepts for later, more refined means.

#### 4.3.1 One-Dimensional Approach

Here it is assumed without loss of generality that both beacons and a sensor are located on the x-axis. If the ratio  $c$  of distances  $d_b$  and  $d_a$  is known, using the relationship of  $D$  with  $d_b$  and  $d_a$  makes identifying the sensor location a trivial matter.

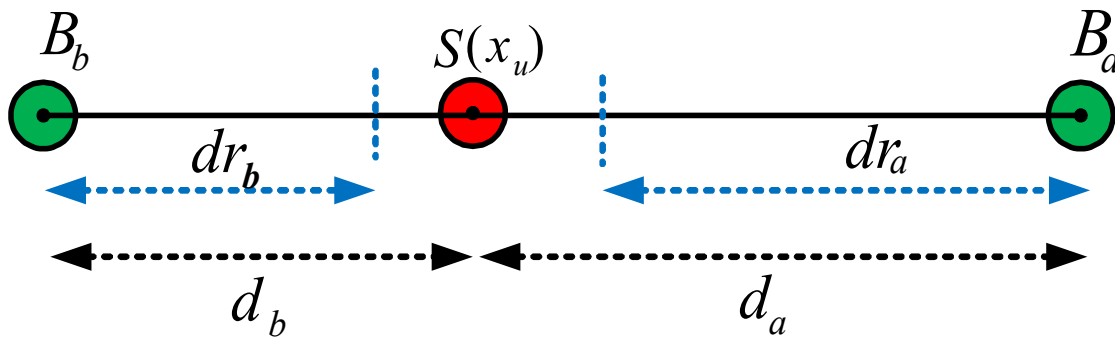


Figure 4.3-1 1-D-Basic Rough Method Layout

Some observation and using equation 4.3 and the ratio ( $c = \frac{d_b}{d_a}$ ) yields to:

$$d_b = D \cdot \frac{c}{c+1}, \quad (4.9)$$

$$d_a = D \cdot \frac{1}{c+1}, \quad (4.10)$$

Due to fluctuations in power, the beacon power readings taken by a sensor may have a certain percentage of error. These error ratios ( $r_b$  and  $r_a$ ) correspond to shortened distance measurements ( $dr_b$  and  $dr_a$ ) by factors of distance measurement errors ( $eb$  and  $ea$ ).

The summation of equations 4.7 and 4.8 and using equation 4.3 yields to:

$$dr_b + dr_a \leq D \quad (4.11)$$

as it shown in Figure 4.3.1

In the case of equality in equation 4.11 plus doing some simple observation leads to the conclusion that the two measured distances must both be completely accurate, meaning that  $dr_b = d_b$  and  $dr_a = d_a$ . This is due to the fact that by assumption each measured distance can never exceed the actual distance it is representing, making it mathematically impossible to draw any other conclusion [71, 72, 73].

Note:  $dr_b \leq d_b$  and  $dr_a \leq d_a$ .

More generally, for any pair of measured distances ( $d_{rbi}$ ,  $d_{raj}$ ), if  $d_{rbi} + d_{raj} + (j - i) \cdot \Delta m = D$ , then  $d_{rbi} = d_{bi}$  and  $d_{raj} = d_{aj}$ . By selecting the “before” and “after” measurements that provide the closest approximation to this equality, it is possible to derive a crude, though possibly effective, means of estimating the location of a sensor.

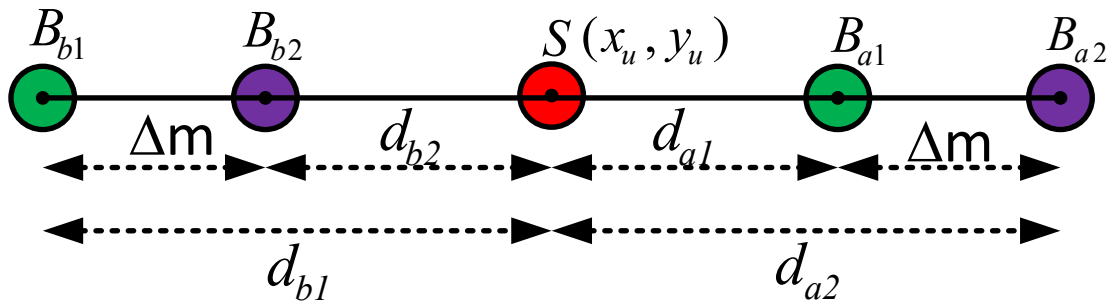


Figure 4.3-2 1-D-Multi Sending Case Basic Rough Method Layout

Though the quality of estimation of such a crude method is highly dependent upon quantities of measurements producing nearer results through a type of “trial and error”, it does, nonetheless, form the basis of concept for the more refined methods discussed in later sections that attempt to “bound” the location of the sensor by knowing that the sensor cannot be located within the range covered by any  $d_{rb}$  or  $d_{ra}$ , which forms a kind of “floor” for the possible location of a sensor.

It will most often be the case that  $dr_b + dr_a < D$ . It is from this fundamental premise that we explore a method involving estimation of  $c$  in order to provide a primitive means of hopefully eliminating some of the incurred error. This method involves the use of a ratio of received signal powers in the form of calculated measured distances.

$$\hat{c} = \frac{dr_b}{dr_a} = \frac{d_b}{d_a} \cdot K, \text{ where } K \text{ is an unknown error factor}$$

Given a pair of “before” and “after” readings from two paired beacon transmissions, we are able to relate the measured distances obtained from them.

*From*

$$\frac{dr_b}{dr_a} = \frac{d_b}{d_a} \cdot k,$$

$$d_b = dr_b + e_b , \text{ and}$$

$$d_a = dr_a + e_a$$

we find that 
$$\frac{dr_b \cdot dr_a + dr_b \cdot e_a}{dr_a \cdot dr_b + dr_a \cdot e_b} = k \quad (4.12)$$

If we assume that  $\hat{c} = c$ , meaning that  $K = 1$ ,

we find that 
$$\frac{dr_b}{dr_a} = \frac{e_b}{e_a}$$

When we relate this to

$$d_b + d_a = (dr_b + e_b) + (dr_a + e_a) = D ,$$

we find that  $(dr_b + e_b) + \left(dr_a + \frac{dr_a}{dr_b} \cdot e_b\right) = \left(dr_b + \frac{dr_b}{dr_a} \cdot e_a\right) + (dr_a + e_a) = D$

yields 
$$e_b = \frac{D - (dr_b + dr_a)}{\frac{dr_b}{dr_a} + 1} \quad (4.13)$$

and 
$$e_a = \frac{D - (dr_b + dr_a)}{\frac{dr_a}{dr_b} + 1} \quad (4.14)$$

From this point it is a trivial matter to find  $d_b$  and  $d_a$  using the fundamental relationship  $d = d_r + e$ . This method can also be generalized to use alternative, potentially more accurate replacement for  $dr_b$  and  $dr_a$  based on additional readings using the method described just prior. Since this method utilizes an assumption that is often untrue, proper quantification of results dictates that we have really found  $\widehat{e}_b$  and  $\widehat{e}_a$ , indicating that our final conclusions are still in fact  $\widehat{d}_b$  and  $\widehat{d}_a$ .

### 4.3.2 Two-Dimensional Approach

The use of the methods described above as extended to the two-dimensional realm requires additional considerations. Fundamentally, the problem is exactly the same if the

sensor lies on the axis of movement between the two beacons. However, this is likely not the case in question. Thus, it is necessary to determine two factors: distance along the axis of movement (position) and distance from the axis of movement (offset). This approach follows from the known mathematical fact that the shortest distance between a line (the axis of movement) and a point (the sensor) is a line perpendicular to the first line (the offset).

It should be immediately noted that with the case of two beacons there are in fact three distances relative to the position on the axis of movement. These three distances are from the position and the sensor, before-beacon, and after-beacon with before and after being relative to the direction of movement. It should be clear that the two triangles formed from this geometry have the same height, a property that is exploited thoroughly throughout the two-dimensional approaches in this work. The figure below illustrates this geometry [39].

From observation it can be noted that

$$[d_{bx} + d_{ax} = D] \tag{4.15}$$

where  $d_{bx}$  and  $d_{ax}$  are the components of  $d_b$  and  $d_a$  respectively along the axis of movement. Similar to the single-dimensional case, we must consider that

$$[dr_{bx} + dr_{ax} \leq D] \tag{4.16}$$

Additionally, we must also consider that  $[d_{by} = d_{ay} = d_y]$  with particular attention paid to the fact the  $dr_{by}$ ,  $dr_{ay}$ , and  $d_y$  may be different due to the errors present in  $dr_b$  and  $dr_a$ . This is another fact that is thoroughly exploited throughout the two-

dimensional approaches in this research. The following Figure shows the one sending case layout for tow dimension [71].

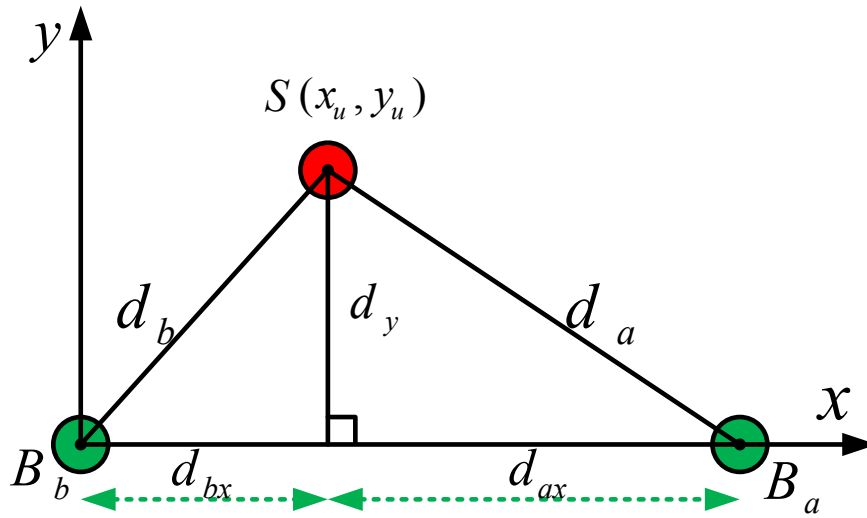


Figure 4.3-3 2-D Basic Layout

Ideally, if  $[B_b + dr_{bx} = B_a + dr_{ax}]$ , then  $[dr_{by} = dr_{ay}]$  and the sensor position is known. However, it is fundamentally impossible to separate  $dr_b$  and  $dr_a$  into their constituent components. What is known is that the errors associated with  $dr_b$  and  $dr_a$  will follow the components of each to scale.

$$\text{Thus, } \left[ \frac{dr_{by}}{dr_{bx}} = \frac{e_{by}}{e_{bx}} = \frac{d_y}{d_{bx}} \right] \text{ and } \left[ \frac{dr_{ay}}{dr_{ax}} = \frac{e_{ay}}{e_{ax}} = \frac{d_y}{d_{ax}} \right].$$

As a rough attempt at localization, we could assume that the read distances are correct (without error) and draw a circle centered at each beacon with radius equal to the read distance corresponding to that beacon. The intersection of the circles would then yield the sensor's position as shown in the next figure.

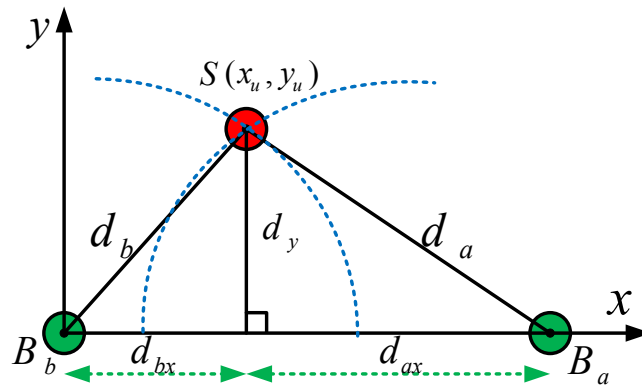


Figure 4.3-4 2-D- Radial Range for Ratios Uses

While this crude method can be executed from a single set of readings, the assumption that there are no errors creates an imminent hazard. If more than one set of readings are used, it may be possible to obtain a more accurate location for the sensor. This is one of the founding tasks to be accomplished for this work. The figure below outlines the structure of the task in case of two pair of readings.

In the case of two or more readings, we draw for each pair of readings a circle centered at each beacon with radius equal to the corresponding  $d_r$ . Because we know that any detected sensor must be at least  $d_r$  away from a transmitting beacon, we can assume that the sensor is above these circles with the lowest possible location for the sensor being the intersection of the two circles. This intersection makes a probable estimation point for the sensor's location. When determining which pair of readings to consider, those two readings that produce the highest intersection point are taken as the best candidates due to their elimination of the estimated locations produced by other candidates.

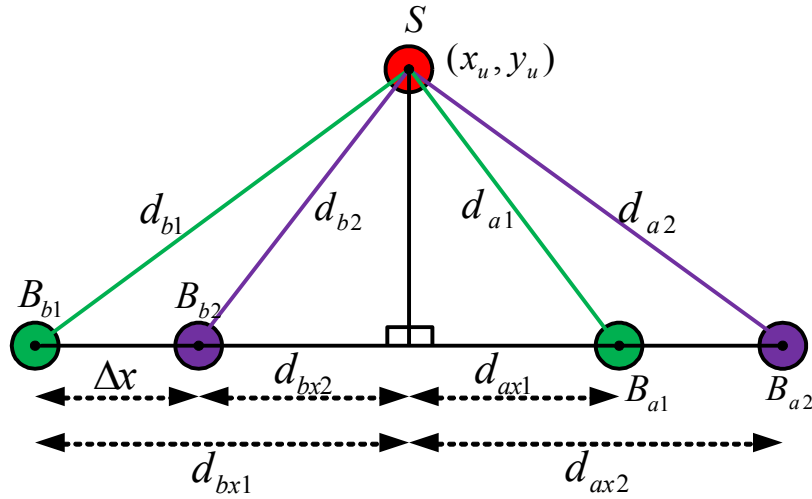


Figure 4.3-5 2-D-Multisendig Case Layout

If the condition occurs that there exist no overlapping pairs of beacons, it must be true that the sums of all pairs of readings are less than the distances between their corresponding beacons. In other words, equation 4.11 can be rewritten as:

$$d_{rbi} + d_{raj} \leq d_{ij} \quad (4.17)$$

Here,  $d_{ij}$  is the distance between beacons  $B_{bi}$  and  $B_{aj}$ . In order to resolve this situation, we identify the pair of beacons that produces a sum of readings closest to the corresponding distance between the beacons and utilize the ratio of the individual readings compared with the total sum of the readings to apply small extension factors to each reading such that the two extended readings produce an overlap point. To identify the candidate pair of beacons, we minimize the following relationship:

$$d_{ij} - (d_{rbi} + d_{raj}) \geq 0$$



We utilize the minimal value produced by the relationship in order to produce the necessary extension factors by doubling it and multiplying by the relational ratios. Mathematically, this follows as:

$$\hat{d}_{bi} = d_{rbi} + \frac{d_{rbi}}{(d_{rbi} + d_{raj})} * 2[d_{ij} - (d_{rbi} + d_{raj})] \quad (4.18)$$

$$\hat{d}_{aj} = d_{raj} + \frac{d_{raj}}{(d_{rbi} + d_{raj})} * 2[d_{ij} - (d_{rbi} + d_{raj})] \quad (4.19)$$

These new extended readings produce an intersection point that becomes the estimated location for the sensor [38].

### 4.3.3 Three-Dimensional Approach outlines

The beacons and overall processing system are mounted within a flying vehicle that could be manned or unmanned. One of the critical components of the onboard system is the ability to accurately measure altitude. In the simple case that we consider, the sensors are located in a flat, two-dimensional plane above which our surveying vehicle passes at a fixed altitude. Thus, we can assume that both the before and after beacons should be located at the same altitude when performing broadcasts. Mathematically, the relationship between the sensor-plane and the beacon-plane is:

$$S_{pl} = B_{abpl} - h$$

For estimation purposes to tolerate a certain degree of realistic error, we locate the sensor plane with the following relationship:

$$S_{pl} = 0.5[(B_{bpl} - h) + (B_{apl} - h)]$$

The location of the sensor plane becomes the value of the z-coordinate for calculation purposes. By observing the figure below, it can be seen that the readings

taken from beacon broadcasts now represent the shape of a cone Here, we consider a pair of readings as accurate candidates ( $d_b = d_{rb}$ , and  $d_a = d_{ra}$ ) if and only if they are greater than the altitude and their circular-projections onto the sensor plane intersect. Given these conditions, we can consider this a two-dimensional problem and solve for the estimation of the x and y coordinates as explained in Section 4.3.2. The estimated sensor position is the intersection of these circles. If the condition occurs that we do not find a pair of candidates that meet the altitude condition, extension factors are added to the most appropriate candidates. Thus, if a reading is smaller than the altitude ( $d_r < h$ ), the following incremental transformation is applied until the altitude condition (h) is met:

$$d_b = d_{rb} + n \frac{d_{rb}}{h} * d_{rb} \quad \text{where } n = 1,2,3,\dots \quad (4.20)$$

$$d_a = d_{ra} + n \frac{d_{ra}}{h} * d_{ra} \quad (4.21)$$

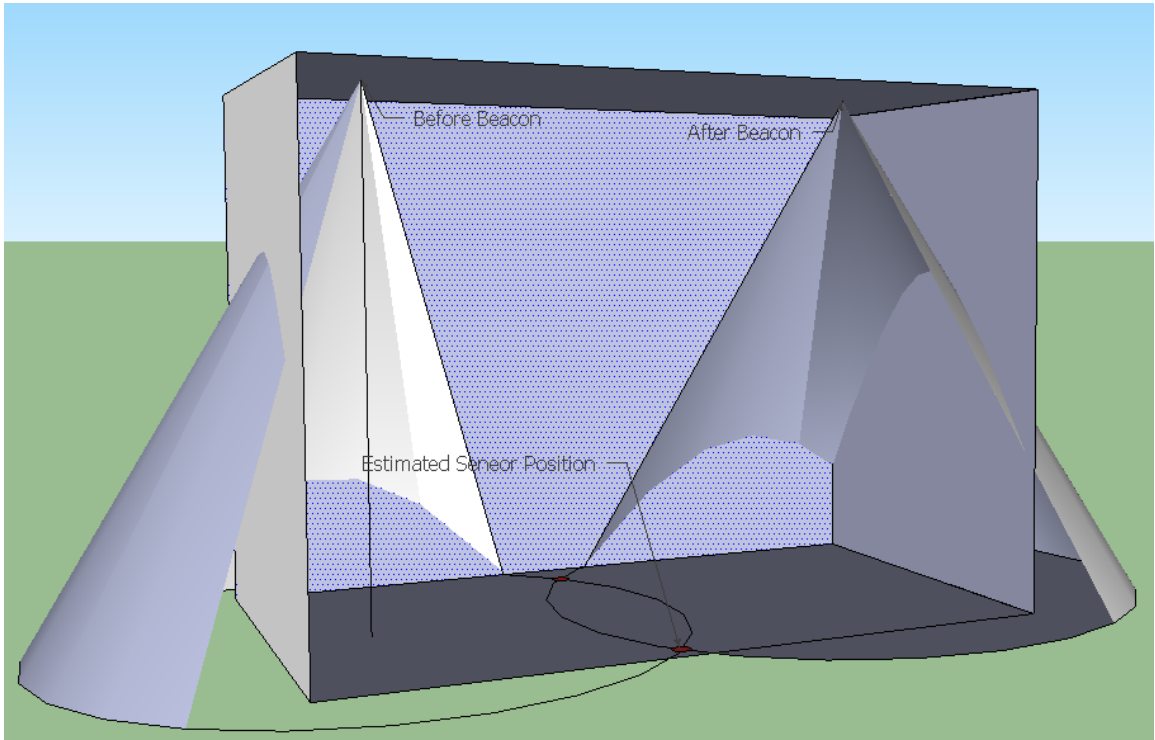


Figure 4.3-6 3-D-Onesendig Case Layout

#### 4.4 Sensor Localization Using Magnitude Bounding Method

In this section, we hold the assumption that the sensor is located between the two beacons as in task one and can receive wireless signals from both anchors. The received signals are gathered and sent to the system and they will be translated to distances. In this area we are going to find the line where the sensor can be in 1-D, the area in 2-D, and the volume in 3D. In addition to the general assumption, we assume that the translated distances from the received powers are greater, equal to the specific percent of the real distance and less, or equal to the real distance itself.

$$(1 - r_{\max})d_{bi} \leq d_{bri} \leq d_{bi}$$

$$(1 - r_{\max})d_{ai} \leq d_{ari} \leq d_{ai}$$

Where  $r_{\max}$  is a random variable that depends on the communication fluctuation.

#### 4.4.1 One-Dimensional Approach

In this task we are going to first determine the minimum and maximum  $x$  coordinates that the sensor cannot exceed for each pair of transmission cases. Then we will minimize the possibility line length for the sensor's position through the combination of all cases [72, 73, 74].

Our assumption now is:

$$(1 - r_{\max})d_{bx} \leq dr_b \leq d_{bx}$$

$$(1 - r_{\max})d_{ax} \leq dr_a \leq d_{ax}$$

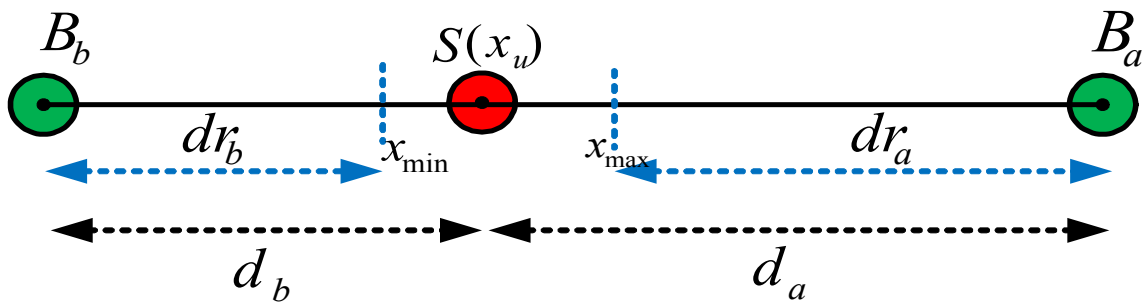


Figure 4.4-1 1-D-Magnitude Bounding Layout

As a result, the sensor is located on the line between  $x_{\min}$  and  $x_{\max}$  as shown in figure 4.4.1.

In the case of more than one reading, we are going to determine  $x_{\min}$  and  $x_{\max}$  for each pair of readings, then we will choose the  $x_{\min}$  and the  $x_{\max}$  that have the closest values to each other as shown in Figure 4.4.2.

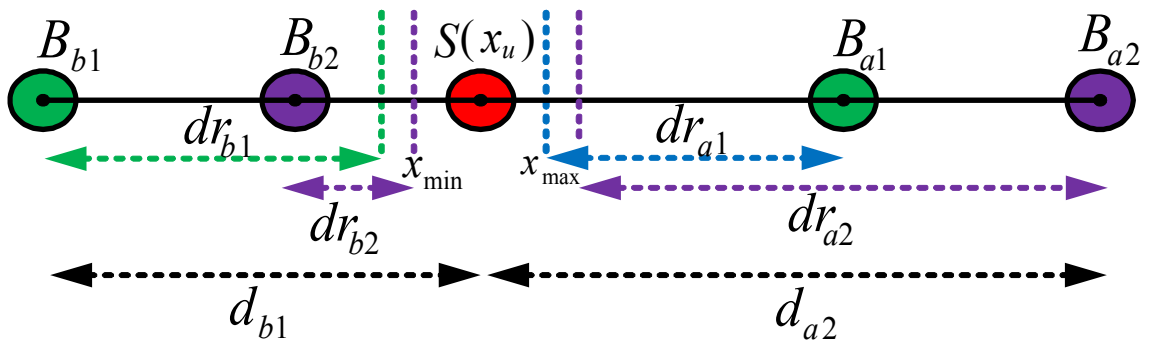


Figure 4.4-2 1-D-Adjusted Magnitude Bounding

#### 4.4.2 Two-Dimensional Approach

The two-dimensional approach to magnitude bounding allows the determination of a “floor” for the location of the sensor based on the fact that the minimum distance to the sensor from a beacon is equal to the read distance for that beacon. For the “ceiling”, the communication range of the sensor is limited and thus the sensor location cannot be out of range of either beacon. The figure below illustrates these points.

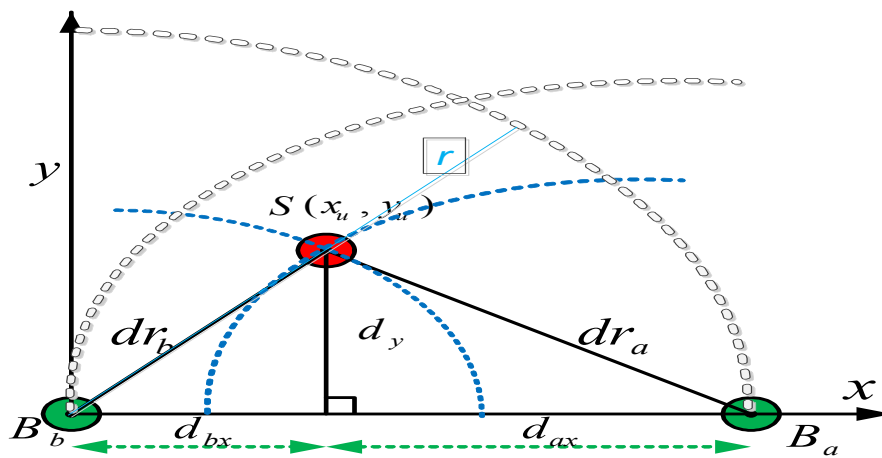


Figure 4.4-3 2-D-Magnitude Bounding

This approach, while completely accurate given the constraining assumptions, is not as precise as more-refined methods because the area of certainty in which the sensor is located is rather large. It follows from these conclusions that a more-refined bounding method is necessary.

#### **4.5 Sensor Localization Using Bounded-Error Method**

The previously discussed methods, despite their inconsistent, error-prone results, form the groundwork of principles and approaches necessary to take a more accurate approach to sensor localization. The method discussed in this section bounds the errors of all readings through correlation of gathered readings. This differs from the previously discussed methods and those methods found within researched works in that it utilizes the magnitudes of unknown error quantities as a means to accurately place sensor locations.

As before, what we desire are accurate estimates of distances  $d_b$  and  $d_a$ , represented as  $\hat{d}_b$  and  $\hat{d}_a$ . Because our error-model  $e = d*r$  relates distance “d” and power loss ratio “r”, it is important to note that  $d = dr + e = d*(1-r) + d*r$ . Thus, when  $dr$  is minimal,  $e$  is maximal and vice versa. It is from this standpoint that we initially assume that  $e$  is maximal, making  $dr$  minimal. When  $e$  is maximal,  $r$  is necessarily maximal as well [6, 63, 70, 74].

Given that  $d = \frac{dr}{1-r}$ ,

When  $d_r$  is minimal,  $d = \frac{dr}{1-r_{\max}}$

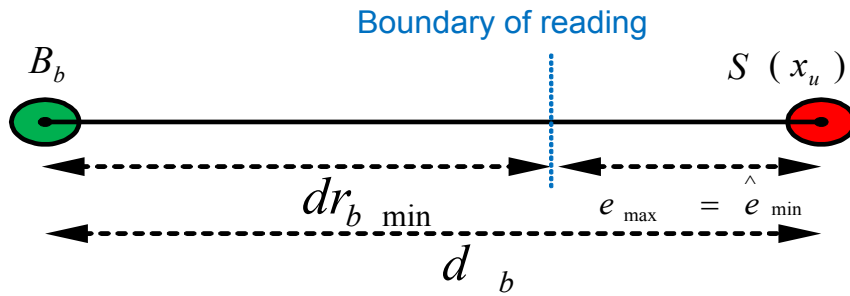


Figure 4.5-1 1-D-Minimum Estimated Error

The previously discussed methods, despite their inconsistent, error-prone results, form the groundwork of principles and approaches necessary to take a more accurate approach to sensor localization. The method discussed in this section bounds the errors of all readings through correlation of gathered readings. This differs from the previously discussed methods and those methods found within researched works in that it utilizes the magnitudes of unknown error quantities as a means to accurately place sensor locations.

As before, what we desire are accurate estimates of distances  $d_b$  and  $d_a$ , represented as  $\hat{d}_b$  and  $\hat{d}_a$ . Because our error-model  $e = d*r$  relates distance “d” and power loss ratio “r”, it is important to note that  $d = d_r + e = d*(1-r) + d*r$ . Thus, when  $d_r$  is minimal,  $e$  is maximal and vice versa. It is from this standpoint that we initially assume that  $e$  is maximal, making  $dr$  minimal. When  $e$  is maximal,  $r$  is necessarily maximal as well.

Given that  $d = \frac{dr}{1-r}$ ,

When  $dr$  is minimal,  $d = \frac{dr}{1-r_{\max}}$

### 4.5.1 One-Dimensional Approach

In the case of a single dimension,  $d_b + d_a = D$  as previously established. Because  $d_b$  and  $d_a$  lie within the same plane, their reading counterparts  $d_{rb}$  and  $d_{ra}$  are directly correlated within that plane. The fundamental inequality between them is that they may have different error ratios “ $r$ ”. As the following figure depicts, the readings obtained for the “before” and “after” sides provide means of establishing “floor” values for their respective sides. Simple observation leads to the conclusion that the “before” side also provides a “ceiling” for the “after” side and vice versa. This becomes especially important when taking into account multiple combinations of “before” and “after” readings.

Even with these observations and relationships, it should be noted that our efforts ought to be concentrated on locating the exact position of S. Theoretically, the sensor position can be computed using equations 4.1, 4.4, and 4.5 as follows:

$$s = B_b + d_b = B_b + dr_b + e_b = B_a - d_a = B_a - (dr_a + e_a)$$

Since the errors are not known, we can calculate the minimum and the maximum possible positions of the sensor.

$$s_{\min} = \max(B_b + dr_b, B_a - \frac{dr_a}{1-r_a}) \quad (4.22)$$

$$s_{\max} = \min(B_b + \frac{dr_b}{1-r_b}, B_a - dr_a) \quad (4.23)$$

$$s_{\min} \leq S \leq s_{\max}$$

Figures 4.4.2 A and B illustrate two different reading cases of the one sending bounding case.



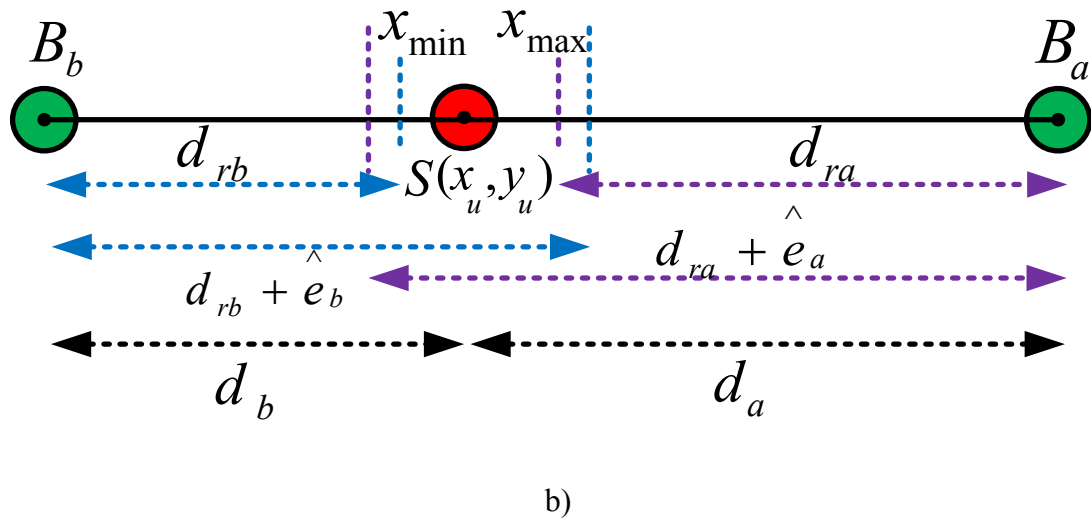
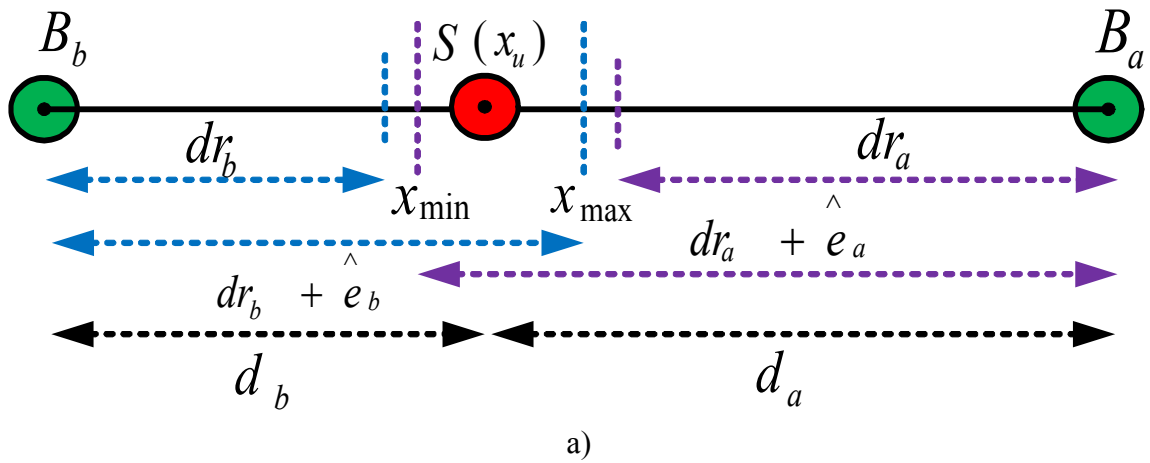


Figure 4.5-2 1-D- Estimated Error Bounding

a) Estimated Error determine Bounding points

b) Real Reading determine Bounding points

When multiple combinations of “before” and “after” readings are utilized per the previously discussed methods, it becomes possible to iteratively update these boundaries of “S” by ensuring that only the most maximal minimum and minimal maximum are kept. From new readings, it is possible to minimize previous “r” estimations.

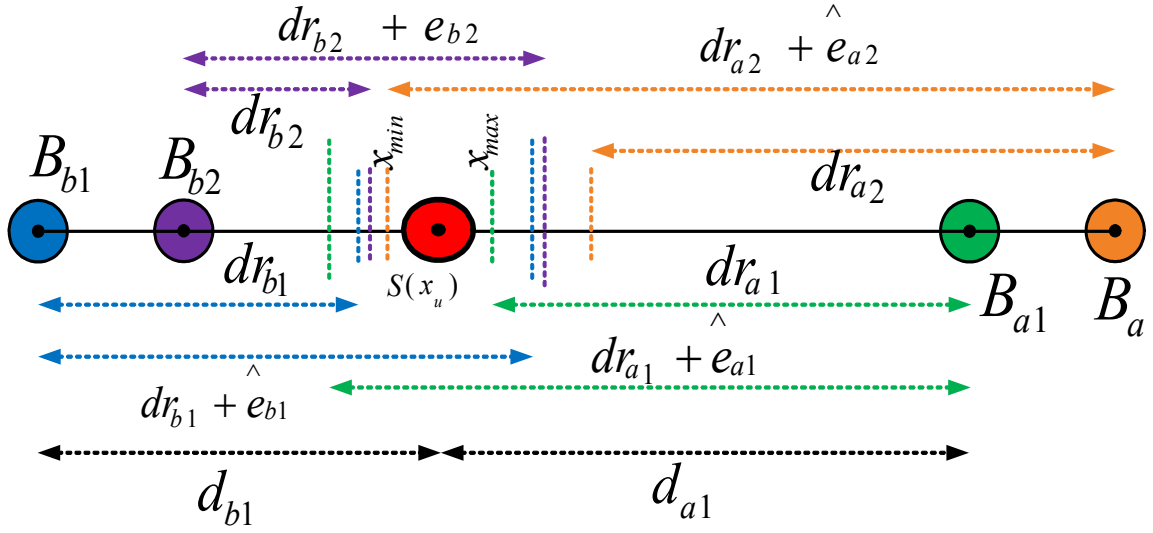


Figure 4.5-3 1-D- Adjusted Estimated Error Bounding

For any given set of readings,

$$r_{bmin} = \frac{\hat{e}_{bmin}}{\hat{d}_{bmin}} = \frac{1}{\frac{dr_b}{\hat{e}_{bmin}} + 1} = \frac{1}{\frac{dr_b}{S_{min} - (B_b + dr_b)} + 1}$$

$$r_{bmax} = \frac{\hat{e}_{bmax}}{\hat{d}_{bmax}} = \frac{1}{\frac{dr_b}{\hat{e}_{bmax}} + 1} = \frac{1}{\frac{dr_b}{S_{max} - (B_b + dr_b)} + 1}$$

$$r_{amin} = \frac{\hat{e}_{amin}}{\hat{d}_{amin}} = \frac{1}{\frac{dr_a}{\hat{e}_{amin}} + 1} = \frac{1}{\frac{dr_a}{(B_a - dr_a) - S_{max}} + 1}$$

$$r_{amax} = \frac{\hat{e}_{amax}}{\hat{d}_{amax}} = \frac{1}{\frac{dr_a}{\hat{e}_{amax}} + 1} = \frac{1}{\frac{dr_a}{(B_a - dr_a) - S_{min}} + 1}$$

$$r_{bmin} \leq r_b \leq r_{bmax}$$

$$r_{amin} \leq r_a \leq r_{amax}$$

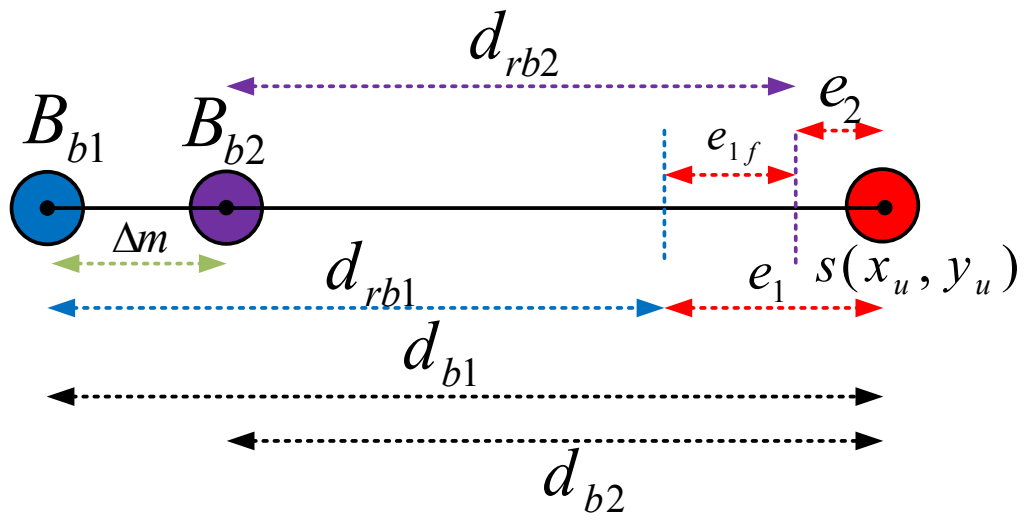


Figure 4.5-4 1-D-Part of Estimated Error Cancellation

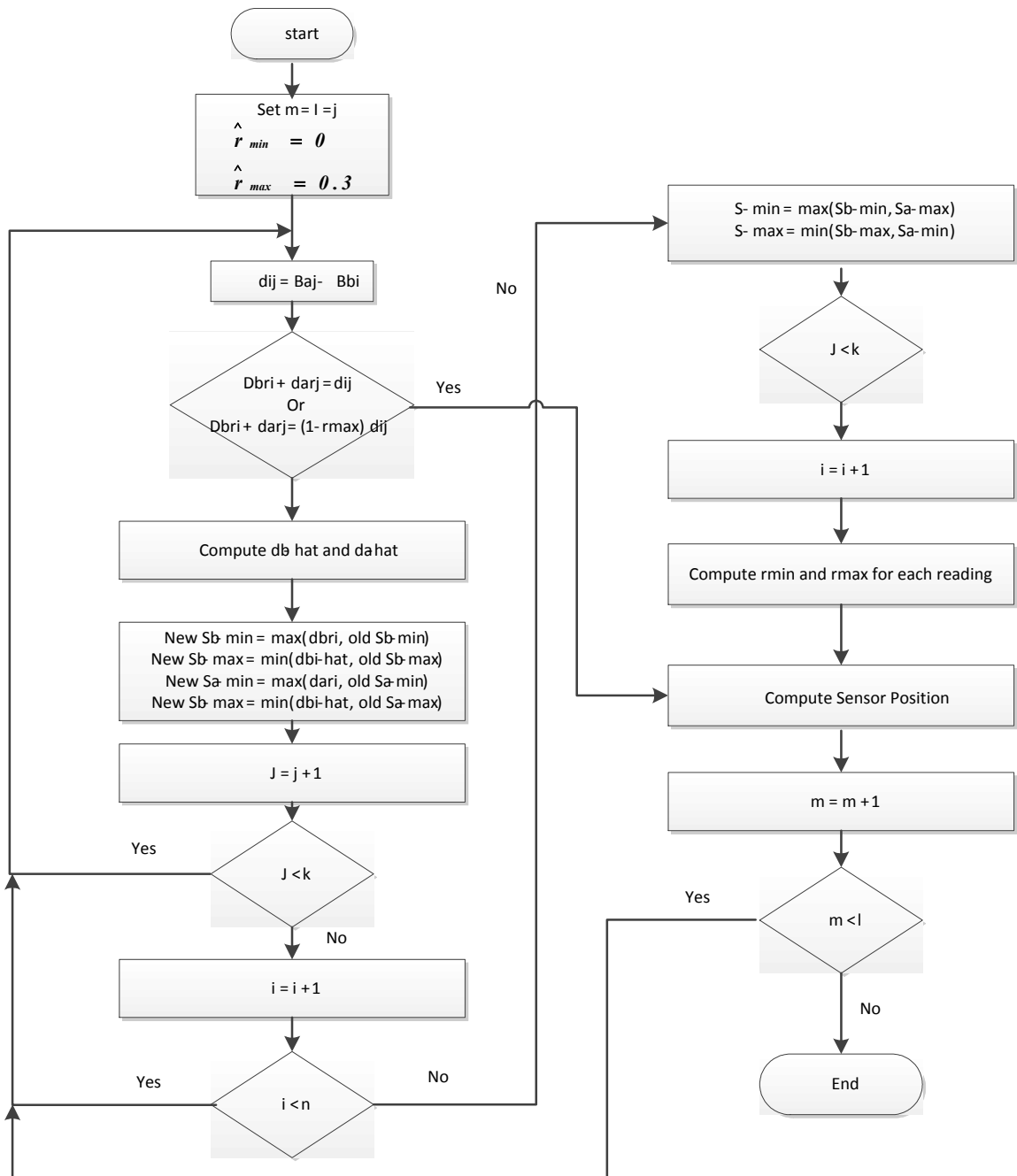


Figure 4.5-5 Flow Chart for 1-D- Bounding Algorithm

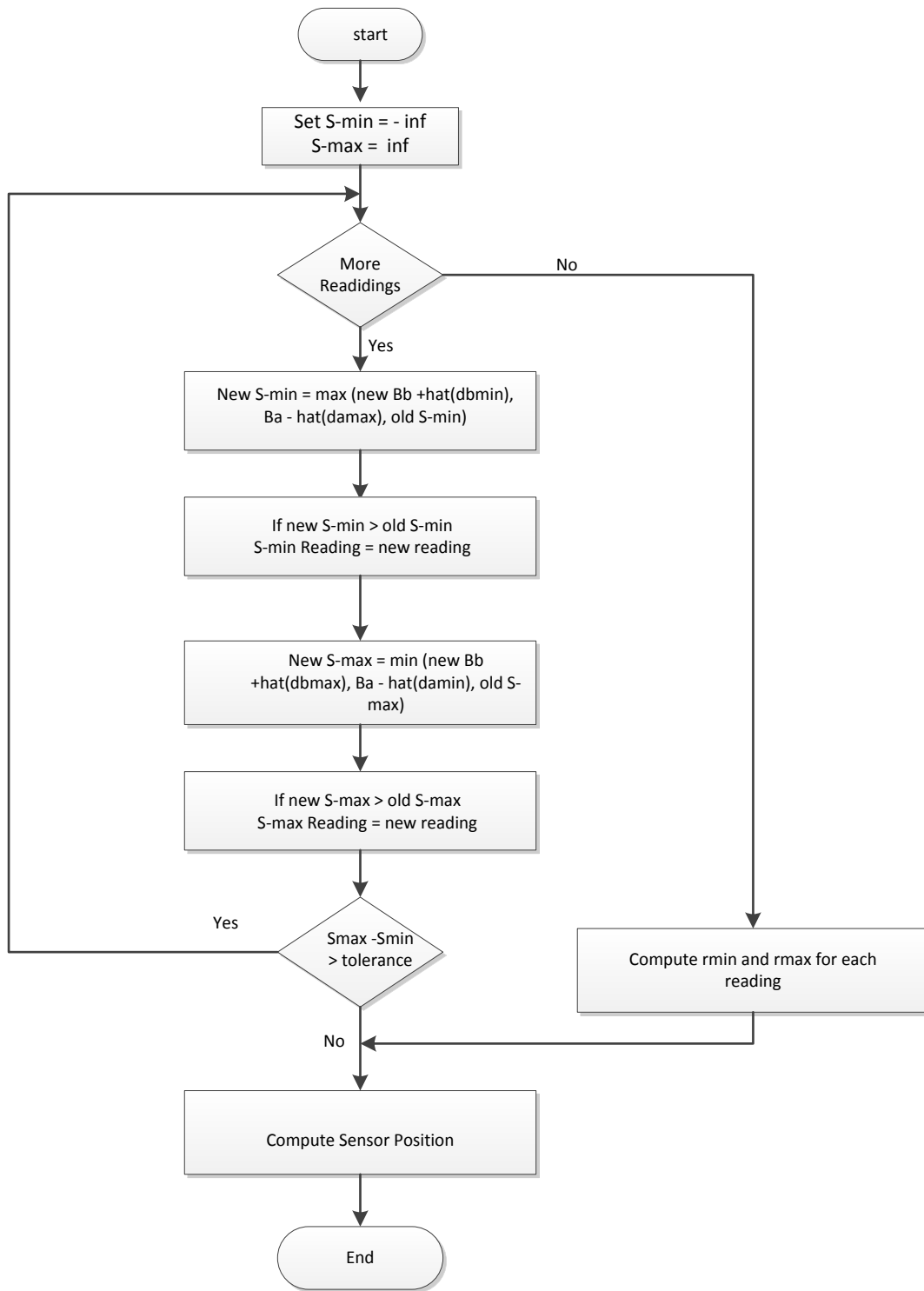


Figure 4.5-6 Simplification of the Flow Chart for 1-D- Bounding Algorithm

Bounding Algorithm (BA):

- 1- Compute the sums of readings( $dr_{bi} + dr_{aj}$ ), for all readings  $i= 1 \dots n$ , and  $j = 1, 2 \dots n$  where  $n$  is the total number of readings.
- 2- Compare all the sums of the pair readings computed above with

$$(d_{ij} = B_{aj} - B_{bi})$$

- 3- If any  $dr_{bi} + dr_{aj} = d_{ij}$  then compute sensor position

$$S = B_b + dr_{bi} = B_a - dr_{aj} \text{ and stop}$$

Or any  $d_{bri} + d_{arj} = (1 - r_{max}) d_{ij}$  then compute sensor position

$$S = B_b + \left(\frac{dr_{bi}}{1 - r_{max}}\right) = B_a - \left(\frac{dr_{aj}}{1 - r_{max}}\right)$$

and stop

else go to the next step

- 4- Compute  $r_{bi}$  and  $r_{aj}$  ranges using the above equations and chose the smallest ranges
- 5- Find the measured readings related to them and then compute the real distances as follow:

$$\frac{dr_{bi}}{dr_{aj} + dr_{bi}} = \frac{d_b}{d_{ij}} \text{ or } d_b = \frac{dr_{bi}}{dr_{aj} + dr_{bi}} d_{ij}$$

$$\frac{dr_{aj}}{dr_{aj} + dr_{bi}} = \frac{d_a}{d_{ij}} \text{ or } d_a = \frac{dr_{aj}}{dr_{aj} + dr_{bi}} d_{ij}$$

- 6- Compute the sensor location as follow:

$$S = B_b + d_b = B_a - d_a$$

### 4.5.2 Two-Dimensional Case

The two-dimensional application of the error-bounding method follows from the principles established for single-dimensional application. From a single transmission, it is our task to utilize the read distances to perform a radial bounding rather than a linear bounding [31, 32]. Thus, the single-dimensional case can be seen as a specialized version of the two-dimensional case in which the sensor lies directly between the beacons. The figure below illustrates the geometry of this aspect of the problem.

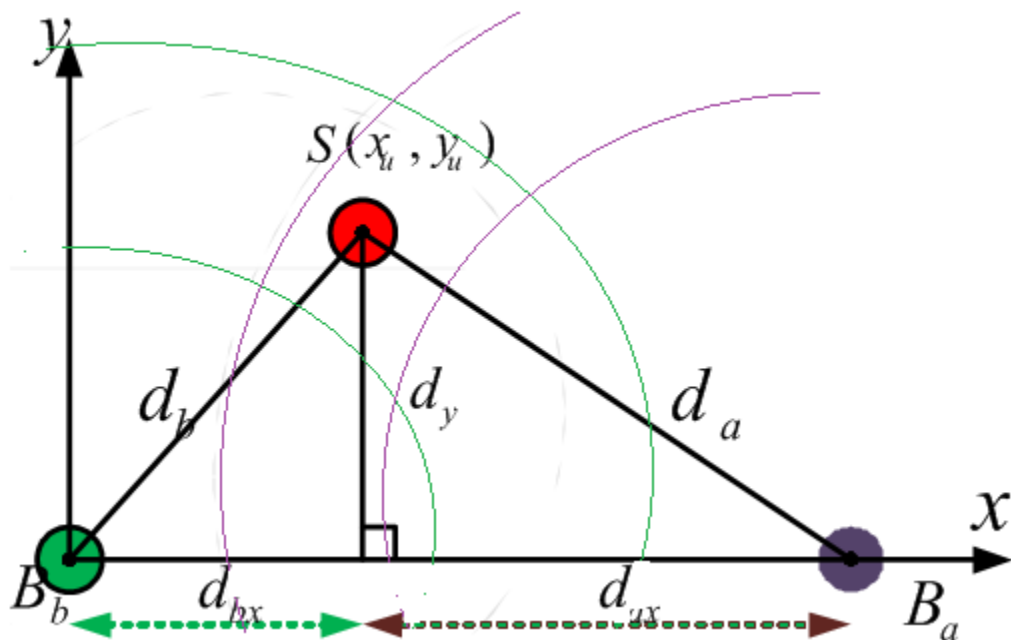


Figure 4.5-7 2-D-Estimated Error Bounding Layout

However, given a developed method, it is necessary to utilize additional readings to further bound the area of certainty for the sensor location. This constitutes a type of iterative algorithmic process of refining the error assumptions of previous readings in order to minimize the area of certainty of sensor location. The following figure

demonstrates the geometry of the expanded approach. The simulation results are shown in chapter 5 illustrate the approached process in creating and refining radial bounds for the sensor location. It should be noted that a fundamental observation regarding this process is that of extreme-values, meaning that refinement relies on bounding conditions that exceed previously-demonstrated conditions.

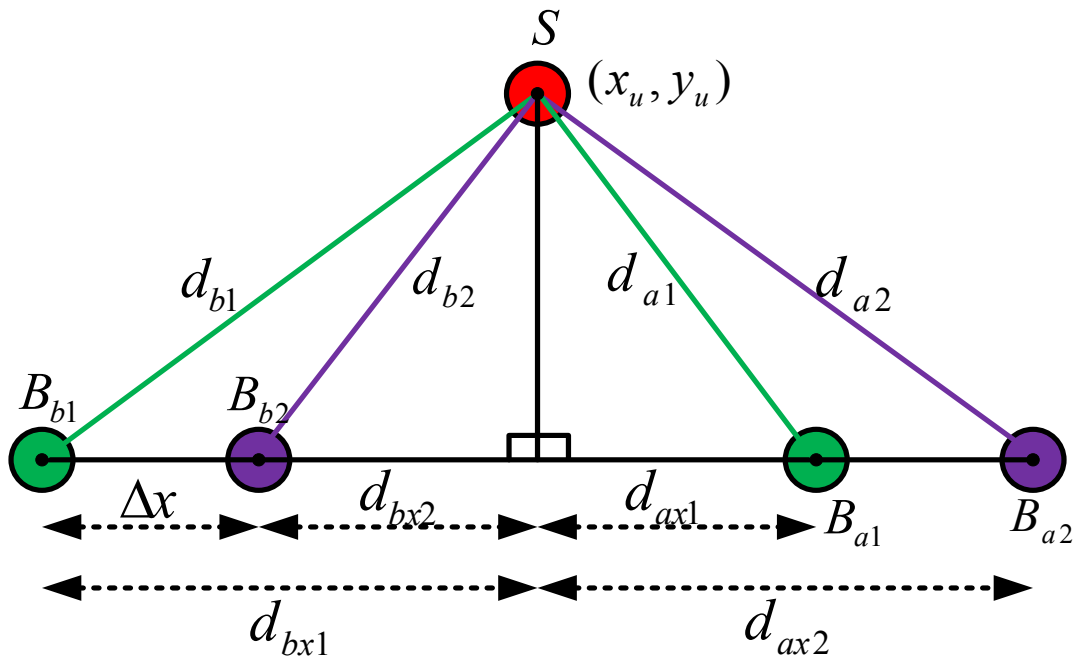


Figure 4.5-8 2-D-Two Sending Case Estimated Error Bounding Layout

Since the shortest distance between the sensor's location and the line between the beacons, which is on the x-axis, is the perpendicular line as shown in figure 4.5.8. The following equations control the estimated sensor position:

$$\left. \begin{aligned} d_{bx1}^2 + d_y^2 &= d_{b1}^2 \\ d_{bx2}^2 + d_y^2 &= d_{b2}^2 \end{aligned} \right\} d_{b1}^2 - d_{b2}^2 = d_{bx1}^2 - d_{bx2}^2$$



$$\left. \begin{aligned} d_{ax1}^2 + d_y^2 &= d_{a1}^2 \\ d_{ax2}^2 + d_y^2 &= d_{a2}^2 \end{aligned} \right\} d_{a2}^2 - d_{a1}^2 = d_{ax2}^2 - d_{ax1}^2$$

$$\left. \begin{aligned} d_{bx1}^2 + d_y^2 &= d_{b1}^2 \\ d_{ax1}^2 + d_y^2 &= d_{a1}^2 \end{aligned} \right\} d_{b1}^2 - d_{a1}^2 = d_{bx1}^2 - d_{ax1}^2$$

$$\left. \begin{aligned} d_{bx2}^2 + d_y^2 &= d_{b2}^2 \\ d_{ax2}^2 + d_y^2 &= d_{a2}^2 \end{aligned} \right\} d_{b2}^2 - d_{a2}^2 = d_{bx2}^2 - d_{ax2}^2$$

**Lemma:**

$$d_{b2}^2 - d_{a2}^2 = d_{bx1}^2 - d_{ax1}^2 - 2\Delta x D$$

**Proof:**

To find the square differences' relationship between the second and the first reading for before beacon, we can do the following:

$$\begin{aligned} d_{b2}^2 - d_{a2}^2 &= d_{bx2}^2 - d_{ax2}^2 = (d_{bx1} - \Delta x)^2 - (d_{ax1} + \Delta x)^2 \\ &= d_{bx1}^2 - 2\Delta x d_{bx1} + \Delta x^2 - d_{ax1}^2 - 2\Delta x d_{ax1} - \Delta x^2 \\ &= d_{bx1}^2 - d_{ax1}^2 - 2\Delta x (d_{ax1} + d_{bx1}) \\ &= d_{bx1}^2 - d_{ax1}^2 - 2\Delta x D \end{aligned}$$

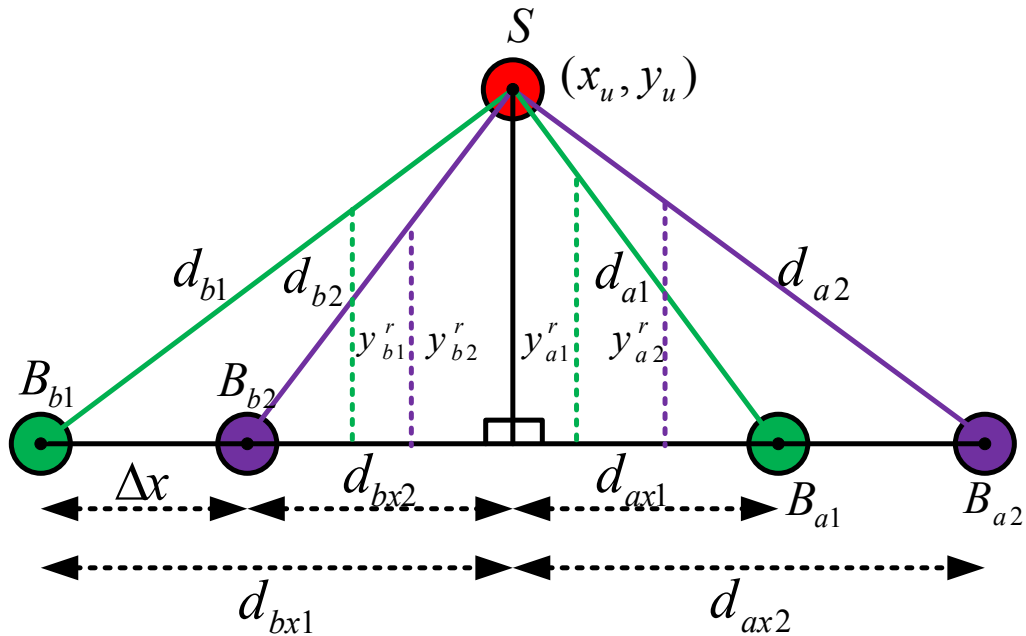


Figure 4.5-9 2-D-Two Sending Case Estimated Error Bounding using Similar Triangulation

### 4.5.3 Three-Dimensional Approach outlines

As considered in the two-dimension section above, we still hold the assumption that the reading taken from a beacon cannot be smaller than a partial part of a related distance and cannot be bigger than the distance itself. First, we must apply any necessary extension factors based on the altitude per process explained in Section 4.5.2 until both cones' sides are greater than their altitude. From this point, we compute estimated distances as illustrated in Section 4.3.3 resulting in two cones for each reading as illustrated in figure 4.5.10. Given the projections of two sets of concentric circles with some degrees of overlap, the problem can be considered in two dimensions per the methodology discussed in Section 4.5.2.

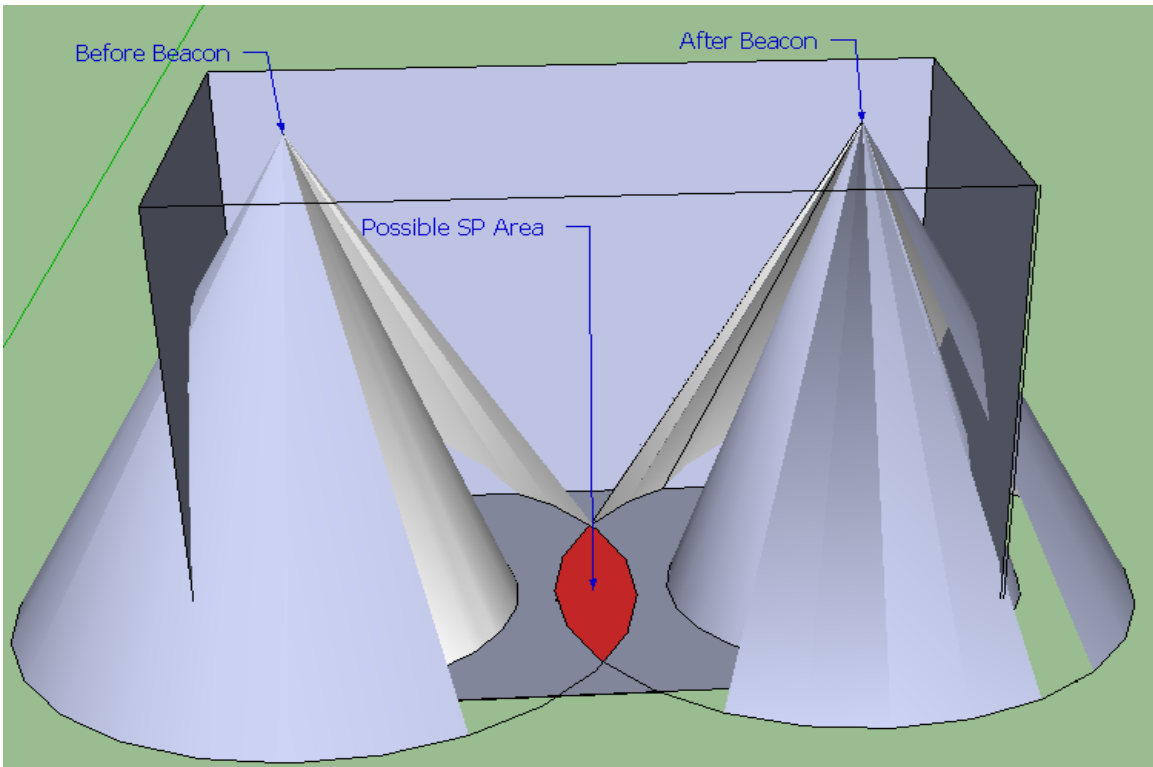


Figure 4.5-10 3-D-One Sending Case Estimated Error Bounding using Similar Cones

When we have multiple readings, just like in the 2D section, we once again try to minimize the area in which the sensor is located within the overlap of the 2 cones in the 3D model. Then, we can find the estimate sensor position's volume and calculate its estimated location regarding the nearest beacons. After that, we can find the estimated  $x$ , and  $y$  coordinates.

#### 4.6 Sensor Localization Using Bounded-Angle Method

This method is an offshoot of the bounded-error method that could serve as a substitute and may demonstrate quality as a supplement to that method. While it is known that certain regions incrementally fall outside of the area of certainty for sensor location through the process of further refinement, it must be noted that some of the area included

using the bounded-error method area actually unfeasible possible locations for the sensor due to the geometry of the problem. As the figure below illustrates. It is necessary that the angle created between the sensor and before-beacon and the before-beacon and location on the access of movement must increase with further readings taken after beacon movement. This is illustrated in table 2.

Table 2 Before Angles for different DX when D = 5

	$dy/dbxi$	$\theta_{bi}$	$\theta_{b(i+1)} - \theta_{bi}$	$dy/dbxi$	$\theta_{bi}$	$\theta_{b(i+1)} - \theta_{bi}$	$dy/dbxi$	$\theta_{bi}$	$\theta_{b(i+1)} - \theta_{bi}$
<b>Horizontal B</b> B step size =	1/5	11.309	2 5/7	2/5	21.801	4 3/4	3/5	30.963	6
	1/4	14.036	4 2/5	1/2	26.565	7 1/8	3/4	36.869	8 1/8
	1/3	18.434	8 1/8	2/3	33.690	11 1/3	1	45	11 1/3
	1/2	26.5651	18 3/7	1	45	18 3/7	1 1/2	56.309	15 1/4
	1	45	0	2	63.434		3	71.565	
<b>Horizontal B</b> step size = 2	1/5	11.309	7 1/8	2/5	21.801	11 8/9	3/5	30.963	14
	1/3	18.434	26 4/7	2/3	33.690	29 3/4	1	45	26 4/7
	1	45	0	2	63.434		3	71.565	0
<b>Horizontal B</b> B step size	1/5	11.309	15 1/4	2/5	21.801	23 1/5	3/5	30.963	25 1/3
	1/2	26.565	0	1	45	0	1 1/2	56.309	

The angles created by the after-beacon and its movement must decrease with movement. While having single-dimensional implications, this method is most appropriately applied to multi-dimensional cases.

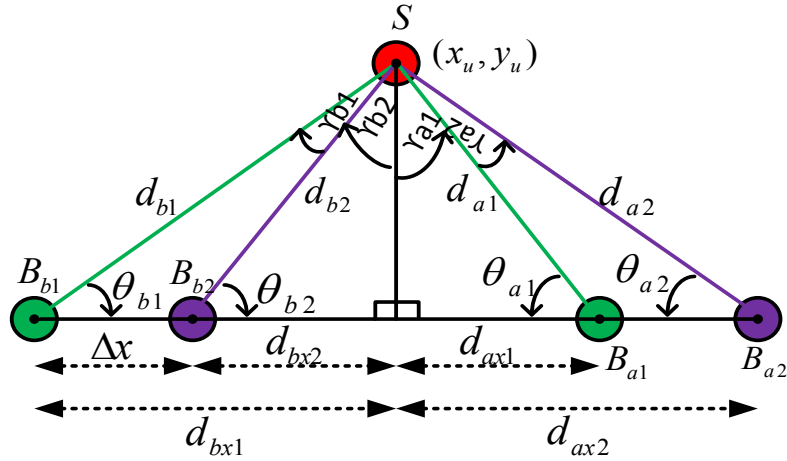


Figure 4.6-1 Angular Bounding Layout

From the figure above we can read:

$$\theta_{b(i+1)} \geq \theta_{bi}, \quad \theta_{a(j+1)} \leq \theta_{aj}$$

$$d_y = d_{bi} \sin \theta_{bi} = d_{aj} \sin \theta_{aj}$$

$$d_{r_{bi}} \sin \theta_{bi} \leq d_y \leq d_{bi} \sin \theta_{bi}$$

$$d_{r_{aj}} \sin \theta_{aj} \leq d_y \leq d_{aj} \sin \theta_{aj}$$

$$\gamma_{b2} = 90 - \theta_{b2}, \text{ and } \gamma_{b1} = 90 - \theta_{b1} - \gamma_{b2}$$

$$\gamma_{a1} = 90 - \theta_{a1}, \text{ and } \gamma_{a2} = 90 - \theta_{a2} - \gamma_{a1}$$

and from simulation results it's found that:

$$\theta_{bimin} \leq \theta_{bi} \leq \theta_{bimax}, \quad \theta_{aimin} \leq \theta_{ai} \leq \theta_{aimax}$$

The nature of the bounded-angle method is that of utilizing minimal and maximal possible angles for the direction of the sensor. This addresses a problem aspect not found in a single-dimensional case: the direction of the sensor for which we have obtained a distance measurement is unknown, but able to be bounded. It can readily be observed that

although the sensor could be placed on either side of the axis of movement due to a mirror property of the geometry, the addition of a third beacon or many other simple means could be utilized as a future effort to isolate the area of certainty to a single side of the axis of movement.

#### **4.6.1 The Relationship between Angles**

We know that the y-distance ( $dy$ ) is equal for the angles to the sensor of all before-and-after beacon broadcasts,  $S_{xmin}$  and  $S_{xmax}$  are respectively positioned after the last before-beacon ( $B_{bn}$ ) and before the first after-beacon ( $Ba1$ ), and the distance between these two beacons is  $\Delta x$ . Given these strong relationships, being able to constrain the angles from the beacons to the sensors would lead to greatly-increased accuracy of estimating the location of the sensor. In order to simplify the explanation of this process, we assume that the x-position of the sensor ( $S_x$ ) is known in order to explain the relationships between before-before-, after- after-, and before-after-beacon positions.

##### ***4.6.1.1 The Relationship Between Before Angles***

After computing minimum and maximum angles for all steps for each beacon, we can try to constrain these angles by finding relationships among them. Figure 4.6.1 shows the case of two readings.

$$\tan \theta_{b2} = \frac{dy}{d_{bx2}}, \tan \theta_{b1} = \frac{dy}{d_{bx1}}$$

$$\frac{\tan \theta_{b2}}{\tan \theta_{b1}} = \frac{d_{bx1}}{d_{bx2}} = \frac{d_{bx2} + \Delta x}{d_{bx2}} = 1 + \frac{\Delta x}{d_{bx2}}$$

$$\theta_{b2} = \text{atan}\left[\left(1 + \frac{\Delta x}{d_{bx2}}\right) * \tan(\theta_{b1})\right]$$

Similarly, we can find the relationships among  $\theta_{b3}$ ,  $\theta_{b4}$  and  $\theta_{b1}$

$$\frac{\tan \theta_{b3}}{\tan \theta_{b1}} = \frac{d_{bx1}}{d_{bx3}} = \frac{d_{bx3} + 2\Delta x}{d_{bx3}} = 1 + 2 \frac{\Delta x}{d_{bx3}}$$

$$\theta_{b3} = \text{atan}\left[\left(1 + 2 \frac{\Delta x}{d_{bx2}}\right) * \tan(\theta_{b1})\right]$$

$$\frac{\tan \theta_{b4}}{\tan \theta_{b1}} = \frac{d_{bx1}}{d_{bx4}} = \frac{d_{bx4} + 3\Delta x}{d_{bx4}} = 1 + 3 \frac{\Delta x}{d_{bx4}}$$

$$\theta_{b4} = \text{atan}\left[\left(1 + 3 \frac{\Delta x}{d_{bx4}}\right) * \tan(\theta_{b1})\right]$$

In general we can write the relationship between any  $\theta_{bi}$  and  $\theta_{bk}$  under the condition:  $k < i$  as follows:

$$\frac{\tan \theta_{bi}}{\tan \theta_{bk}} = \frac{d_{bk}}{d_{bxi}} = \frac{d_{bxk} + (i - k)\Delta x}{d_{bxi}} = 1 + (i - k) \frac{\Delta x}{d_{bxi}}$$

$$\theta_{bi} = \text{atan}\left[\left(1 + (i - k) \frac{\Delta x}{d_{bxi}}\right) * \tan(\theta_{bk})\right] \quad (4.24)$$

#### 4.6.1.2 The Relationship Between After Angles

We can identify similar relationships regarding after-beacon angles.

$$\tan \theta_{a2} = \frac{d_y}{d_{ax2}}, \quad \tan \theta_{a1} = \frac{d_y}{d_{ax1}}$$

$$\frac{\tan \theta_{a2}}{\tan \theta_{a1}} = \frac{d_{ax1}}{d_{ax2}} = \frac{d_{ax1}}{d_{ax1} + \Delta x}$$

Or

$$\theta_{a2} = \text{atan}\left[\left(\frac{d_{ax1}}{d_{ax1} + \Delta x}\right) * \tan(\theta_{b1})\right]$$

Similarly, we can find the relationship among  $\theta_{a3}$ ,  $\theta_{b4}$  and  $\theta_{a1}$

$$\frac{\tan \theta_{a3}}{\tan \theta_{a1}} = \frac{d_{ax1}}{d_{ax3}} = \frac{d_{ax1}}{d_{bx1} + 2\Delta x}$$

or

$$\theta_{a3} = \text{atan}\left[\frac{d_{ax1}}{d_{bx1} + 2\Delta x} * \tan(\theta_{a1})\right]$$

$$\frac{\tan \theta_{a4}}{\tan \theta_{a1}} = \frac{d_{ax1}}{d_{ax4}} = \frac{d_{ax1}}{d_{ax4} + 3\Delta x}$$

or

$$\theta_{a4} = \text{atan}\left[\frac{d_{ax1}}{d_{ax4} + 3\Delta x} * \tan(\theta_{a1})\right]$$

In general we can write the relationship between any  $\theta_{aj}$  and  $\theta_{al}$  under the condition:

$j < l$  as follows:

$$\frac{\tan \theta_{aj}}{\tan \theta_{al}} = \frac{d_{axl}}{d_{axj}} = \frac{d_{axl}}{d_{axj} + (j-l)\Delta x}$$

or

$$\theta_{aj} = \text{atan}\left[\left(\frac{d_{axl}}{d_{axj} + (j-l)\Delta x}\right) * \tan(\theta_{al})\right] \quad (4.25)$$

#### 4.6.1.3 The Relationship between Before and After Angles

Now all that remains is to establish the critical, connecting relationships between before and after angles.



$$\tan \theta_{bi} = \frac{d_y}{d_{bxi}}, \tan \theta_{aj} = \frac{d_y}{d_{axj}}$$

$$\frac{\tan \theta_{bi}}{\tan \theta_{aj}} = \frac{d_{axj}}{d_{bxi}} = \frac{B_{aj} - S_x}{S_x - B_{bi}}$$

Or

$$\theta_{bi} = \text{atan}\left[\left(\frac{B_{aj} - S_x}{S_x - B_{bi}}\right) * \tan(\theta_{aj})\right] \quad (4.26)$$

In the case of  $i = j$  and considering the position of  $S_x$ , we can determine if  $\theta_{bi}$  is greater than, equal to, or smaller than  $\theta_{aj}$ . There are several important points to consider when determining these relationships between before and after beacons.

- *The middle point*

$$S_x = \frac{B_{bi} + B_{ai}}{2}$$

*Lemma*  $\theta_{bi} = \theta_{ai}$

*Proof:*

$$\frac{\tan \theta_{bi}}{\tan \theta_{ai}} = \frac{d_{axi}}{d_{bxi}} = \frac{B_{ai} - S_x}{S_x - B_{bi}} = \frac{B_{ai} - \frac{B_{bi} + B_{ai}}{2}}{\frac{B_{bi} + B_{ai}}{2} - B_{bi}} = \frac{B_{ai} - B_{bi}}{B_{ai} - B_{bi}} = 1$$

$$\tan \theta_{bi} = \tan \theta_{ai}$$

Or

$$\theta_{bi} = \text{atan}[\tan \theta_{ai}] = \theta_{ai}$$

- *The first half-distance interval*

$$S_x < \frac{B_{bi} + B_{ai}}{2}$$

Here, the y-distance ( $d_y$ ) is equal for both angles and  $S_x$  is located in the first half of the region ( $\Delta x$ ) between  $d_{axi}$  and  $d_{bxi}$ , This means that  $d_{axi} > d_{bxi}$  and

$$\frac{B_{ai} - S_x}{S_x - B_{bi}} > 1$$

and

$$\tan \theta_{bi} > \tan \theta_{ai}$$

As a result

$$\theta_{bi} > \theta_{ai}$$

- *The second half distance interval*

$$S_x > \frac{B_{bi} + B_{ai}}{2}$$

Similarly, but opposite, this case means that  $d_{axi} < d_{bxi}$  and

$$\frac{B_{ai} - S_x}{S_x - B_{bi}} < 1$$

and

$$\tan \theta_{bi} < \tan \theta_{ai}$$

As a result

$$\theta_{bi} < \theta_{ai}$$

#### 4.6.2 Problem Transform From 2-D to 1-D and X Coordinate Estimation

After constraining the angles as much as possible, we can compute the new  $rb_{minn}$ ,  $rb_{maxn}$ ,  $ra_{minn}$ , and  $ra_{maxn}$  as follows:

$$d_{b1min} = \frac{d_{rb}}{1-r_{bnmin}} \text{ or } r_{bnmin} = 1 - \frac{d_{rb}}{d_{b1min}}$$

$$d_{b1max} = \frac{d_{rb}}{1-r_{bnmax}} \text{ or } r_{bnmax} = 1 - \frac{d_{rb}}{d_{b1max}}$$

Given these constrained distances, we can utilize the concepts from our one-dimensional analysis for computing the minimum and maximum values for each reading in the x-space ( $d_{rbxmin}$ ,  $d_{rbxmax}$ ,  $d_{riaxmin}$ , and  $d_{riaxmax}$ ) and then perform some calculations to estimate the x-coordinate of the sensor.

$$d_{ribxmin} = d_{ribx} * \tan \theta_{bimax}$$

$$d_{ribxmax} = d_{ribx} * \tan \theta_{bimin}$$

$$d_{riaxmin} = d_{riax} * \tan \theta_{aimax}$$

$$d_{riaxmax} = d_{riax} * \tan \theta_{aimin}$$

After computing all readings in x-space, we can calculate all of their corresponding estimated distances using the newly-computed  $r_{bmin}$ ,  $r_{bmax}$ ,  $r_{amin}$ , and  $r_{amax}$ .

$$\hat{d}_{ibxminmin} = \frac{d_{ribxmin}}{(1 - r_{bmin})}$$

$$\hat{d}_{ibxminmax} = \frac{d_{ribxmin}}{(1 - r_{bmax})}$$

$$\hat{d}_{ibxmaxmin} = \frac{d_{ribxmax}}{(1 - r_{bmin})}$$

$$\hat{d}_{ibxmaxmax} = \frac{d_{ribxmax}}{(1 - r_{bmax})}$$

In the same way, we can compute all corresponding estimated distances for after beacons.

$$\hat{d}_{iaxminmin} = \frac{d_{riaxmin}}{(1 - r_{aminn})}$$

$$\hat{d}_{iaxminmax} = \frac{d_{riaxmin}}{(1 - r_{amaxn})}$$

$$\hat{d}_{iaxmaxmin} = \frac{d_{riaxmax}}{(1 - r_{aminn})}$$

$$\hat{d}_{iaxmaxmax} = \frac{d_{riaxmax}}{(1 - r_{amaxn})}$$

By comparing these estimated readings with  $S_{xmin}$  and  $S_{xmax}$ , we were able to constrain  $S_{xmin}$  and  $S_{xmax}$  along with  $d_{rbxmin}$  and  $d_{rbxmax}$  and  $d_{raxmin}$ , and  $d_{rbxmax}$ . Finally we can estimate the x-coordinate of the sensor location ( $S_{xi}$ ) as we did in Section 4.5.1 and then compute the estimated reading distances in the x-space  $\hat{d}_{ribx}$  and  $\hat{d}_{riax}$ .

#### 4.6.3 Problem Retransform From 1-D to 2-D and Y-Coordinate Estimation

After computing the estimated reading distances in the x-space  $\hat{d}_{ribx}$ , and  $\hat{d}_{riax}$ , we are now able to calculate the estimated angles for all sensors in the field for each reading as follows:

$$\hat{\theta}_{ib} = \text{acos}\left(\frac{\hat{d}_{ribx}}{d_{rib}}\right)$$

$$\hat{\theta}_{ib} = \text{acos}\left(\frac{\hat{d}_{riax}}{d_{ria}}\right)$$

By finding the intersection points of rays drawn using these angles originating at their corresponding beacons, we can identify several estimated sensor locations for each sensor. By averaging the x- and y-coordinates of these estimated locations, we can arrive at an estimated location for each sensor that is of high accuracy.

What follows are the flow chart and corresponding algorithm that are preliminarily suggested for this work. While some proof of concept tests have been used to perform an initial feasibility and solidity evaluation of these attempts, it is a necessary task to verify their uses through simulation and refine them as necessary.

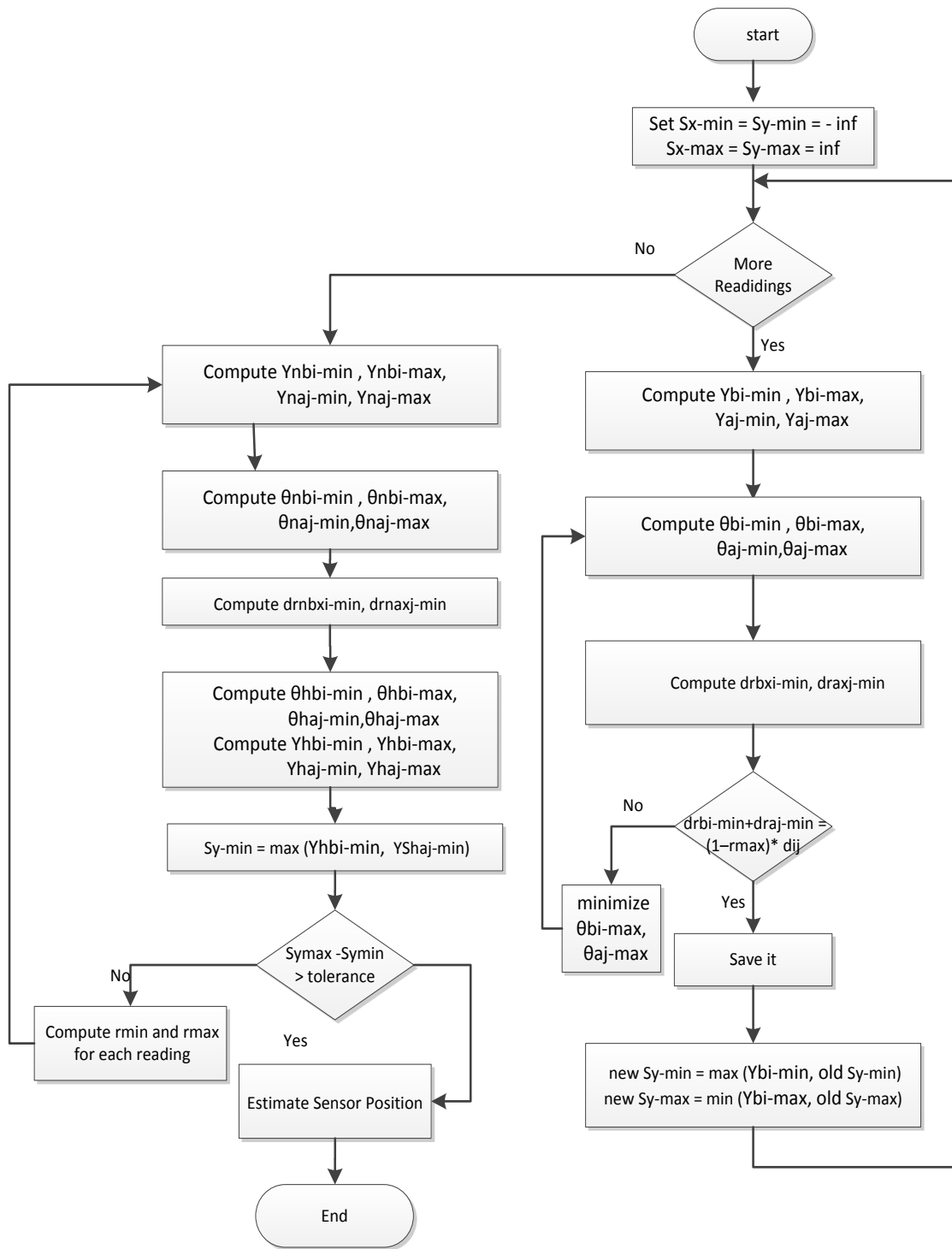


Figure 4.6-2 Flow Chart for Angular Bounding Method Algorithm

Angular Bounding Algorithm (ABA):

- 1- Compute all  $y_{bimin}$  and  $y_{bimax}$

$$y_{bimin} = y_{aimin}, y_{bimax} = y_{aimax}$$

- 2- Find all angles  $\theta_{bimin}$ ,  $\theta_{bimax}$ ,  $\theta_{aimin}$ , and  $\theta_{aimax}$

$$\theta_{bimin} = \tan^{-1}\left(\frac{y_{bimax}}{x_{y_{bimax}}}\right), \theta_{aimin} = \tan^{-1}\left(\frac{y_{aimax}}{x_{y_{aimax}}}\right),$$

$$\theta_{bimax} = \tan^{-1}\left(\frac{y_{bimin}}{x_{y_{bimin}}}\right), \theta_{aimax} = \tan^{-1}\left(\frac{y_{aimin}}{x_{y_{aimin}}}\right)$$

- 3- Compute the sum of  $dr_{bixmin} + dr_{aixmin}$ ,  $dr_{bixmax} + dr_{aixmax}$

$$\text{Where } dr_{bixmin} = dr_{bi} \cos \theta_{bimax}, dr_{aixmin} = dr_{ai} \cos \theta_{aimax}$$

$$dr_{bixmax} = dr_{bi} \cos \theta_{bimin}, dr_{aixmax} = dr_{ai} \cos \theta_{aimin}$$

- 4- If  $dr_{bixmin} + dr_{aixmin} \geq (1 - r_{max})D$ ,  $dr_{bixmax} + dr_{aixmax} \geq D$  store them  
Else delete them

- 5- Find the new angles  $\theta_{binmin}$ ,  $\theta_{binmax}$ ,  $\theta_{ainmin}$ , and  $\theta_{ainmax}$

$$\theta_{binmin} = \tan^{-1}\left(\frac{\max(y_{bimax})}{x_{y_{bimax}}}\right), \theta_{ainmin} = \tan^{-1}\left(\frac{\max(y_{aimax})}{x_{y_{aimax}}}\right),$$

$$\theta_{binmax} = \tan^{-1}\left(\frac{\min(y_{bimax})}{x_{y_{bimin}}}\right), \theta_{ainmax} = \tan^{-1}\left(\frac{y_{aimin}}{x_{y_{aimin}}}\right)$$

- 6- Compute the sum of  $d_{rbinxmin} + d_{rainxmin}$ ,  $d_{rbinxmax} + d_{rainxmax}$

- 7- Apply the bounding algorithm for 1D

- 8- Compute the new angles

- 9- Solve for x, and y

#### 4.6.4 Three-Dimensional Approach Outlines

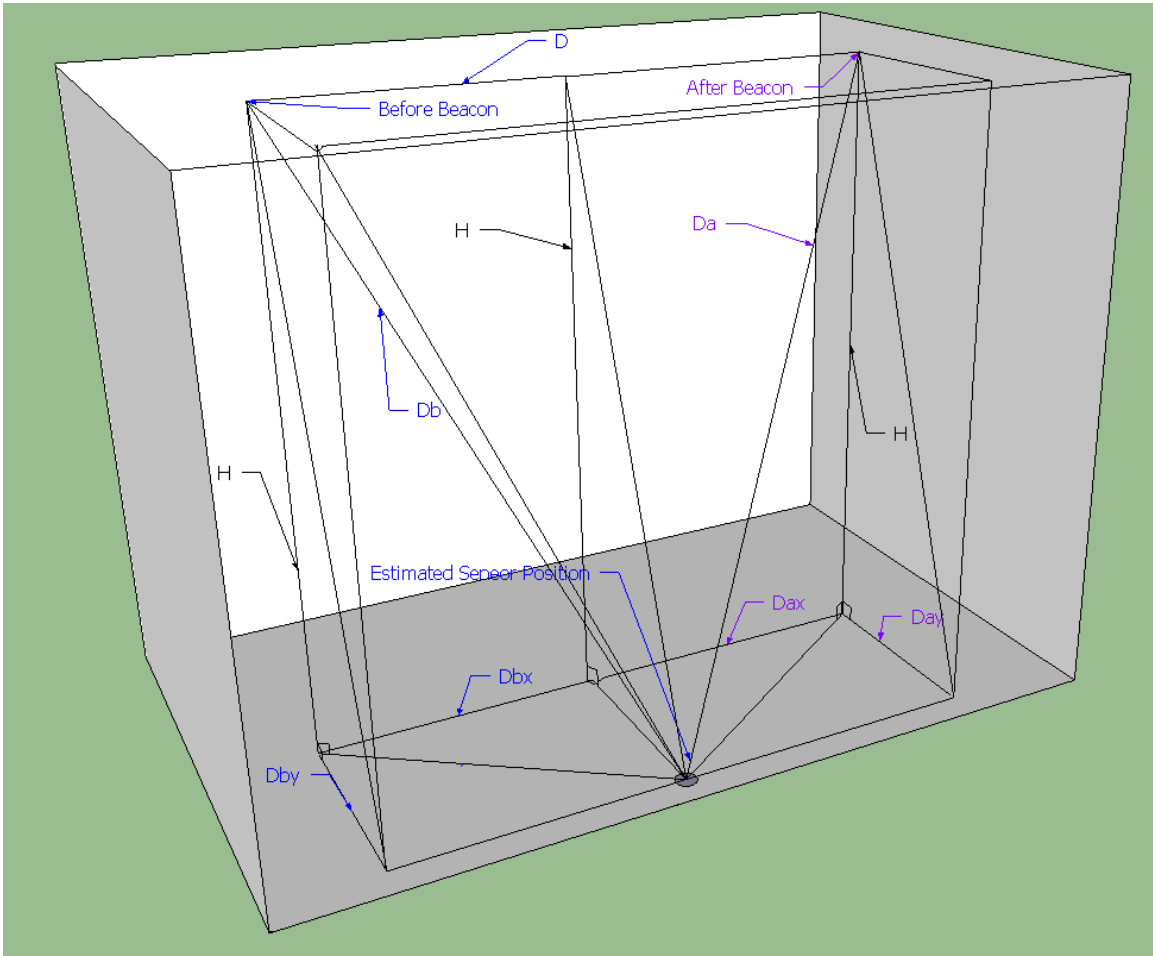


Figure 4.6-3 3-DAngular Bounding Method Layout

As noted before, the angular bounding method is a developed method of estimated error. After determining the volume or in some cases the area, we can once more minimize the bounded volume, or the bounded area, by using the relationships between the angles as illustrated in the previous section.

$$D_b^2 = D_{bx}^2 + D_{by}^2 + H^2$$

$$D_a^2 = D_{ax}^2 + D_{ay}^2 + H^2$$



## 4.7 Mobile Beacons Trajectory

In regards to the paths taken by mobile-beacon-carrying vehicles for purposes of field coverage, there are many possible options. Figure 4.7.1 illustrates what is known as the Sparse-Straight-Line (SSL) movement pattern, which is shown in Figure. This pattern is typically unable to localize every sensor node due to its broad vertical spacing. The second figure, figure 4.7.2 illustrates the Dense-Straight-Line (DSL) movement pattern. The methods developed for this dissertation utilize this pattern to ensure the highest-likelihood of complete sensor network localization. The use of these patterns allows for both horizontal and vertical isolation of broadcast steps so that the information gained as a result of such broadcasts is uniform in spacing and able to be subjected to mathematical analyses that take advantage of this fact [55, 56].

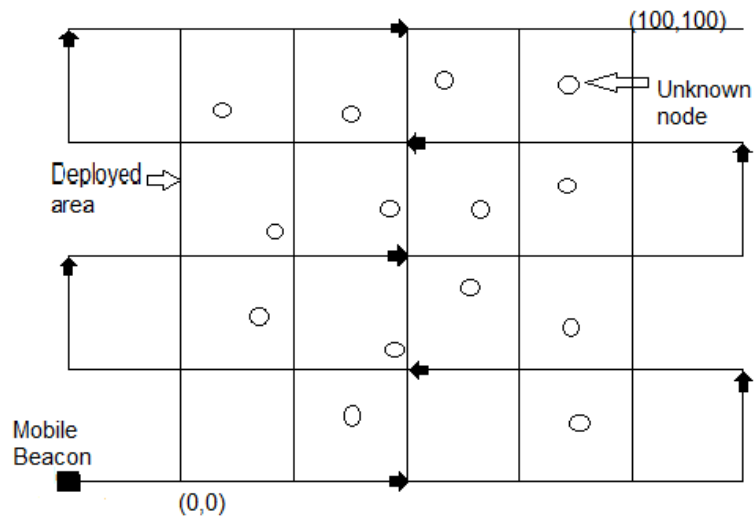


Figure 4.7-1 SSL Mobile Trajectory

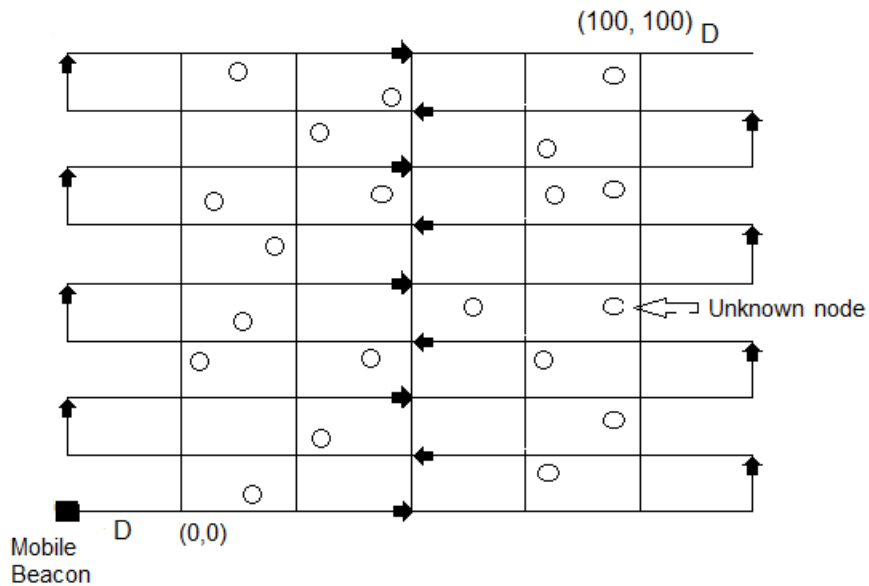


Figure 4.7-2 DSL Mobile Trajectory

#### 4.8 Measurement-Error Ratio Distribution Assumptions

Two different forms of measurement-error ratio distribution were considered for this dissertation. Both were considered over an adjustable segment within the range from 0 to 1.0 with the values within this range being missing portions of the distance-measurements calculated based on beacon broadcasts. The first distribution was that of a uniform distribution, which considers all parts of the segment from which measurement-error ratios were drawn to be equally-likely. Based on this assumption, the localization methods leveraged during simulation considered the final localization positions within their bounded regions to be equally-likely. This assumption no longer held when considering a Gaussian distribution, which considers the segment from which measurement-error ratios were drawn to be normally-likely with mean focused at the center of the segment. The construction of such a constrained, normal distribution

required that four standard deviations in the positive and negative directions from the mean be fitted within the segment with the remaining, highly-unlikely tails of the distribution being truncated to zero probability. Under the Gaussian assumption, the localization methods leveraged during simulation, being aware of the initial segment and distribution of measurement-error ratios, considered sensor positions closer to the Gaussian mean to be of much greater likelihood than those further from the mean. This created a considerable effect when the mean was eliminated as a possibility based on the efforts of the localization methods.

## **Chapter Five: Simulation and results of Sensor Localization**

### **5.1 Introduction**

In the previous chapter we discussed various mathematical models and methods for estimated sensor locations. The models that we established were proven based on the localization problem definitions established previously and fundamentals of trigonometry and mathematical relationships. While the methods suggested are firmly-grounded in proof, what remains is to measure the magnitude of success of the application of these methods. It would theoretically be possible to use algorithmic and proof-based methods to establish accuracy given the definitions and constraints established. However, doing so would be tedious and prone to error and skepticism. It is for these reasons that we opted to develop a means of gathering concrete, objective proof capable of being subjected to theoretical and statistical scrutiny. In establishing such a means, there are several principles aspects to be mentioned, the first of which is the definition of magnitude of correctness.

Given that the nature of the localization problem is in identifying the locations of sensors, the logical conclusion to measuring correctness of a localization method is in measuring the error of identifying the locations of large bodies of randomly-located sensors. While this would be possible to do in a real-world scenario given the proper equipment and experimental arrangements, for the scope of this work such an endeavor would have been extremely inefficient and cost-prohibitive. Thus, for this research, we

designed a fully-featured simulation environment for placing large arrays of sensors in a virtual field and a virtual set of beacons to traverse this field. Because the base-information utilized by all of the suggested methods in this work is the same, we were able to achieve high efficiency in implementation by passing the gathered beacon information for each sensor to each implemented method to simultaneously gather individual results. The obviously-desired result of each method is a single, definitive estimated location for each sensor in the field. Given these goals and constructions, we next must establish the parameters of consideration.

The parameters utilized for our simulation were those that were deemed to produce obvious effects on the outcome of sensor localization based upon the models discussed in the previous chapters. These specifically include:

- Step Size in the Direction of Travel (DX)
- Step Size Perpendicular to the Direction of Travel (DY)
- Separation of Beacons (D)
- Broadcast Angle of Beacons (A)
- Communication Range of Beacons (C)
- Number of Sensors (Sensors)
- Minimum Measurement Error (RMIN)
- Maximum Measurement Error (RMAX)

Given these parameters, we established the following gathered results:

- Mean Error (for each method)
- Minimum Error (for each method)

- Maximum Error (for each method)
- Mean Sensors Detected
- Minimum Sensors Detected
- Maximum Sensors Detected

In order to accurately and efficiently administer the necessary parameters to our simulation and gather the requisite results, a separate result-gathering environment was developed to administer set numbers of trials per each set of parameters and encapsulate execution of the simulation environment. This allowed for the execution of many random trials with each desired set of parameters in order to perform statistical averaging to minimize the effects of random occurrences that might unduly benefit or harm the results being gathered. Because our primary concern was the mean and range of effectiveness of sensor localization, the gathered-results were tailored as such. Once we gathered the desired results, we next needed to present them in a meaningful and analytical way.

Although tabular results would have sufficed for proof of concept, we felt that detailed graphical results would much more effectively lend themselves to proper analysis and reveal characteristics specific to each method that might be left unnoticed in a tabular form. Thus, we created an automated graphing environment to effectively and efficiently display the encapsulated results of the result-gathering environment. The results of this effort are displayed liberally throughout this chapter.

It should be kept in mind that results were gathered for both one-dimensional and two-dimensional variations of each method. We strongly believe that future expansion to three dimensions would be able to utilize the same foundations and tools established and

designed for this work. When displaying actual simulated fields in graphical form throughout this chapter, it should be noted that beacon locations are denoted by an “x” and sensor locations are denoted by an “o”. The model’s performance depends on whether or not the beacon separation distance is less than or equal to a meter.

## **5.2 1-D- Methods**

The software used in this Section was the Matlab 7.8. In it, we used a line length of 500 units. We distributed 100 nodes randomly and their localization job is to receive and gather beacon signals and then send them back to the system but with an addition of their ID information. In this section, there are three methods: Rough, Magnitude Bounding, and Error Bounding; we will compare all of the methods with each other and they will be analyzed profoundly with different parameter values. The communication range of beacons is equal to the beacons’ separation distance to ensure all sensors are detected. To obtain more average accuracy for the mean error, we run the simulation programs 50 times.

### 5.2.1 Rough Method

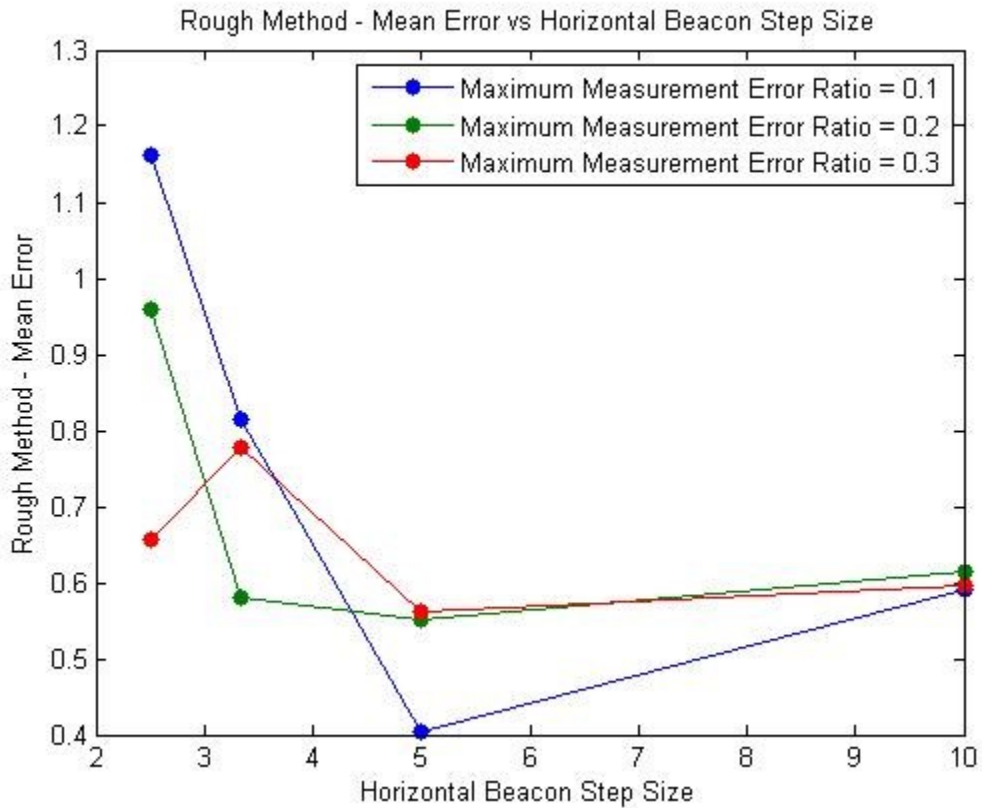


Figure 5.2-1 Accuracy of Rough Method vs  $\Delta x$  for different  $R_{max}$ 's

At the Horizontal Beacon Step Size of 2.5 units ( $D/4$ ), all of the Maximum Measurement Error Ratios ( $R_{max}$ ) had different mean errors; more specifically, the 0.1  $R_{max}$  had a mean error of approximately 1.18 units while the 0.2  $R_{max}$  had a mean error of about 1 units and the 0.3  $R_{max}$  had a mean error of approximately 0.7 units. Then the 0.1 and the 0.2  $R_{max}$ s rapidly dropped while the 0.3  $R_{max}$  increased. After that, all 3  $R_{max}$ s decreased, and then they all increased again all reaching almost the same mean error value of 0.6 units.



The previous figure, figure 5.2.1, shows the rough method's mean error vs the horizontal beacon step sizes for different  $R_{\max}$ s while the following figure, figure 5.2.2, also shows the rough method's mean error vs horizontal beacon step sizes but it will demonstrate it by testing different beacon separation distances.

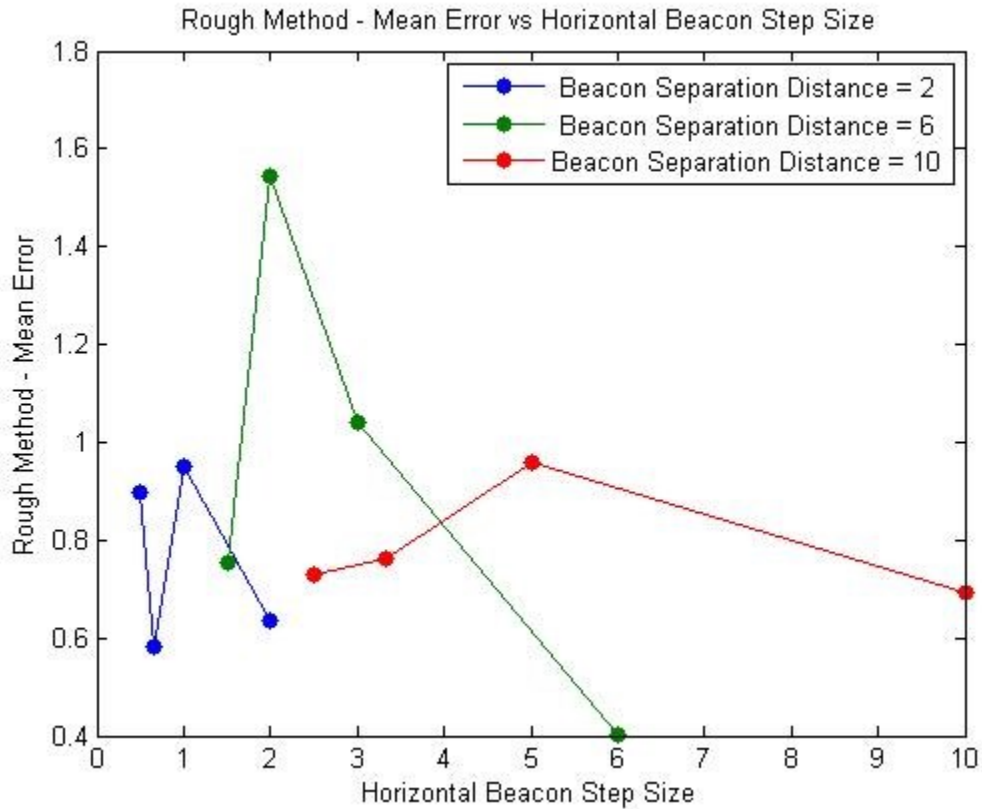


Figure 5.2-2 Accuracy of Ruogh Method vs  $\Delta x$  for different D's

The rough method's mean error fluctuates 0.59 and 1 for the beacon with a separation distance of 2. For the beacon with the separation distance of 6, the mean error is approximately 0.75 units when the horizontal beacon step size is  $6/4$  and then rises to its peak of approximately 1.6 units and decreases sharply afterwards a mean error of 1 at  $D/2$ . It then continues to decrease but does so at a far less rapid rate reaching its lowest

mean error of 0.4 units at the step size of 6. The beacon with the separation distance of 10 starts out with a mean error of approximately 0.7 units and then increases and then increases slightly between the step size of 2.5-3.5; after that it continues to increase but at a faster rate than before reaching its peak at the step size of 5 and then decreases reaching a mean error of 0.7 by the step size of 10.

To sum up, there's no specific rule for the mean error as a function in the horizontal beacon step size and for different  $D_s$  and  $R_{max}$ s. This is because the rough method depends on the actual reading distances as explained in Section 4.3.1.

### 5.2.2 Magnitude Bounding Method

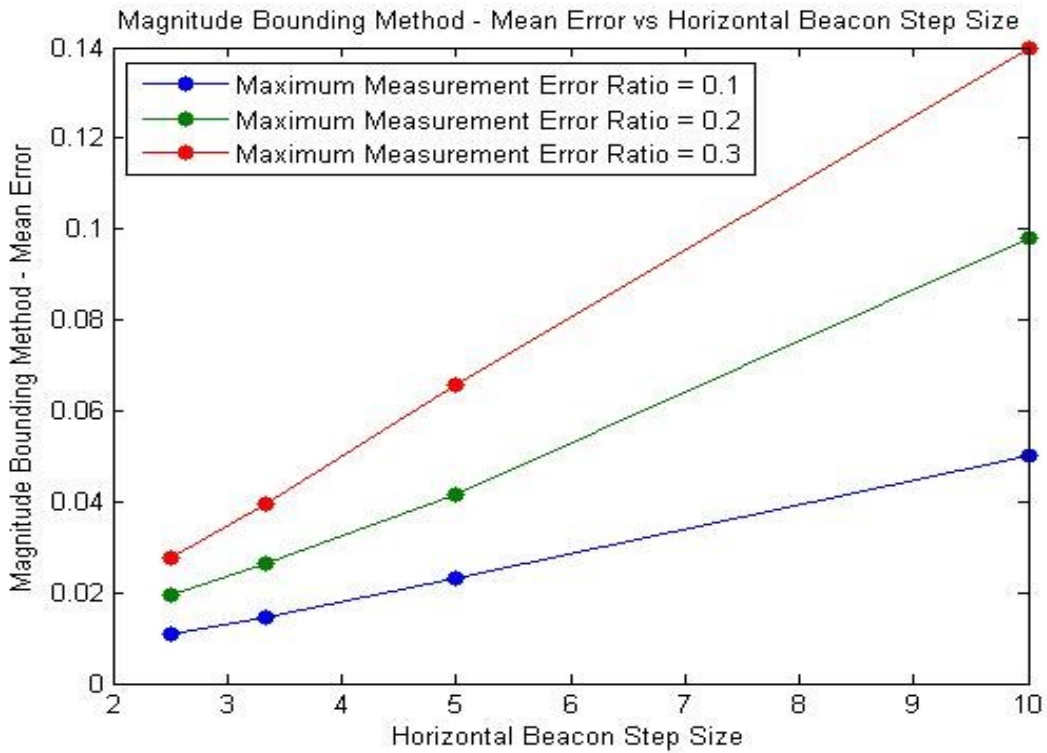


Figure 5.2-3 Accuracy of Magnitude Bounding Method for different  $R_{max}$ 's

Overall, all the 3  $R_{\max}$ s increased. Each of the  $R_{\max}$ s increased at almost a constant rate, making the relationship between the horizontal beacon step size and the mean error seem like a linear one. At the horizontal beacon step size of  $D/4$ , the 0.3  $R_{\max}$  had the highest mean error at 0.03 units while the 0.2  $R_{\max}$  had a mean error of 0.02 and the 0.1  $R_{\max}$  had a mean error of 0.01. They all increased but at different rates; the 0.3  $R_{\max}$  increased with the most rapid rate reaching a mean error of about 0.04 units while the 0.2  $R_{\max}$  increased to a mean error of approximately 0.03 units and the 0.1  $R_{\max}$  increased to a mean error of 0.015 units. Then, they all continued to increase at the same rate they increased by before.

The prior figure, figure 5.2.3, demonstrates the mean error's relationship with the horizontal beacon step size for the Magnitude Bounding method by testing different  $R_{\max}$ s while the following figure, figure 5.2.4, will demonstrate the same relationship but it will do so by testing different beacon separation distances.

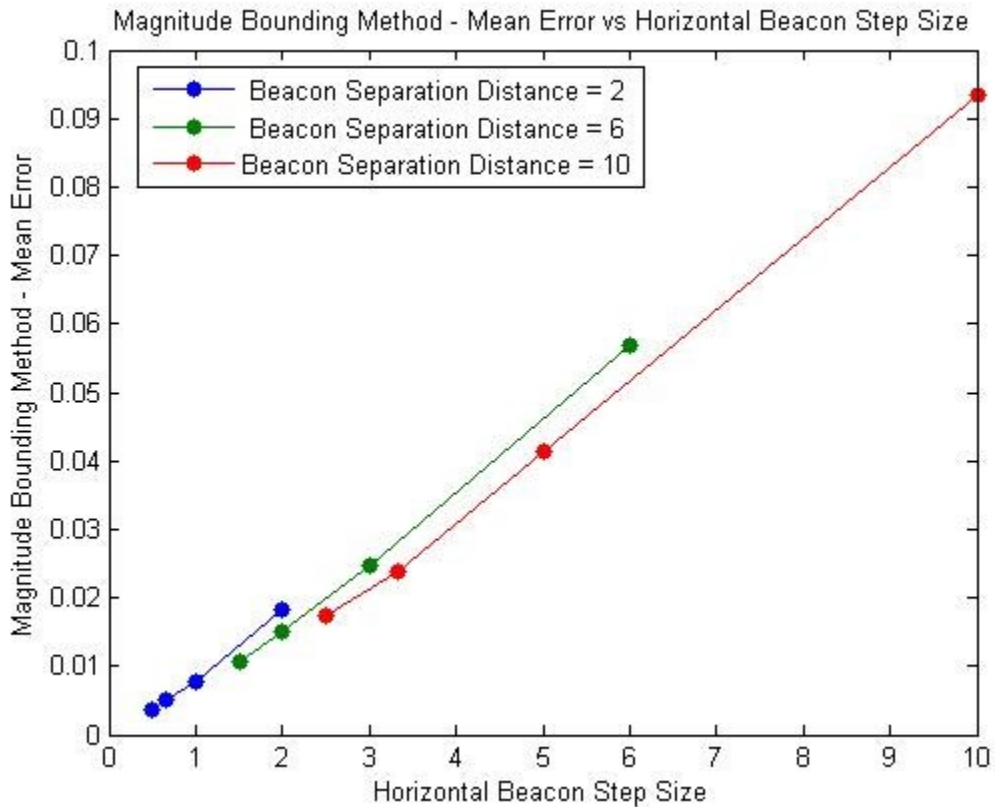


Figure 5.2-4 Accuracy of Magnitude Bounding Method for different D's

In contrast to the rough method, the magnitude bounding method's mean error depends on the beacon separation distance and the horizontal beacon step size. It's clearly demonstrated that the smaller the distance, the smaller the mean error and that the higher the horizontal beacon step size, the higher the mean error.

### 5.2.3 Error Bounding Method

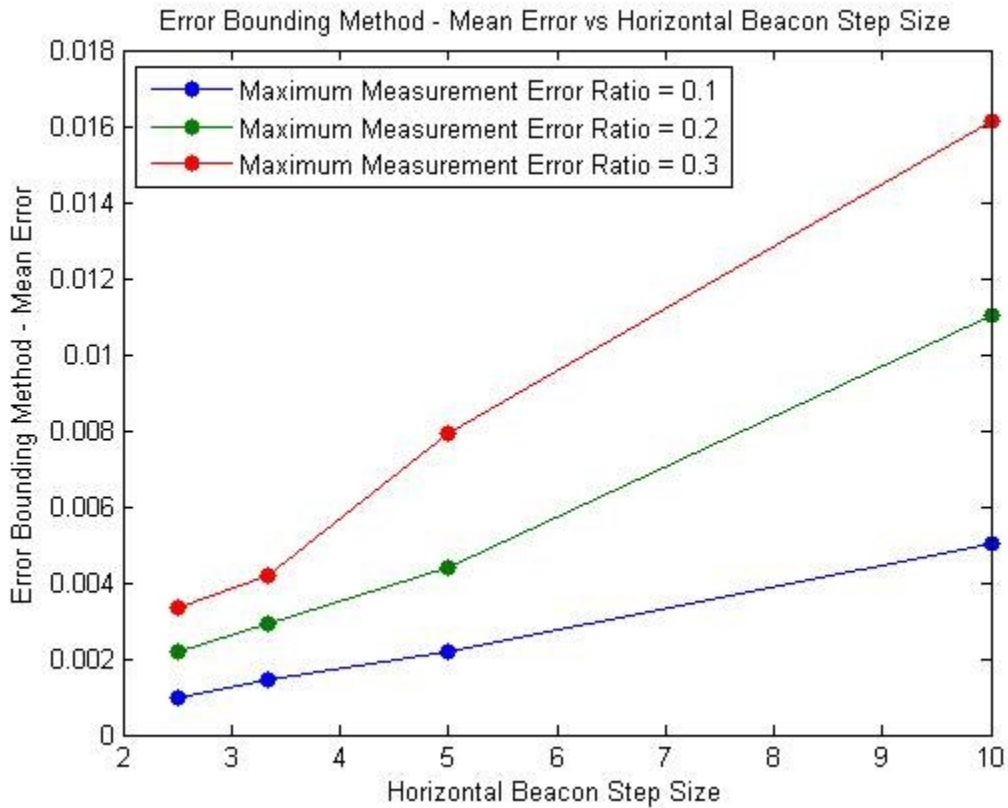


Figure 5.2-5 Accuracy of Error Bounding Method for different  $R_{\max}$ 's

In general, all of the 3  $R_{\max}$ s increased at the same rate for the horizontal beacon step sizes of 2.5-3.5. The 0.1  $R_{\max}$  was the only  $R_{\max}$  that remained almost stable at this rate throughout all of the step sizes. The 0.2  $R_{\max}$ , on the other hand, changed its rate of growth becoming more rapid every time as the step size increased while the 0.3 step size seemed to grow at a rapid rate but then started to grow at a less rapid rate at the step size of 5.

Figure 5.2.5 shows the error bounding method's mean error vs the horizontal beacon step size by testing different  $R_{\max}$ , while the following figure, figure 5.2.6, will

look at the same relationship between the mean error and the horizontal beacon step size but by testing beacon separation distances instead.

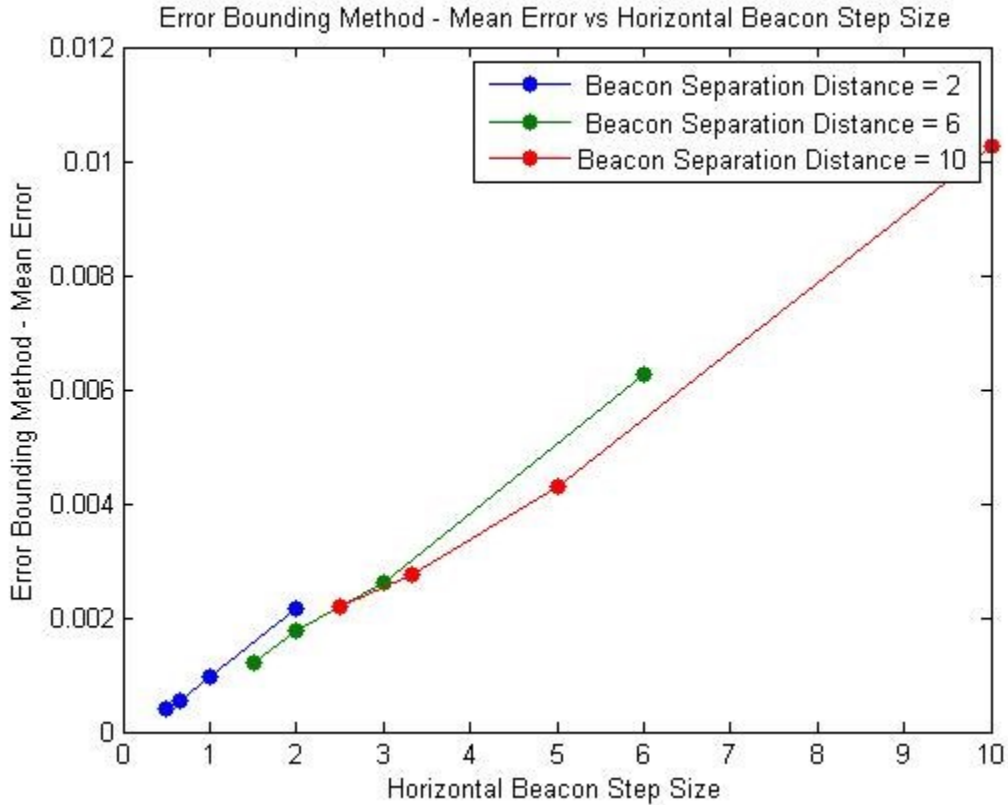


Figure 5.2-6 Accuracy of Error Bounding Method vs DX

Like the magnitude bounding method's mean error, the error bounding method's mean error depends on  $D$  and the horizontal beacon step size but has a much smaller range of mean errors because the bounding values ( $S_{x_{min}}$  and  $S_{x_{max}}$ ) are determined by the before and after beacons as illustrated in Section 4.5.1.

### 5.3 2-D-Methods

In this Section, we used the same software that was used in section 5.2 with the 1D method, but instead of using a 500 unit field, we used a square field with the length of

100 units. The simulation codes are run 50 times as in 1-D to obtain high average accuracy.

### 5.3.1 Finding the Best Beacon Transmission Angle

The three following figures illustrate the sensor detection as a function of different transmission angles (15, 30, 45, 60, 75, 90) for diverse  $R_{max}$ 's (0.1, 0.2, 0.3) respectively.

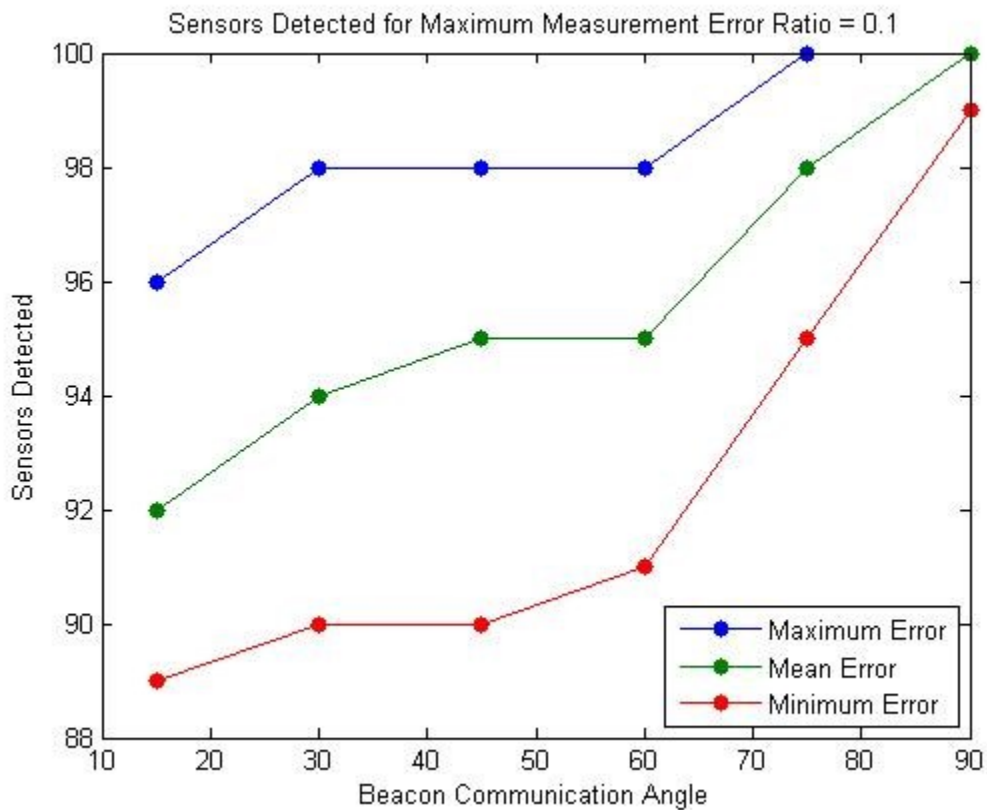


Figure 5.3-1 Sensor Detection for  $R_{max} = 0.1$

Figure 5.3.1 shows the number of minimum, maximum, and mean sensors detected when the maximum measurement error ratio is 0.1 as a function of the beacon communication angle. In general, the figure demonstrates that the higher the beacon

communication angle, the higher the sensor detection. The minimum sensor detection is 87 of all distributed sensors.

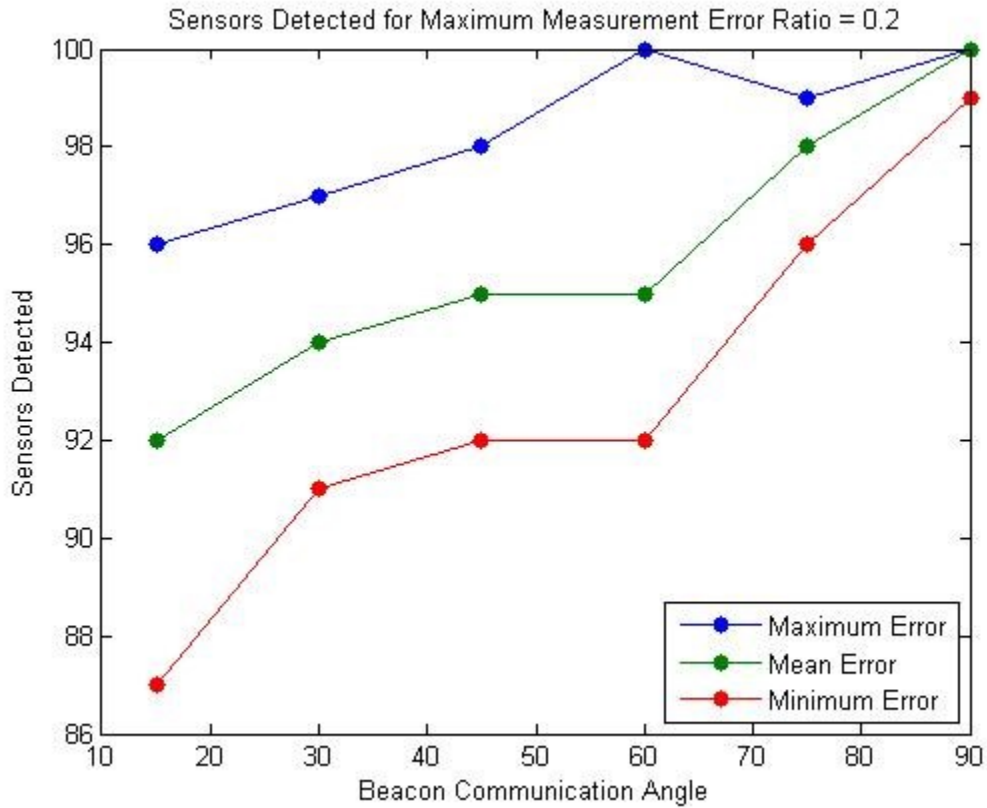


Figure 5.3-2 Sensor Detection for  $R_{\max} = 0.2$

The figure 5.3.2 also shows the number of minimum, maximum, and mean sensors detected when the maximum measurement error ratio is 0.2 as a function of the beacon communication angle. For the most part, the figure illustrates that the higher the beacon communication angle, the higher the sensor detection. The minimum sensor detection is 87 of all distributed sensors.



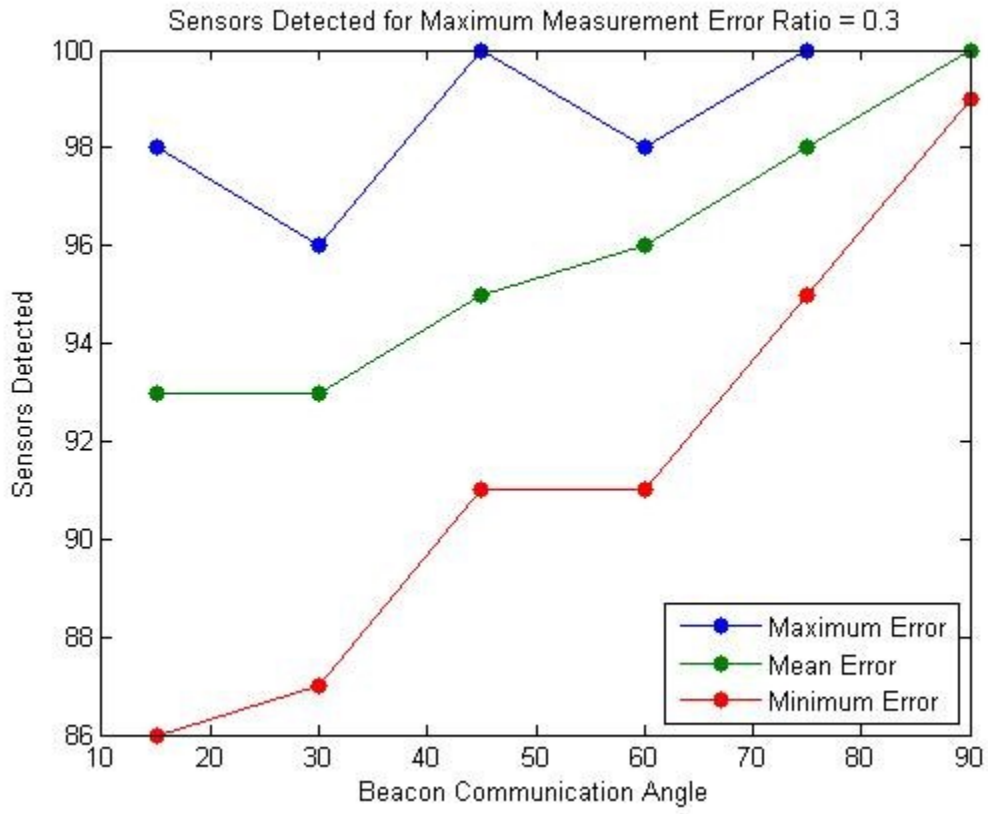


Figure 5.3-3 Sensor Detection for  $R_{\max} = 0.3$

In this figure, it is illustrated that the sensor detection is extremely dependent on the sensor communication angle. The figure also illustrates that the minimum sensor detection and the maximum sensor detection fluctuate while the mean sensor detection stays almost the same for all the different beacon communication angles.

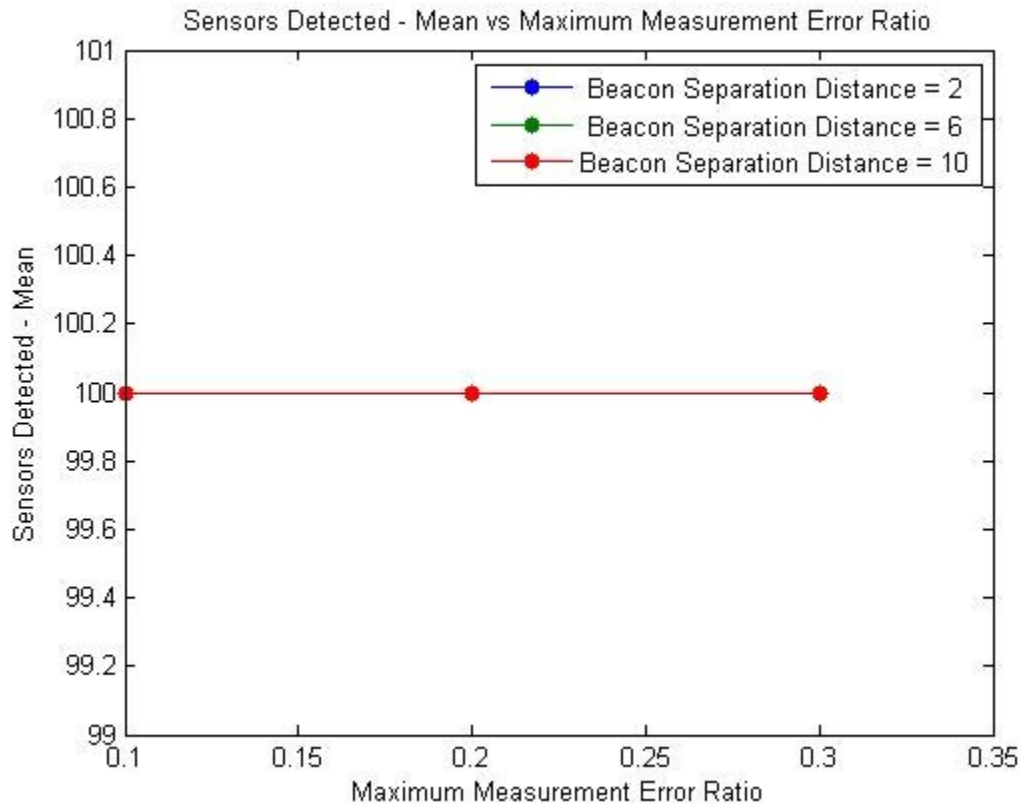


Figure 5.3-4 Sensor Detection for A = 90

Figure 5.3.4 demonstrates that all the sensors for all of the different beacon separation distances and all the three different Rmax's are detected when the beacon transmission angle is equal to 90 degrees which is we used the beacon transmission angle of 90, in all of the two dimension simulations to ensure all sensora in the field are detected.

### 5.3.2 Rough Method

Figure 5.3.5 shows the actual and the estimated sensor positions in the whole field. The actual sensors' positions are marked as small red rhombuses and the rough method sensors' estimated positions are marked as small light blue circles.

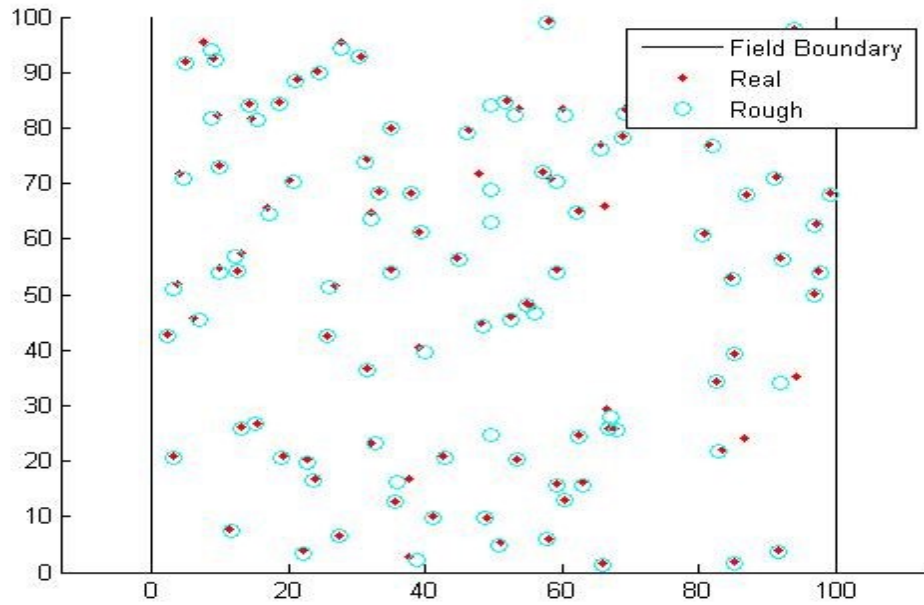


Figure 5.3-5 Localization Results of Rough Method

Figures 5.3.6 and 5.3.7 show the comparison results when the mean error of the rough method is a function of the horizontal beacon step size for different  $D$ 's and  $R_{max}$ 's respectively.

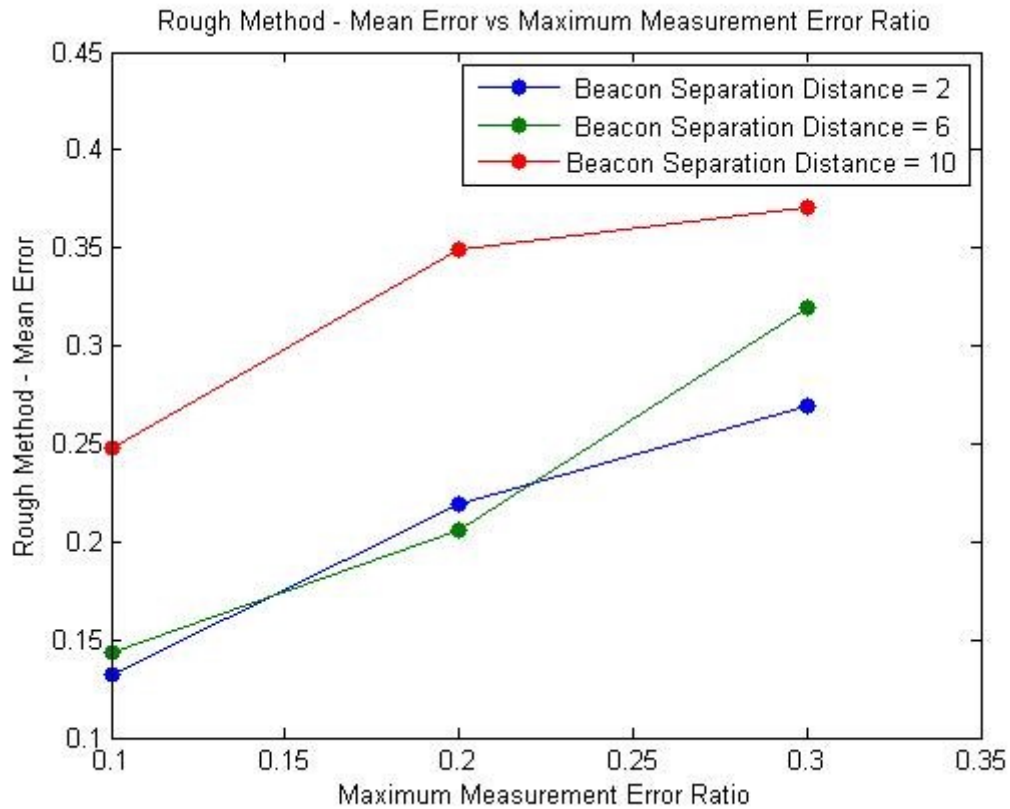


Figure 5.3-6 Accuracy of the Rough Method vs.  $R_{max}$

Generally, the beacon separation with a distance of 10 units has the highest mean error and this remains so throughout the other error ratios. The beacon separation distance of 10 has a mean error of 0.25 units at the error ratio of 0.1 while the two other measurements have a mean error below 0.15 units. Afterwards, all of the three beacon separation distances increased; more specifically, at the error ratio of 0.2, the beacon separation distance of 10 reached a mean error of 0.35 units while the beacon separation distance of 6 and the beacon separation of 2 reached a mean error of more than 0.2. Then, from the error ratio of 0.2-0.3, the beacon separation with a distance of 2 and the beacon separation distance 10 both increased at a less dramatic rate than before with the beacon

separation distance 10 reaching a mean error of more than 0.35 units and the beacon separation distance of 2 reaching a mean error of about 0.25. Unlike the two other beacon separation distances, the beacon separation distance of 6 rises with a more significant rate reaching a mean error of about 0.3 units at the error ratio 0.3.

The preceding figure shows the rough method's mean error vs Rmax for different D's, while the preceding figure also shows the rough method's mean error but it's vs the Dx this time for different Rmaxs.

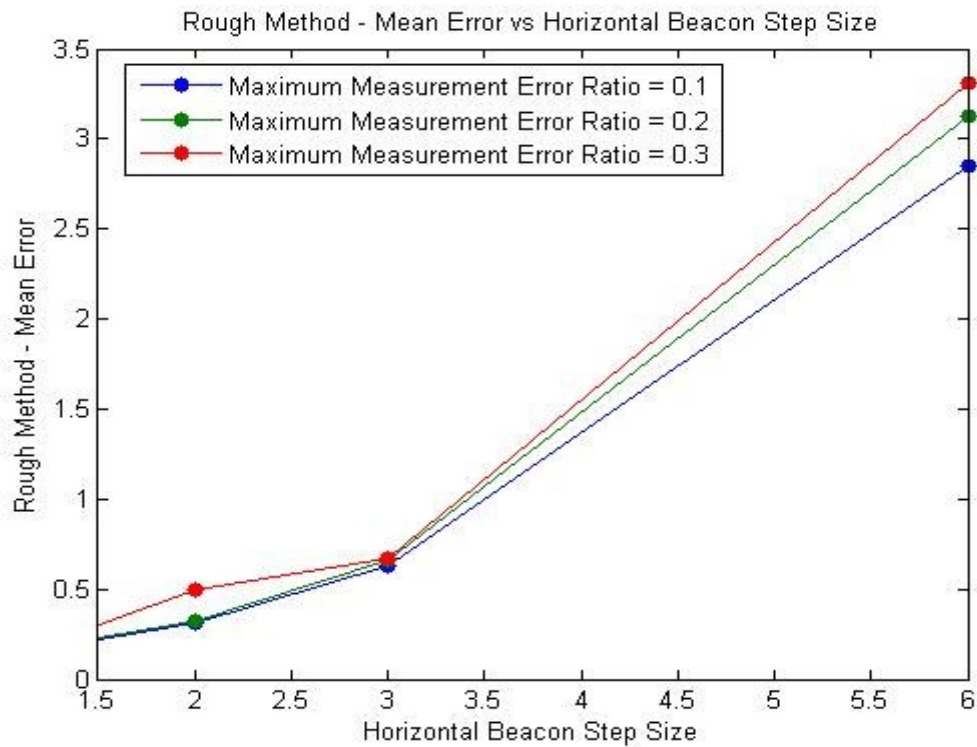


Figure 5.3-7 Accuracy of Rough Method vs DX

### 5.3.3 Error Bounding Method

In Figure 5.3.8, the sub figures a, b, c, and d shows the principle of EBM for 4 sending cases respectively. The small circles represent the RMIN values and their radius is equal to the actual reading distances. As explained in Section 4.5.2, based on our assumption, the readings are equal to the minimum distance, so that we can compute the maximum estimated distance, which equal to the estimated distance, for each reading from both sides. These are represented with the big circles. Then, the possible location area for the sensor is bounded and it's clear that the higher the sending cases the smaller the area, where the sensor can be located.

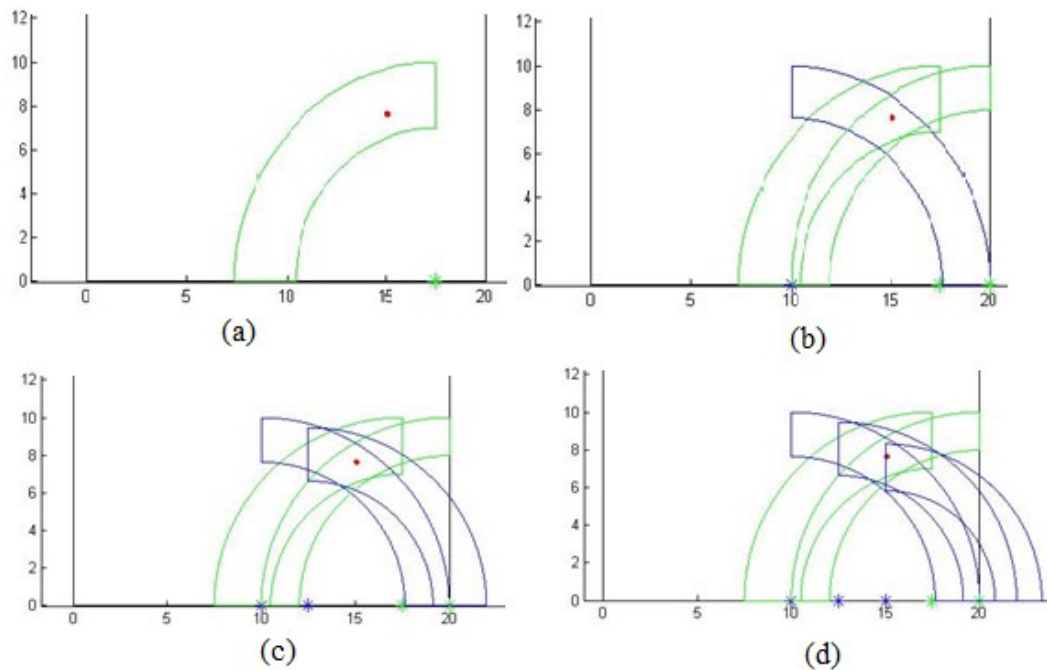


Figure 5.3-8 2-D Four Sending Case-Bounded-Error Method

a) First Sending b) Second Sending c) Third Sending d) Furth Sending

Figure 5.3.9 shows the actual and the estimated sensor positions in the whole field. The true positions are marked as small red dots and the error bounding method estimated positions are marked as small blue squares.

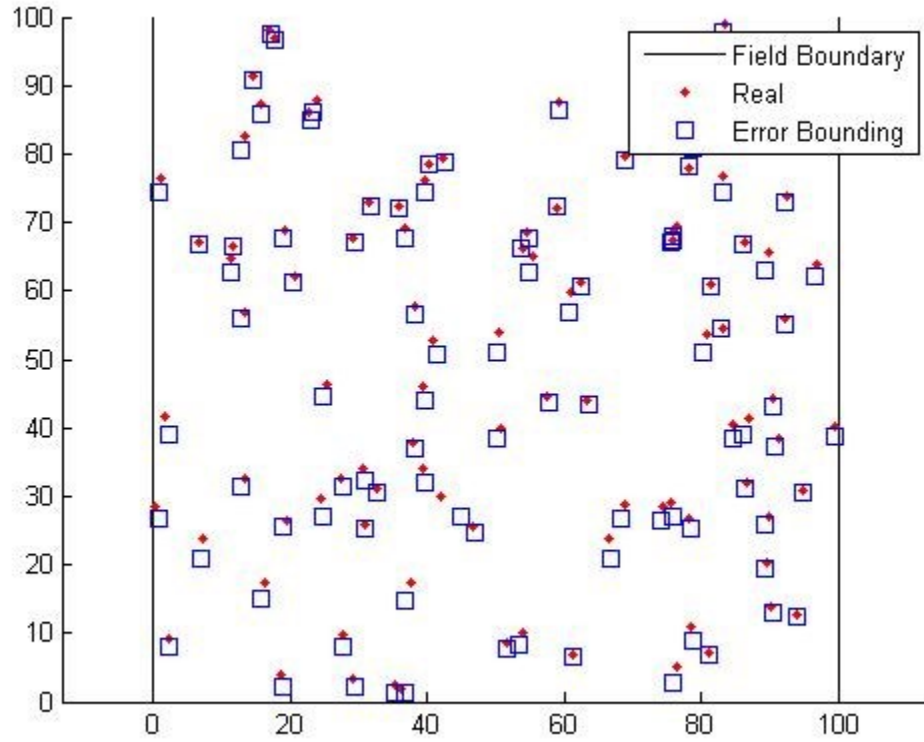


Figure 5.3-9 Localization Result of Error Bounding Method

The accuracy of Error Bounding Method as a function in  $R_{max}$  and  $DX$  for different  $D$ 's is illustrated in figures 5.3.10 and 5.3.11 respectively.

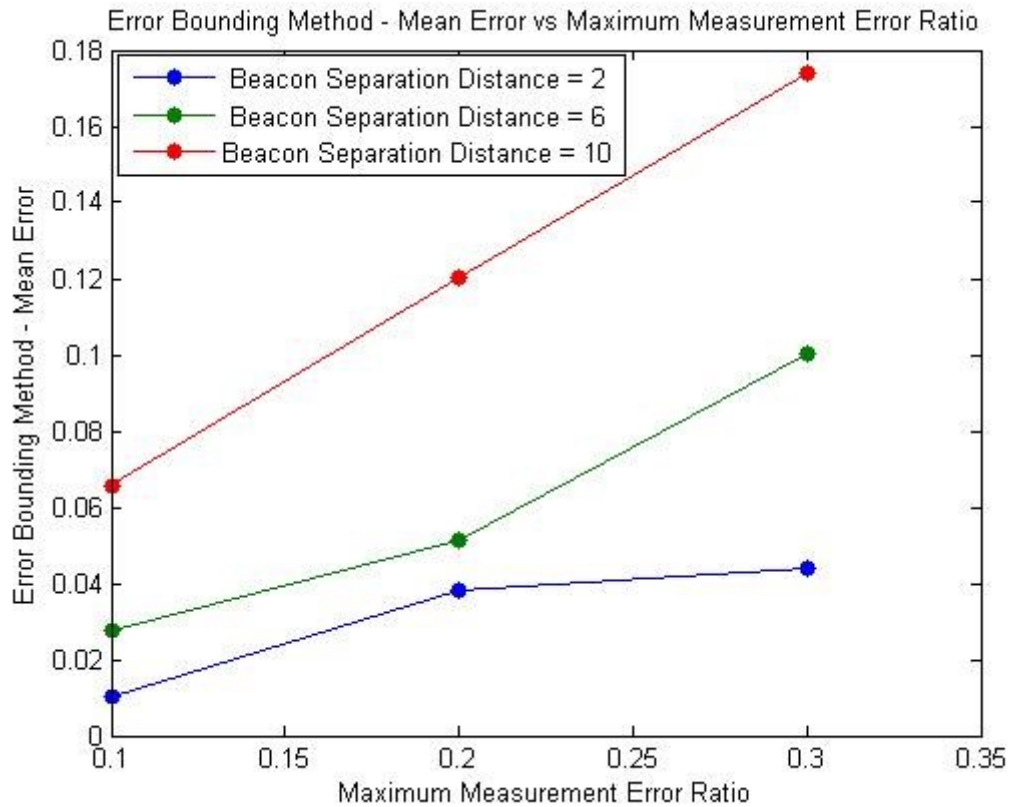


Figure 5.3-10 Accuracy of the Error Bounding Method vs.  $R_{max}$  for different  $D$ 's

This figure shows that the beacon separation distance of 10 has once again managed to get the highest mean error throughout all of the maximum measurement error ratios ( $R_{max}$ ) that were tested. All of the mean errors for the 3 separation distances increased-sometimes more rapidly than other times. At the  $R_{max}$  0.1 units, the beacon separation distance of 10 has a mean error of more than 0.6 units while the beacon separation distance of 6 has a mean error of 0.3 units and the beacon separation distance of 2 has a mean error of 0.1. Then, at the  $R_{max}$  of 0.2 units, the beacon separation distance of 10 increased very significantly reaching a mean error of 0.12 while the beacon separation distance of 6 rose to a mean error of 0.5 and the beacon separation distance of



2 grew at a faster rate than the beacon separation distance of 6 reaching a mean error of approximately 0.4. After that, the beacon separation distance of 10 continued to increase at the same linear rate with a slope of 5.5 reaching a mean error of about 0.18 at the error ratio of 0.3 while the beacon separation distance of 6 grew at a more rapid rate than before reaching a mean error of about 0.1 while the beacon separation distance of 2 rose at a far less dramatic rate than before almost as if it didn't change at all.

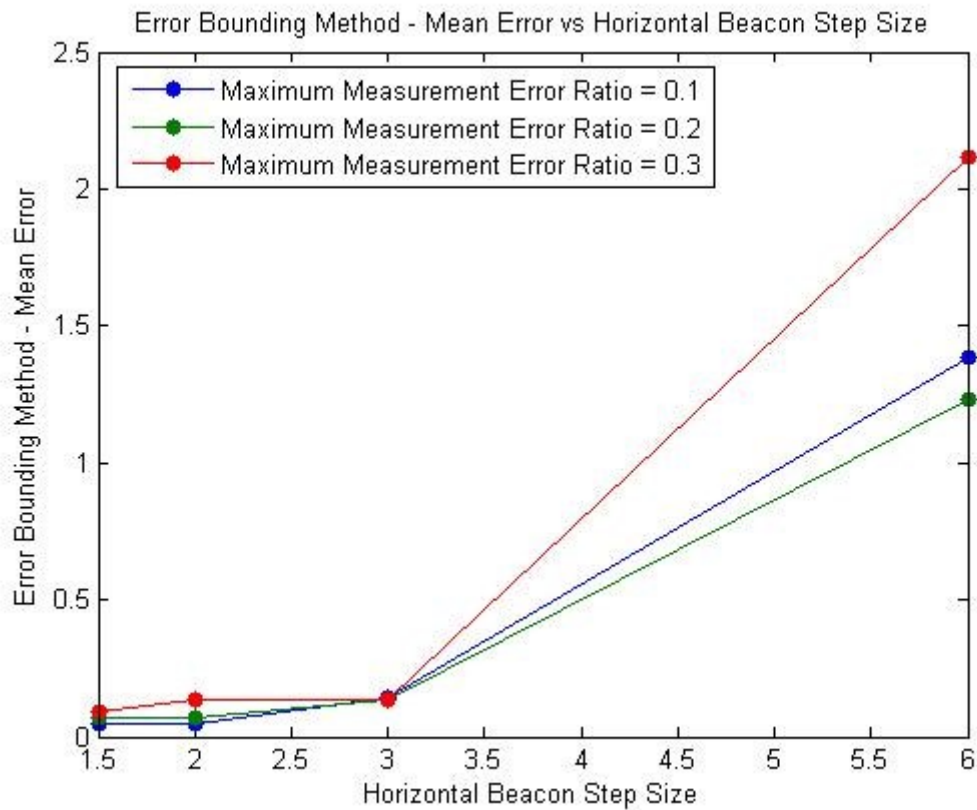


Figure 5.3-11 Accuracy of the Error Bounding Method vs DX for different D's

All the three maximum measurement error ratios ( $R_{max}$ s) had little to no change from the horizontal beacon step size (DX) of 1.5-3 units until they all got to the same

mean error at the  $\Delta x$  of 3 units. Then, they all began to grow at rapid rates. The 0.3  $R_{\max}$  grew at a faster rate than the others reaching a mean error of more than 2 units while the 2 other  $R_{\max}$ s managed to reach a mean error of approximately 1.5 units. It's clearly seen that the mean error isn't all dependent on the  $R_{\max}$  when  $\Delta x$  is equal to half of the distance between the beacons. On the other hand, when  $\Delta x$  is equal to the distance between the beacons, the mean error is extremely affected by  $R_{\max}$ .

In conclusion, the mean error of the Bounded-Error Method depends on the beacon separation distance and on the horizontal beacon step size as shown in figure 5.3.2. The smaller the  $D$ , and the  $DX$ , the smaller the error. On the other hand, the Error Bounding Method mean error does not depend on the  $R_{\max}$  in the majority of the cases when  $DX$  is equal to or less than  $D/2$ .

It's illustrated in table 5.2 that the higher the transmission angle the higher the localize percentage and vice versa. In the other hand, the smaller the transmission angles the better accuracy can be obtained.

#### **5.3.4 Angular Bounding Method**

Figure 5.3.12 shows the actual and the estimated sensor positions in the whole field. The true positions are marked as small squares and the estimated positions are marked as small circles.

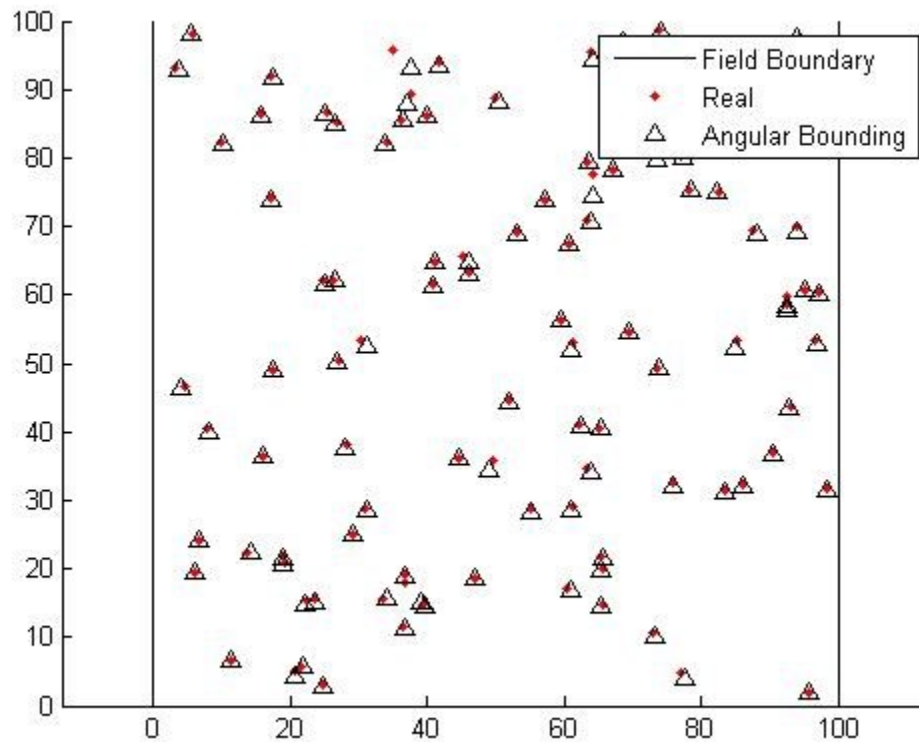


Figure 5.3-12 Localization Result of Angular Bounding Method

Table 3 shows a matlab result example for the sensor 52. The first four lines illustrate the original minimum angle (further left) and the maximum angle (further right) from detected before beacons. The other two left and right columns are the improvement results and the angle between partases is the actual angle. The other four lines explain the same idea for after detected beacons. The last two lines in the table shows the results for minimum (left side) and maximum (right side) bounding values of x- and y- coordinate respectively for the sensor 52. The actual sensor position is the left side value in partasis and the estimated sensor position is the right value.

Table 3 Angle Minimization and Sensor Location Estimation for Sensor 52

<p>thetab 18: [ 9.826 -&gt; 9.826 -&gt; 9.826 ( 10.598) 14.211 &lt;- 17.214 &lt;- 17.214] degrees</p> <p>thetab 19: [ 13.343 -&gt; 13.343 -&gt; 13.343 ( 14.518) 15.287 &lt;- 24.086 &lt;- 24.086] degrees</p> <p>thetab 20: [ 20.611 -&gt; 20.611 -&gt; 20.611 ( 22.800) 22.741 &lt;- 38.739 &lt;- 38.739] degrees</p> <p>thetab 21: [ 42.230 -&gt; 42.230 -&gt; 44.135 ( 48.141) 54.759 &lt;- 75.646 &lt;- 75.646] degrees</p> <p>thetaa 18: [ 40.887 -&gt; 40.887 -&gt; 40.887 ( 59.588) 62.805 &lt;- 73.839 &lt;- 73.839] degrees</p> <p>thetaa 19: [ 20.239 -&gt; 20.239 -&gt; 20.239 ( 25.786) 37.991 &lt;- 37.991 &lt;- 37.991] degrees</p> <p>thetaa 20: [ 13.182 -&gt; 13.182 -&gt; 13.182 ( 15.720) 23.766 &lt;- 23.766 &lt;- 23.766] degrees</p> <p>thetaa 21: [ 9.738 -&gt; 9.738 -&gt; 9.738 ( 11.232) 15.341 &lt;- 17.046 &lt;- 17.046] degrees</p> <p>S52x: [ 24.388 -&gt; 24.388 -&gt; 24.743 -&gt; 24.743 ( 24.906, 24.856) 24.970 &lt;- 25.061 &lt;- 25.061 &lt;- 25.061]</p> <p>S52y: [78.963 -&gt; 78.963 ( 79.012, 78.975) 78.988 &lt;- 79.514]</p>
--------------------------------------------------------------------------------------------------------------------------------------------------------------------------------------------------------------------------------------------------------------------------------------------------------------------------------------------------------------------------------------------------------------------------------------------------------------------------------------------------------------------------------------------------------------------------------------------------------------------------------------------------------------------------------------------------------------------------------------------------------------------------------------------------------------------------------------------------------------------------------------------------------------------------------------------------------------------------------------------------------------------------------------------------------------------------------------------------------------------

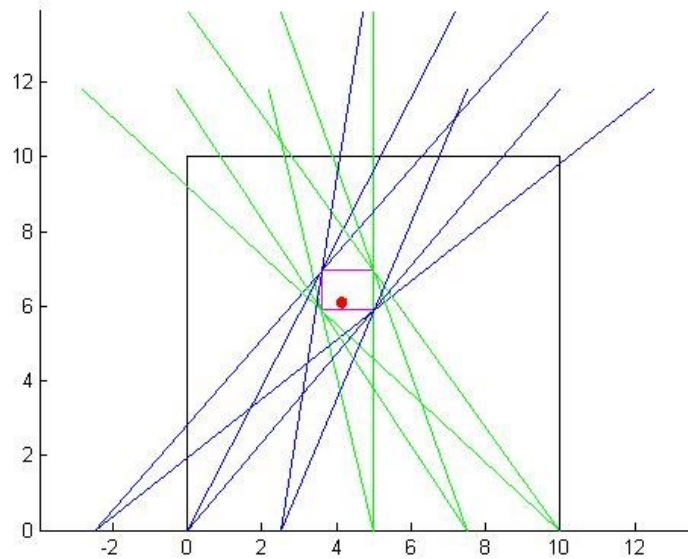


Figure 5.3-13 Angular Bounding Layout

After computing the first step, which determines the minimum and maximum angles for each sending case for before and after beacons, of Angular Bounding Method as it shown in Figure 5.3.13, the angle interval mong minimum and maximum angles for each sending case can be minimized as explained in Section 4.6.1.

Figures 5.3.14 and 5.3.15 present the comparison results when the estimated error is a function of the beacon step size in x direction for Rmax's and different D's respectively.

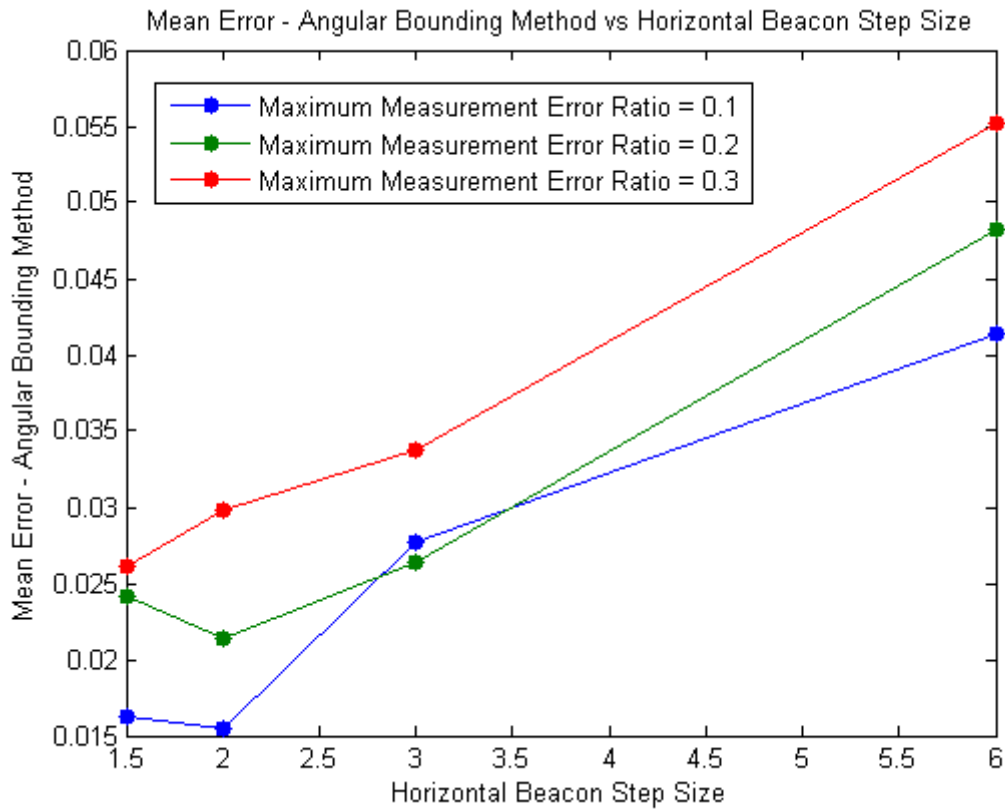


Figure 5.3-14 Accuracy of the Angular Method vs DX for different  $R_{max}$ 's

The Angular Bounding Method is affected by increasing the  $R_{max}$ . This is clear in figure 5.3.14 which demonstrates that the bigger the horizontal beacon step size, the bigger the mean error with an exception of  $R_{max}$  0.2 and  $R_{max}$  0.1 when they were at the horizontal beacon step size.

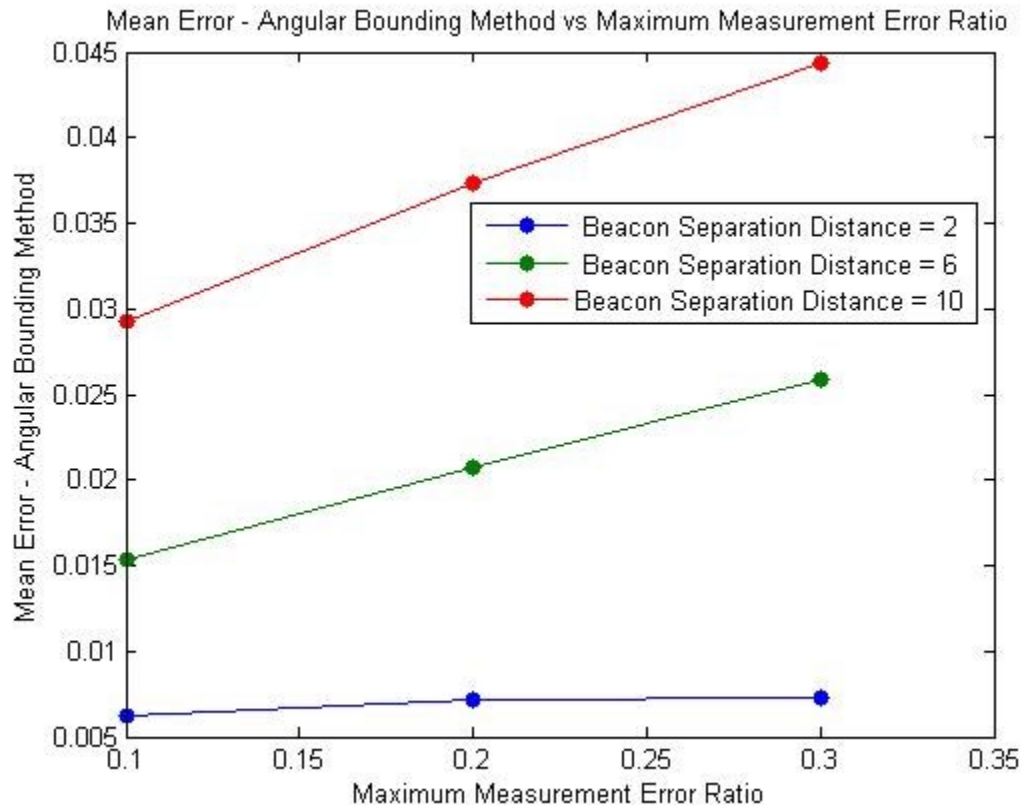


Figure 5.3-15 Accuracy of the Angular Method vs  $R_{max}$  for different  $D$ 's

Overall, it can be seen that most of the significant changes happen when the beacon separation distance=6; it started out at the mean error of approximately 0.4 units and rapidly increased to a mean error of approximately 0.8 units at the maximum measurement error ratio ( $R_{max}$ ) of 0.2 units just like the beacon with the separation distance of 2. Then it continued to increase at the same almost linear rate reaching a high mean error of about 1.2 units. At the beginning, the beacon with the separation distance of 10 has a higher mean error than that of the beacon with the separation distance of 2, but as the  $R_{max}$  increases, the beacon with the separation distance of 2 managed to surpass the beacon with the separation distance of 10.

As a result, the angular bounding method's mean error almost never depends on  $R_{\max}$  if the horizontal beacon step size is equal to a third of the distance and this is accurate for both of the  $R_{\max}$ s 0.2 and 0.3 when the horizontal beacon step size is equal to  $D/2$ , but the angular bounding method does depend on the  $R_{\max}$  when  $DX$  is equal to  $D$  or  $D/4$  as shown in figure 5.3.14. On the contrary, the mean error of the middle value of the beacon separation distance extremely depends on  $R_{\max}$  values and changes almost linearly as a function of  $R_{\max}$  by a slope of 4, while the mean error of  $D=2$  and  $D=10$  almost never changes.

## **5.4 Methods Comparison**

In this Section, we are going to compare all the methods with each other for the best specific parameter values that we obtained from previous discussion.

### **5.4.1 1-D-Methods Comparison**

In this Section, we compare all of the previously studied methods with each other.

#### ***5.4.1.1 1-D-Methods Comparison for different beacon separation distance***

The mean error of all 3 compared methods, rough- magnitude-, and error bounding- method, vs. the horizontal beacon step size for different beacon separation distances,  $D=10$ , 6, 2, are illustrated in figures: 5.4.1, 5.4.2, and 5.4.3 respectively.



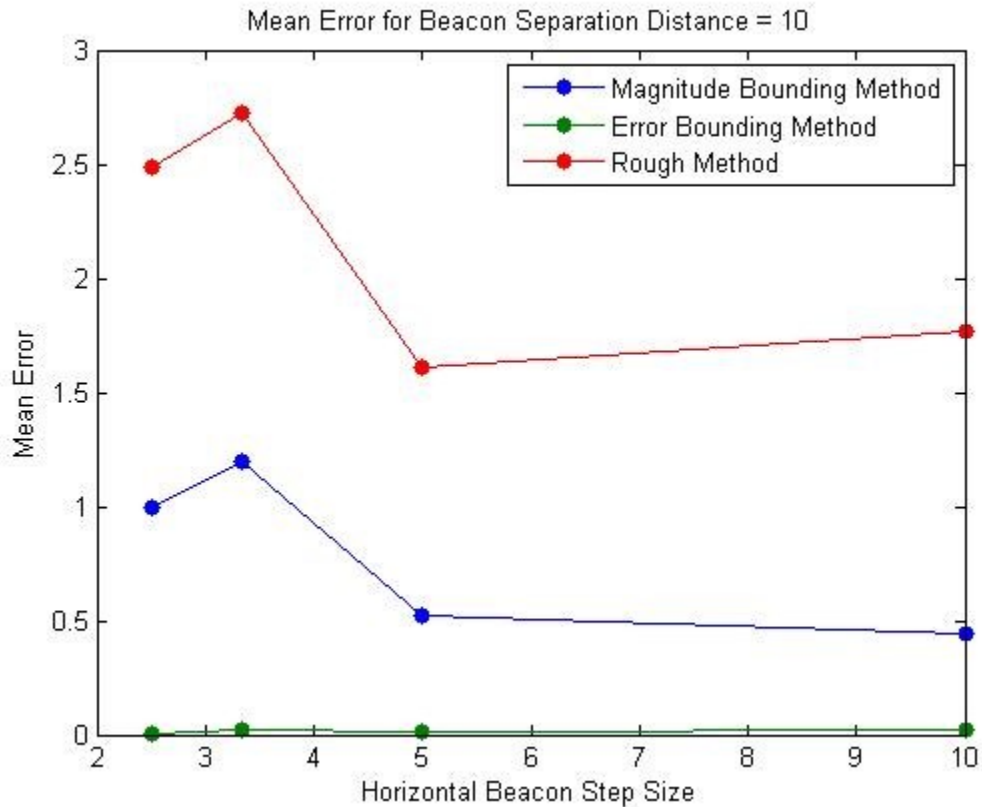


Figure 5.4-1 1-D Methods-Error Comparison for D = 10

The only method whose changes were very significant throughout all of the horizontal beacon step sizes are the rough method's mean errors. It started out with the a very high mean error of 2.5 units at the horizontal beacon step size of 2.5 and then fluctuated in a rapid manner while magnitude bounding method also jumped around but did so in a less significant manner and while the error bounding method had very insignificant slight changes throughout all the horizontal beacon step sizes.

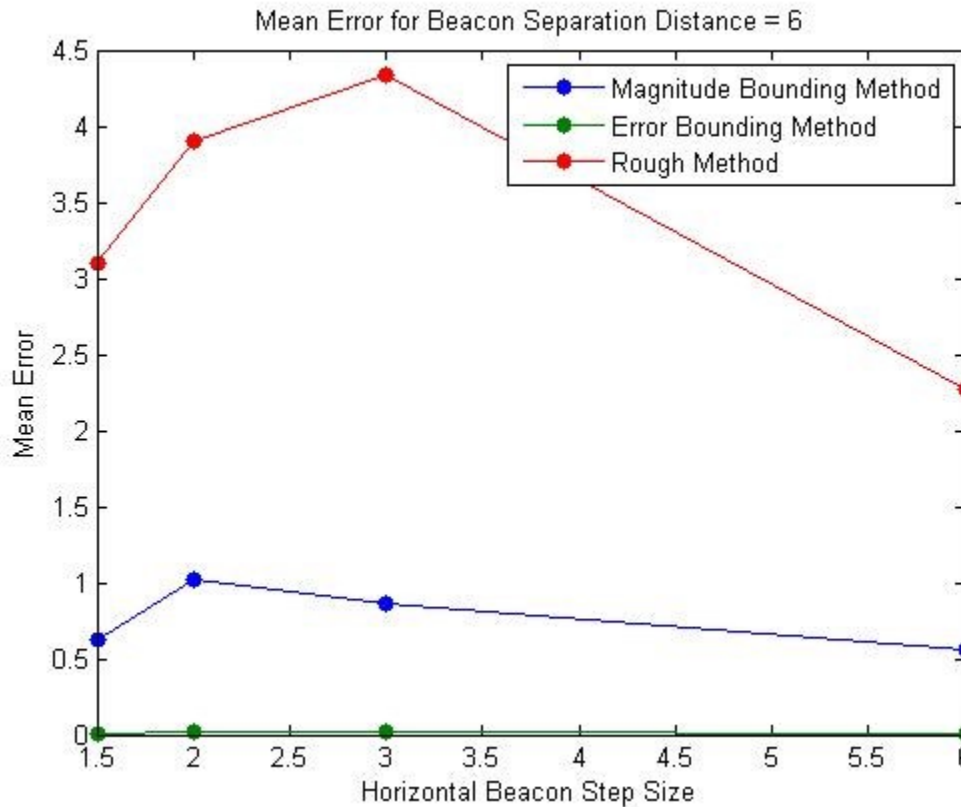


Figure 5.4-2 1-D Methods-Error Comparison for D = 6

Once again, the rough method managed to record the highest mean errors and the most significant changes while the magnitude bounding method came in second when it comes to significant changes and the 3<sup>rd</sup> place goes to the error bounding method because it had almost no mean errors at all for any of the horizontal beacon step sizes. The rough method, on the other hand, started out with the highest number of mean errors at more than 3 units and then continued to grow at a rapid rate reaching a mean error of about 4.5 units which was its highest value. The magnitude bounding method seemed to have reached its highest value of mean errors, approximately 1, at the horizontal beacon step size of 2; and that also seems to be the case for the error bounding method because it got

to its highest value of mean errors, less than 0.5 units, at the same horizontal beacon step size.

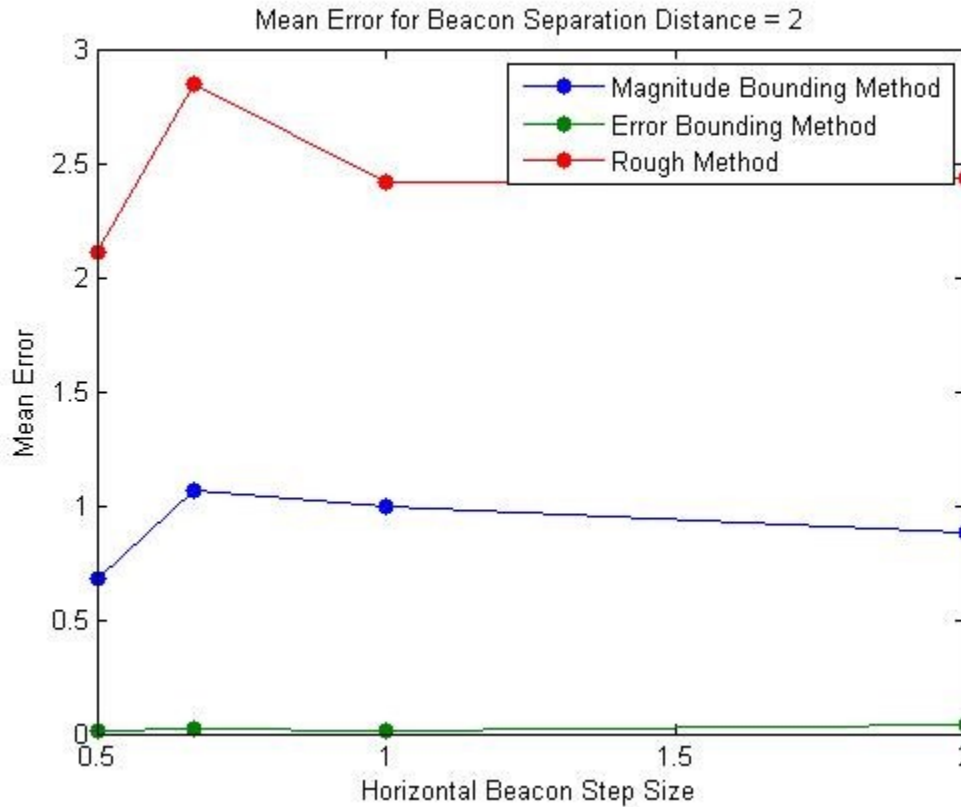


Figure 5.4-3 1-D Methods-Error Comparison for D = 2

Once more, the rough method's mean errors seem to be the highest. The rough method recorded its highest mean error, approximately 3 units, at the horizontal beacon step size of .70 units, while the magnitude bounding method also recorded its highest mean error, approximately 1, at this horizontal beacon step size also. The error bounding method seemed to have almost no mean errors for any of the horizontal beacon step sizes.

To sum up, the rough method did not depend on the horizontal beacon step size for different D's, but as the D gets smaller so does the error range. The mean errors for the

Magnitude bounding method regard almost the same behavior as the rough method's mean errors but with more stability.

**5.4.1.2 1-D-Methods Comparison for different  $R_{max}$ s**

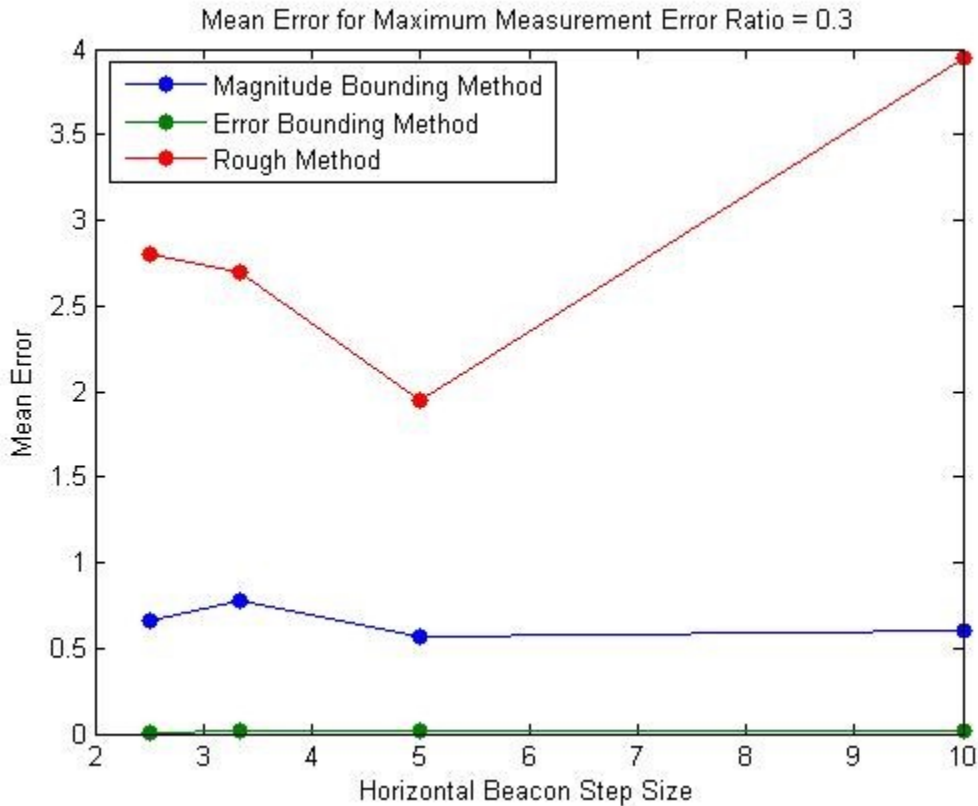


Figure 5.4-4 1-D Methods-Error Comparison for  $R_{max} = 0.3$

The rough method's mean errors were significantly high for all of the horizontal beacon step sizes while the error bounding method seemed to not have recorded almost any mean errors, and the magnitude bounding method's mean errors were somewhat high for all of the horizontal beacon step sizes. The rough method reached its lowest point of mean errors, approximately 2 units, at the horizontal beacon step size of 5 just like the

magnitude bounding method whose mean errors also seem to be the lowest at approximately 0.5 units at this horizontal beacon step size.

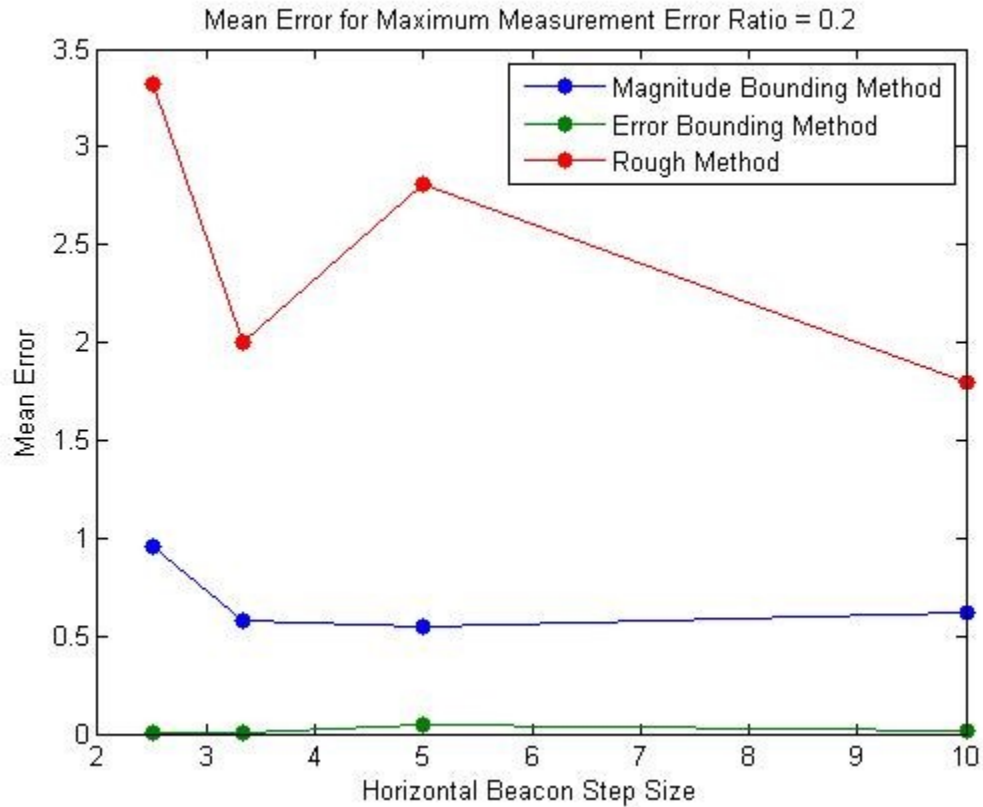


Figure 5.4-5 1-D Methods-Error Comparison for  $R_{max} = 0.2$

The rough method's mean errors were the highest while the magnitude bounding method's mean errors were the 2<sup>nd</sup> highest and the error bounding method's mean errors were the least; in fact, the error bounding method recorded almost no mean errors at all. The rough method recorded its highest mean error, approximately 3.25 units, at the horizontal beacon step size of 2.5 just like the magnitude bounding method which also recorded its highest mean error of approximately 1 at this step size. Then, the rough method recorded its lowest mean error of 2 units at the step size of 3.33 units; after that,

the method's mean errors fluctuated along with the magnitude bounding method's mean errors.

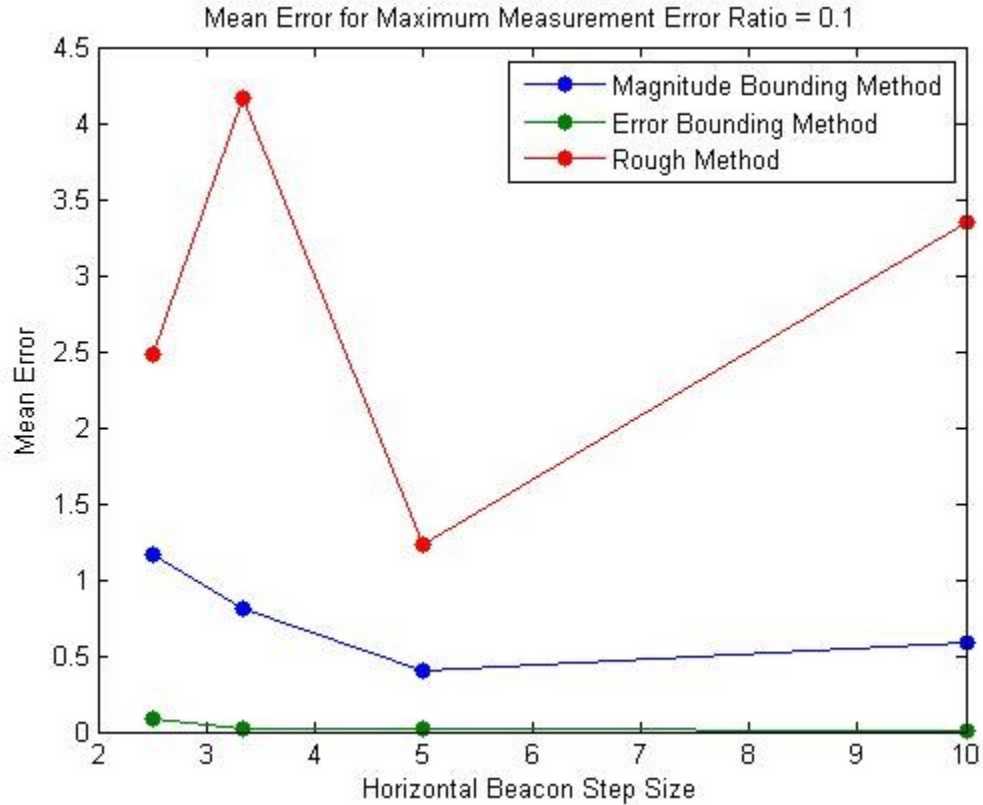


Figure 5.4-6 1-D Methods-Error Comparison for  $R_{max} = 0.1$

From the horizontal beacon step size of 3.33 units, the rough method managed to record its highest mean error, almost 4.25 units and then dropped at a very rapid rate recording its lowest mean error of approximately 1.25 units at the horizontal beacon step size of 5 in which the magnitude bounding method also recorded its lowest mean error, almost 0.5 units. The error bounding method, on the other hand, recorded almost no mean errors at all for any of the horizontal beacon step sizes.

As a result the estimated error method always give us better or at least equal results in compare to other two methods and the rough method give in the majority of running cases the worst results. In addition, the higher the number of steps the higher the obtained accuracy special for magnitude bounding method and the reason for that more parts of the errors are canceled.

#### **5.4.2 2-D-Methods Comparison**

This Section will compare the most important parameters of all the different methods. One of the parameters is the distance between the before and after mobile beacons ( $D$ ) as a function of the number of steps and also as a function of the  $R_{max}$ . Another parameter that will be explored in this section is the  $R_{max}$  as a function of the number of steps and as a function of the beacon transmission angles. To ensure that all the sensors are detected, we made the beacon transmission angle 90 degrees and the communication range equal to the used distance between the beacons.

##### ***5.4.2.1 2-D-Methods Comparison for different beacon separation distances.***

Figure 5.4.7 illustrates the comparison of the 3 different methods by demonstrating the mean error for each of them as a function of the horizontal beacon step size for three different distance values.

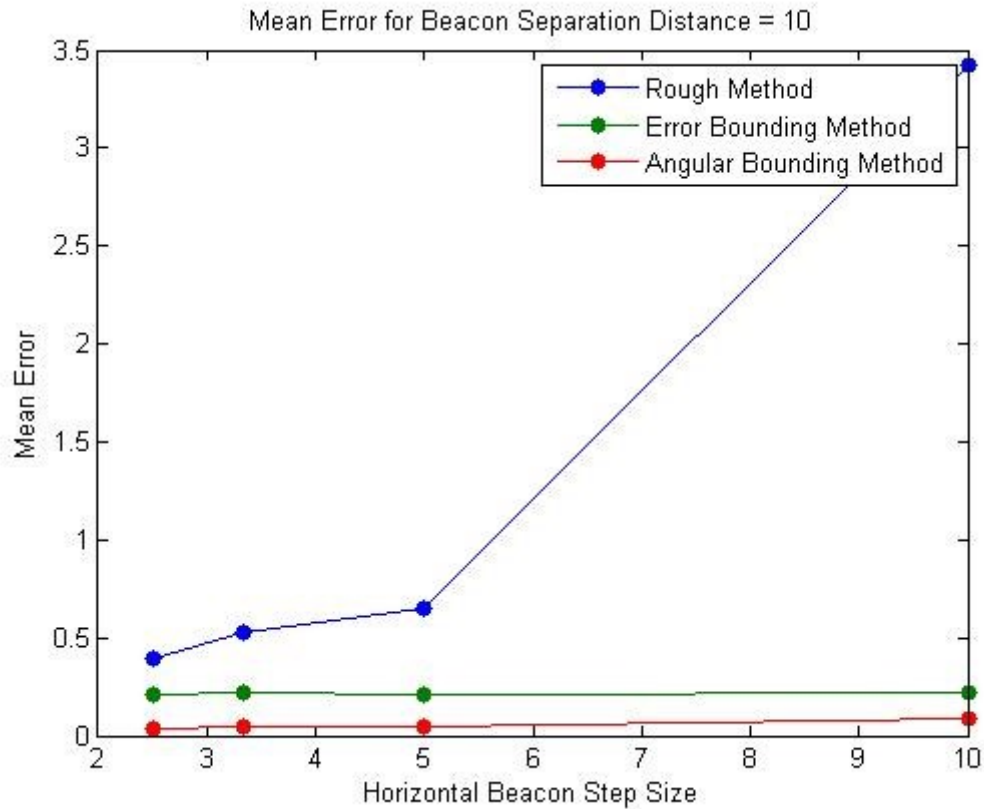


Figure 5.4-7 2-D Methods-Error Comparison for D = 10

Ultimately, the rough method's mean error increases dramatically while the error bounding method's mean error increases and decreases very slightly and the angular method's mean error increases slightly. More specifically, the rough method's mean error increases slowly reaching a mean error of more than 0.5 units at the horizontal beacon step size of 3.33 while the mean error for both error bounding method and the angular bounding method very slightly increases. After that, the rough method's mean error increases at an even slower rate while the error bounding method's mean error decreases very slightly and angular bounding method's mean error stays the same. Then, the mean error for the rough method dramatically rises reaching a mean error of approximately 3.4



units at the horizontal beacon step size of 10, while the mean error for the two other methods slightly increases.

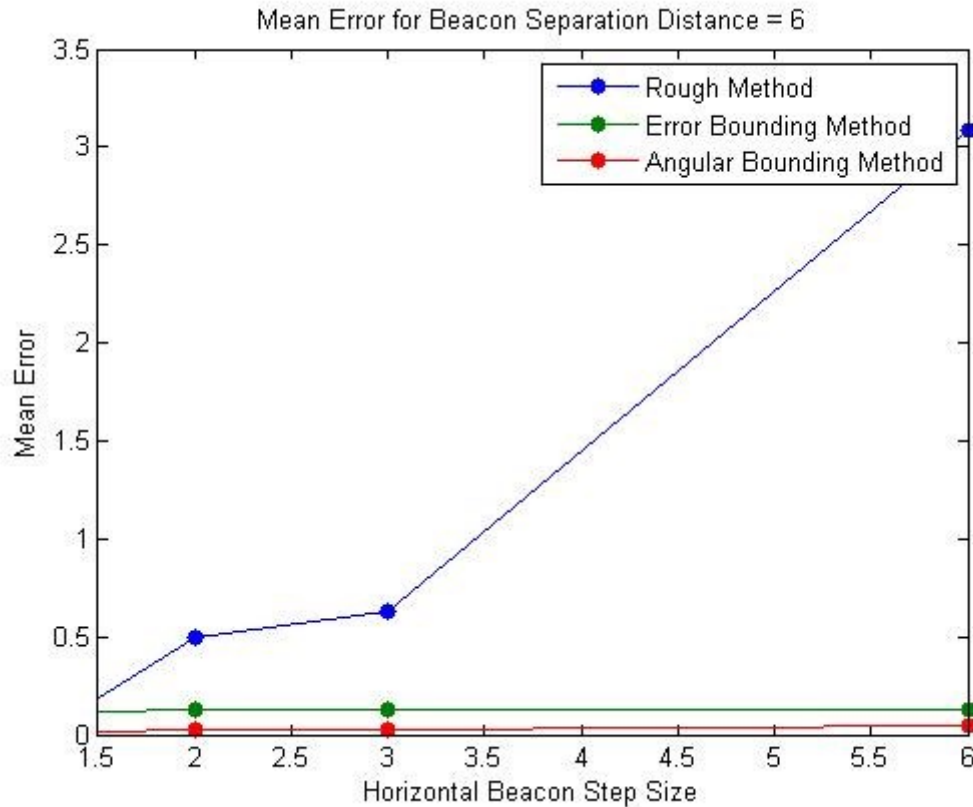


Figure 5.4-8 2-DMethods-Error Comparison for D = 6

Generally, the only method whose mean error has significant changes is the rough method. From the horizontal beacon step size of 1.5-2, the rough method's mean error increases rapidly to a mean error of 0.5 units while the 2 other methods increase very slightly. Afterwards, from the horizontal beacon size of 2-3, the rough method's mean error increases at a slower rate than last time's reaching a mean error of more than 0.5 units while the error bounding method and the angular bounding method's mean error stayed the same. Then, the mean error for the rough method dramatically rose all the way

to a mean error of approximately 3.1 at the step size of 6 while the 2 other methods have little to no change at all.

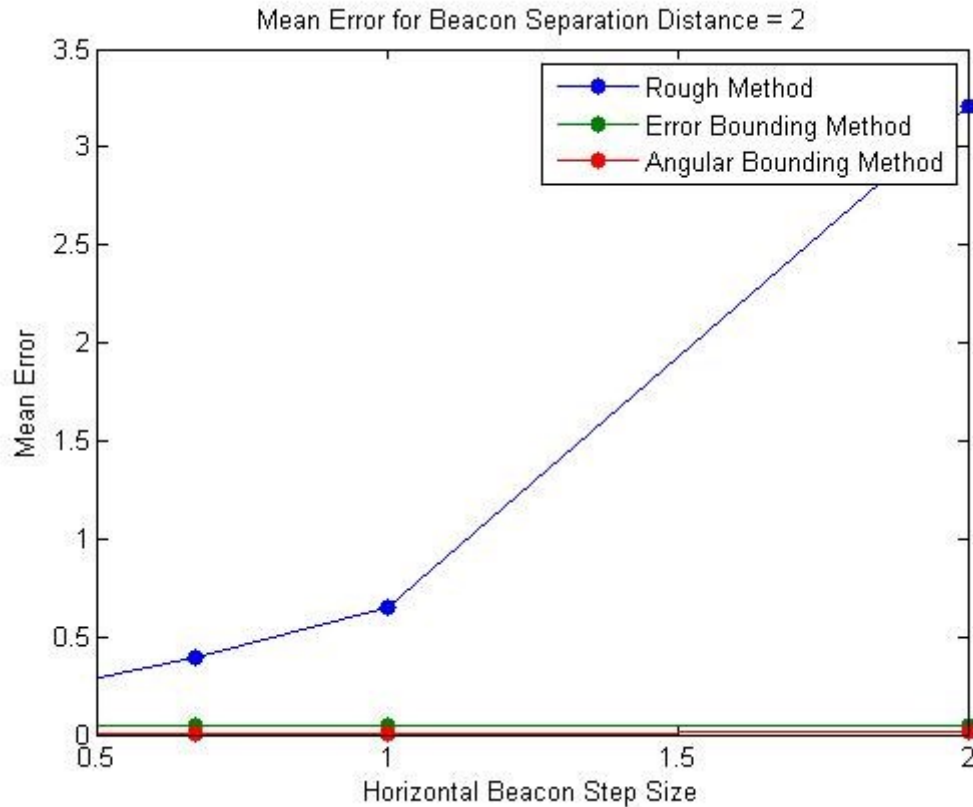


Figure 5.4-9 2-D Methods-Error Comparison for D = 2

For the most part, the error bounding method and angular bounding method had no major changes while the rough method had grown at an almost exponential rate. The rough method grew at a constant rate from the horizontal beacon step sizes of 0.5-1. At that point, the rough method's mean error reached more than 0.5. Afterwards, the rough method increased quickly reaching a mean error of approximately 3.5 at the step size of 2.

To sum it up, the rough method does not depend on the distance between the before and after beacons as illustrated in all the three above figures, but it does extremely depend on the number of steps. On the other hand, the two other methods are affected by the distance between the before and after beacons and it's clearly demonstrated that the smaller the  $D$  the slimmer the chance for error in both methods.

**5.4.2.2 Dense-Straight-Line Mobile trajectory simulation results**

The following figures demonstrate the results of the DSL which is the second path of mobile beacon trajectory as explained thoroughly in Section 4.7.

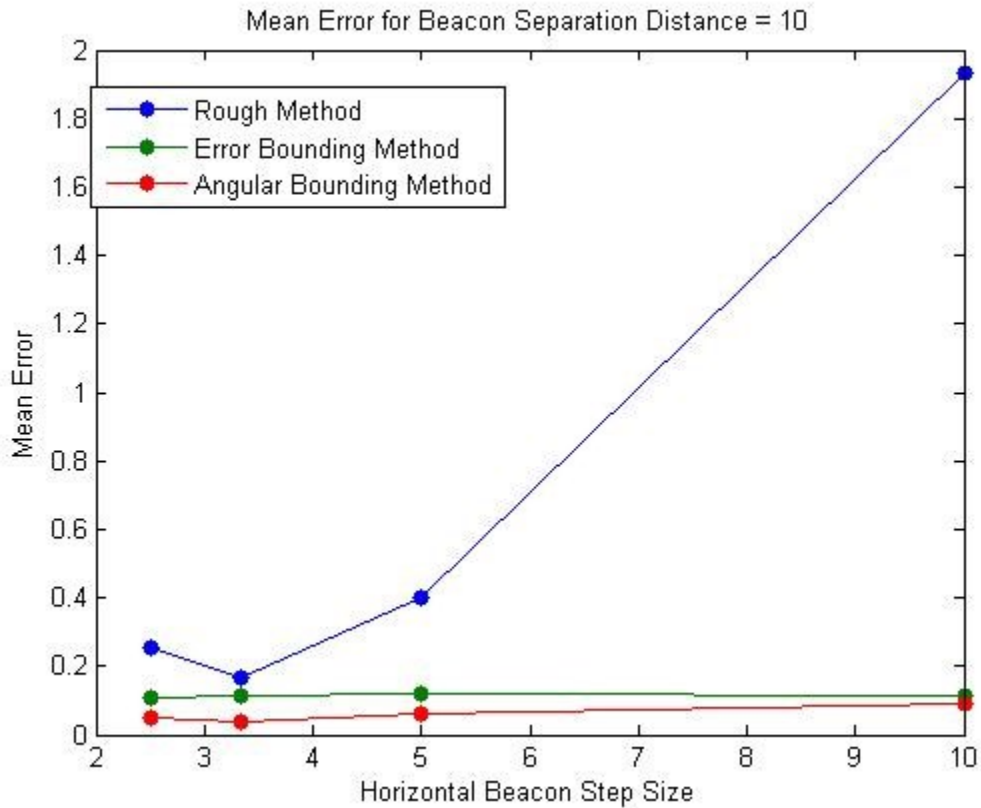


Figure 5.4-10 2-D DSL Methods-Error Comparison for  $D = 10$

The previous figure, figure 5.4.10, presents the comparison results for all 2-D developed techniques when the beacon separation distance is equal to 10.

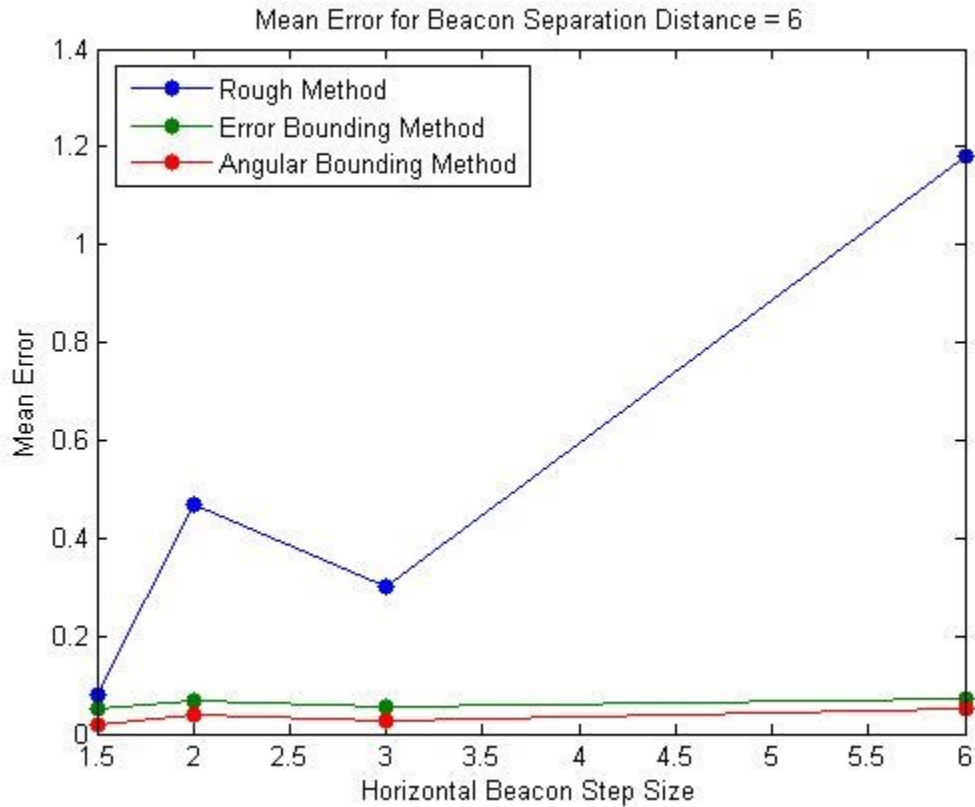


Figure 5.4-11 2-D DSL Methods-Error Comparison for D = 6

The above figure presents the comparison results for all 2-D developed techniques when the beacon separation distance is equal to 6. The following figure, figure 5.4.12, presents the comparison results for all 2-D developed techniques when the beacon separation distance is equal to 10.

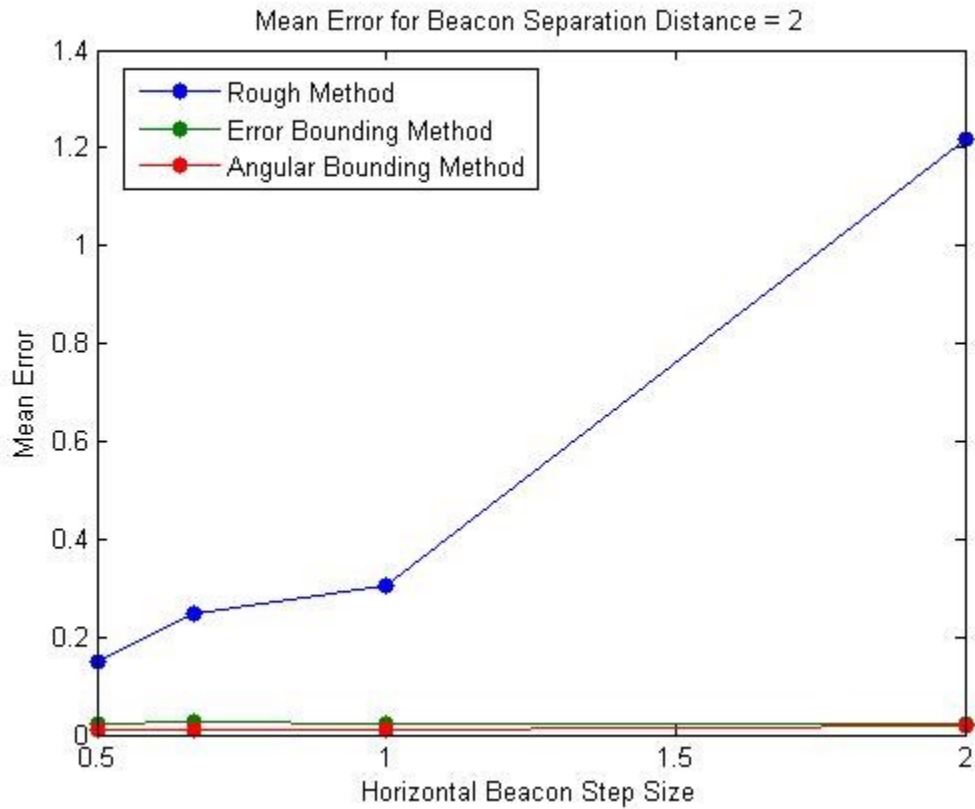


Figure 5.4-12 2-D DSL Methods-Error Comparison for D = 2

To sum up, the DSL trajectory path minimized the mean error especially for the rough method and the cost for that is energy consumption, since the sensors will receive more beacons from mobile beacons.

### 5.4.2.3 2-D-Methods Comparison for different $R_{max}$ s

The below figures illustrate the comparison of the 3 different methods by demonstrating the mean error for each of them as a function of the horizontal beacon step size for three different  $R_{max}$  values.

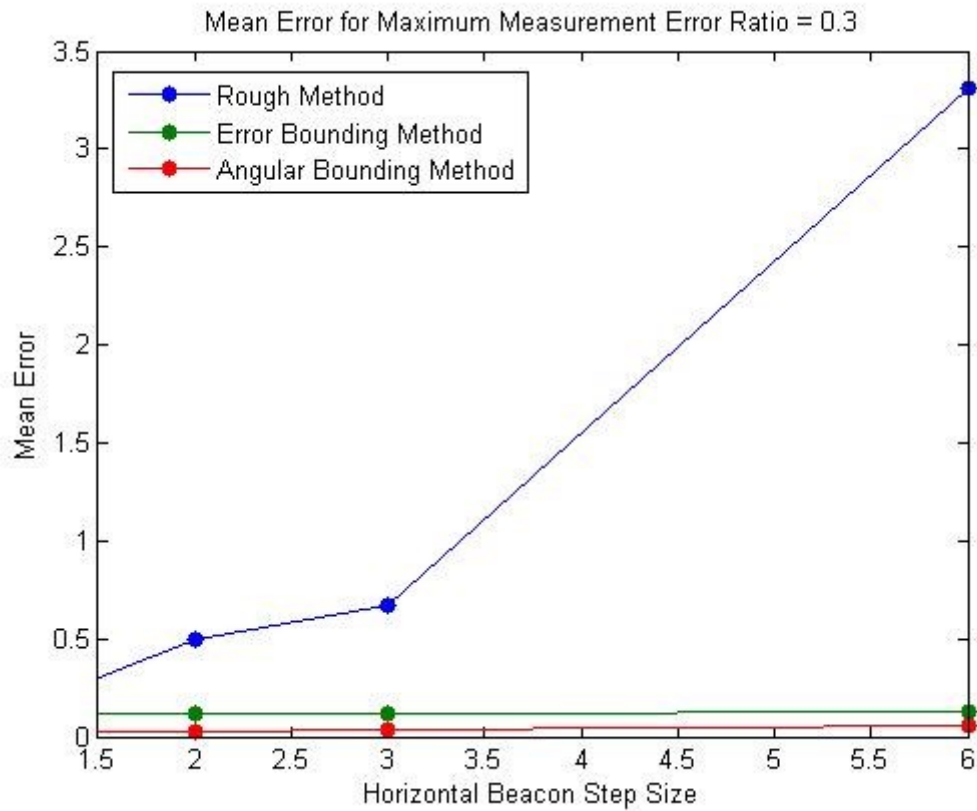


Figure 5.4-13 2-DMethods-Error Comparison for  $R_{max} = 0.3$

Ultimately, the rough method mean error increases from the horizontal beacon step size of 1.5-6 while the two other methods very slightly increase. From the beacon size step of 1.5-2, the rough method increases at a slow rate reaching a mean error of 0.5 at the step size of 2 while the two other methods stay the same. Afterwards, the rough

method increases at an even slower rate from the beacon step size of 2-3 reaching a mean error of 0.7 while the error bounding method stays the same and the angular bounding method very slightly increases. Then, the rough method mean error increases at a significant rate from the step sizes of 3-6 while the error bounding method's mean error and the angular bounding method's mean error slightly increase.

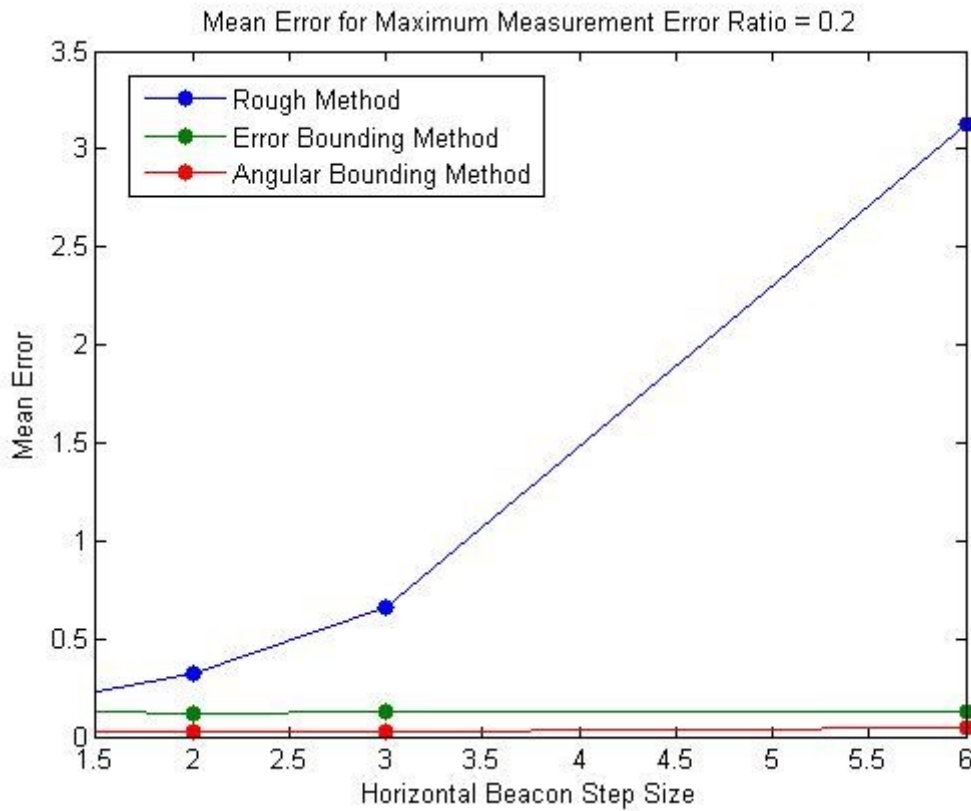


Figure 5.4-14 2-DMethods-Error Comparison for  $R_{max} = 0.2$

From the horizontal beacon step size of 1.5-2, the rough method mean error slightly increases while the error bounding method mean error somewhat decrease and the angular bounding method stay the same. Afterwards, the rough method's mean error continues to increase but does so at a faster rate reaching a mean error of more than 0.5 at

a horizontal beacon step size of 3 while the error bounding method's mean error somewhat increases and the angular bounding method's mean error stays the same once again. After that, the mean error for the rough method significantly increases reaching a mean error of more than 3 at the step size of 6 while the error bounding method's mean error stays the same and the angular bounding method's mean error very slightly increases.

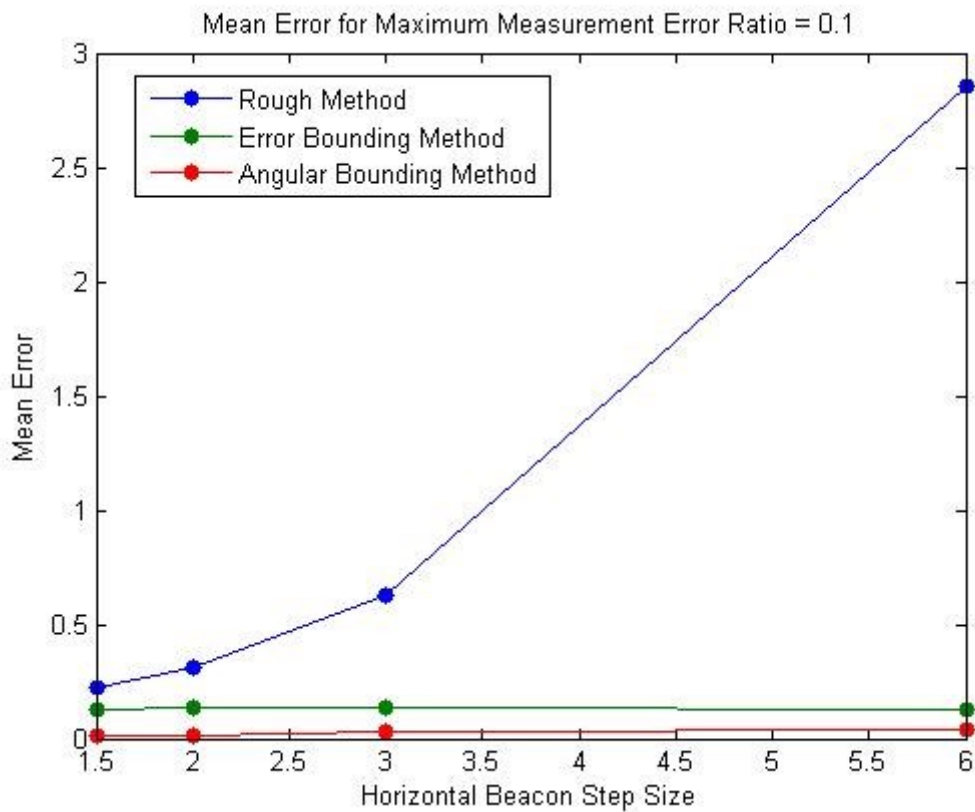


Figure 5.4-15 2-DMethods-Error Comparison for  $R_{max} = 0.1$

The rough method mean error increases at an almost exponential rate from the horizontal step size of 1.5-6 while the angular bounding method increases slightly and the



error bounding method mean error increases very slightly from the step size of 1.5-2 and then decreases also very slightly from the horizontal beacon step size of 2-6.

To put it briefly, the rough method is dependent on the  $R_{max}$  as shown in the three figures above. In addition, the rough method is also extremely dependent on the number of steps. The error in the angular bounding method is a little smaller especially in the case of one step when we compare  $R_{max}0.1$  to  $R_{max} 0.3$ , but the error bounding method stays almost the same.

#### ***5.4.2.4 2-D-Methods Comparison for different beacon separation distances***

The following figures illustrate the comparison of the 3 different methods by demonstrating the mean error for each of them as a function of the  $R_{max}$  for three different distance values. They compare the accuracy of all the three 2-D studied methods as a function in maximum measurement error ratio when the separation beacon distance equal to 10, 6, and 2 units respectively.

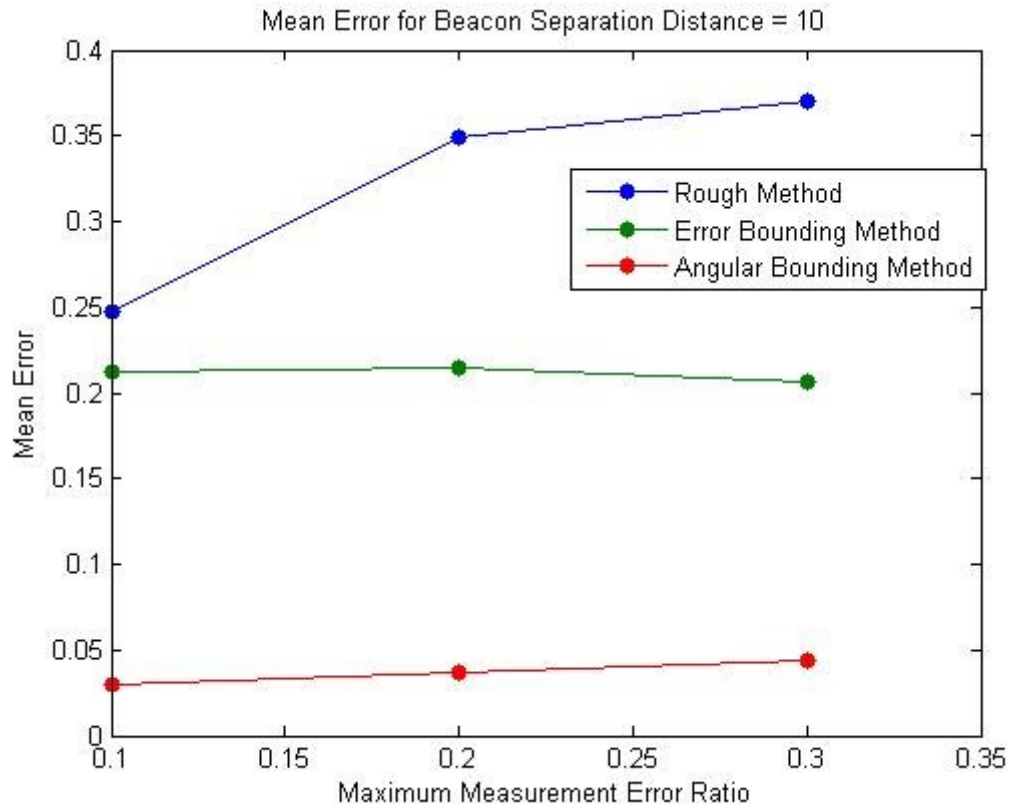


Figure 5.4-16 2-DMethods-Error Comparison for D = 10

This figure shows, once again, significant changes only in the rough method's mean errors. The rough method's mean errors rapidly grew from the maximum measurement error ratio of 0.1-0.2 reaching its peak of 0.35 while the error bounding method stayed almost the same at a mean error of 0.2 and the angular bounding method slightly increased to a mean error of less than 0.05. Then, the rough method continued to grow but did so at a much slower rate from the error ratio of 0.2-0.3 while the error bounding method slightly decreased and the angular bounding method continued to slightly increase.

The second figure compares the accuracy of all the three 2-D studied methods as a function in maximum measurement error ratio when the separation beacon distance equal to six units.

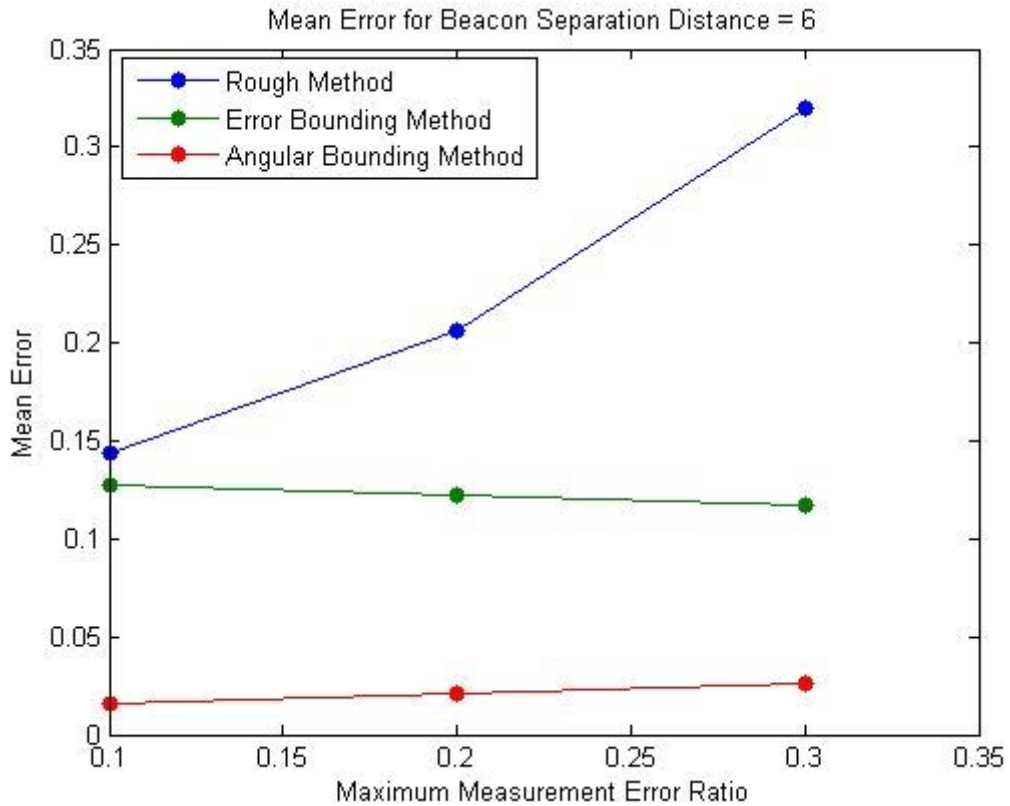


Figure 5.4-17 2-D Methods-Error Comparison for D = 6

Generally, the only method whose mean error has significant changes is the rough method. From the maximum measurement error ratio of 0.1-0.2, the rough methods mean error increases rapidly to a mean error of approximately 0.32 while the error bounding method decreases slightly and the angular bounding method increases slightly, too. Afterwards, from the error ratio of 0.2-0.3, the rough method's mean error increases at a much faster rate than last time reaching a mean error of more than 0.3 while the error

bounding method continued to decrease slowly and the angular bounding method also continued to slightly increase.

. The third one compare the accuracy of all the three 2D studied methods as a function in maximum measurement error ratio when the separation beacon distance equal to two units.

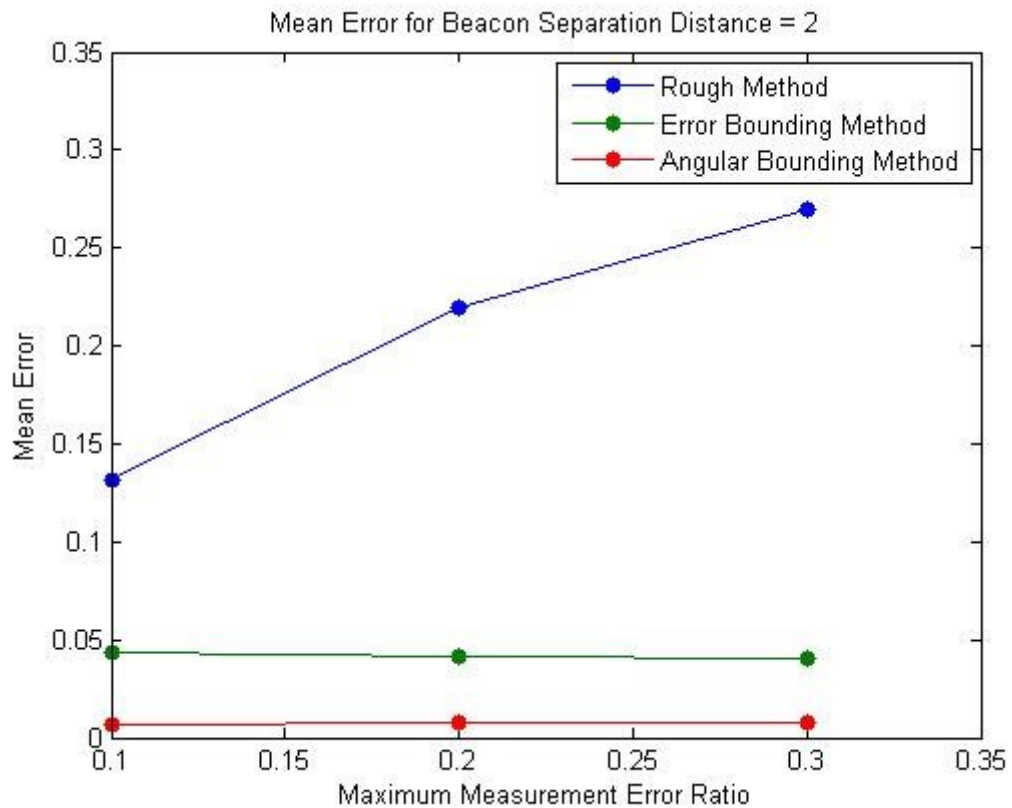


Figure 5.4-18 2-DMethods-Error Comparison for D = 2

For the most part, the error bounding method and angular bounding method had no major changes while the rough method grew rapidly. The rough method grew significantly from error ratios of 0.1-0.2. At that point, the rough method's mean error

reached more than 0.2. Afterwards, the rough method increased at a slower rate than before reaching a mean error of approximately 0.3 at the error ratio of 0.3.

In summary, the rough method is dependent on the  $R_{max}$  as it is demonstrated in the above figures. Moreover, it's also exceedingly dependent on the number of steps. The error in the angular bounding method is a minor one especially in the case of one step when the  $R_{max}0.1$  and the  $R_{max} 0.3$  were compared, but the error bounding method stays almost the same. In addition, the higher the  $R_{max}$ , the higher the rough method's mean error, but the smaller the  $D$ , the smaller the mean error of all the three compared methods. At the same time, the smaller the  $\Delta x$ , the smaller the error for all three separation beacon steps.

#### ***5.4.2.5 2-D-Methods Comparison for different transmission angles***

The following figures illustrate the comparison of the 3 different methods by demonstrating the mean error for each of them as a function of the beacon transmission angles for three different  $R_{max}$  values.

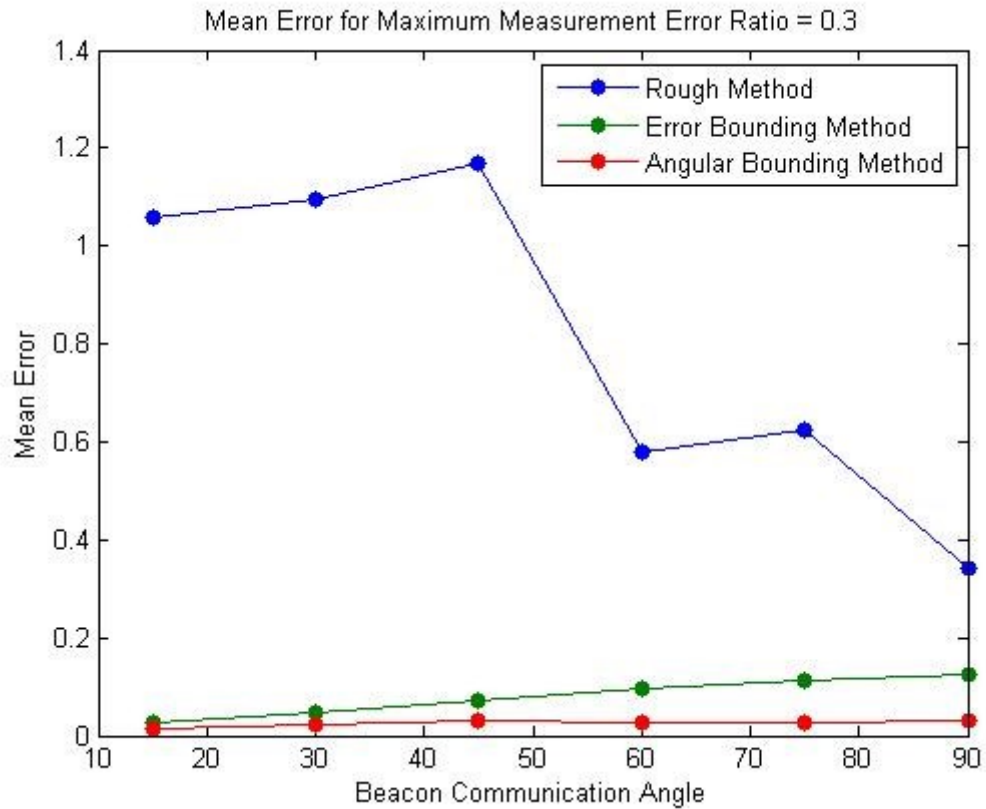


Figure 5.4-19 2-DMethods-Error Comparison for  $R_{\max} = 0.3$

The rough method recorded the highest mean errors for all the beacon communication angles while the angular bounding method recorded the lowest mean errors. The rough method's mean errors fluctuated while the error bounding method's mean errors seemed to grow at a constant rate. The angular bounding method's mean errors, on the other hand, seemed to not change at all for any beacon communication angle.

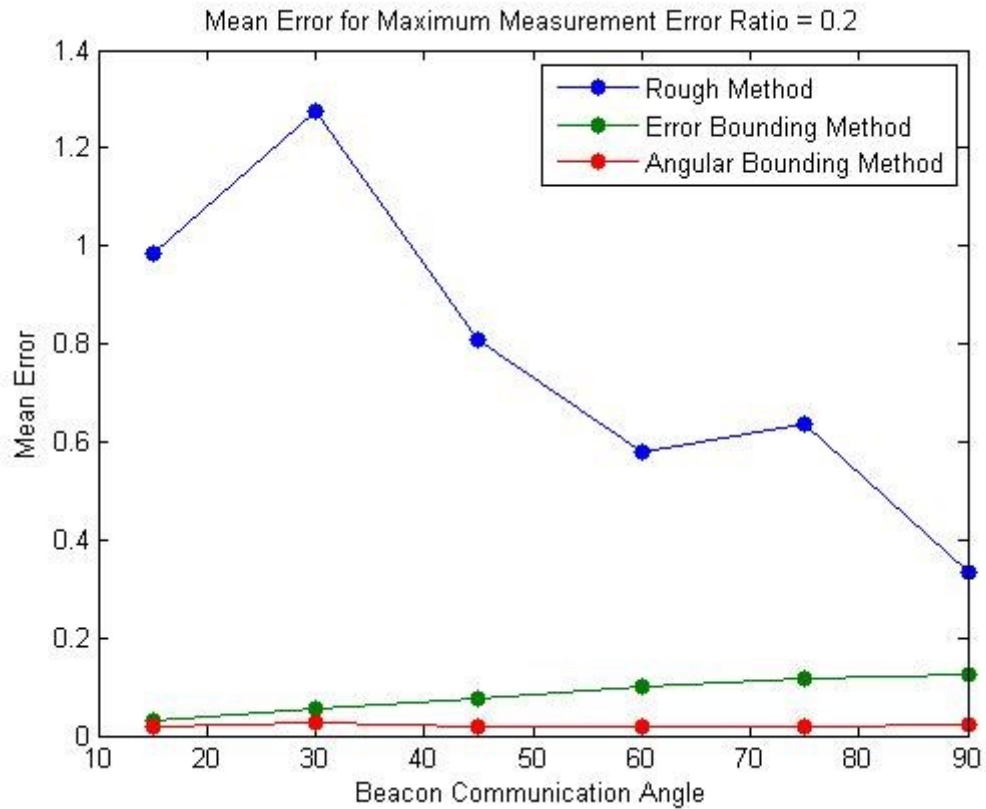


Figure 5.4-20 2-DMethods-ErrorCcomparison for Rmax = 0.2

The mean error rises for all 3 methods from the beacon communication angle of 15-30 degree. The rough method is at its peak on the communication angle of 30 degree, but after that it drops dramatically while the error bounding method increases at an almost constant rate. In the other hand, the angular bounding method does not affected in increasing of beacon transmission angle and has almost the same error values.

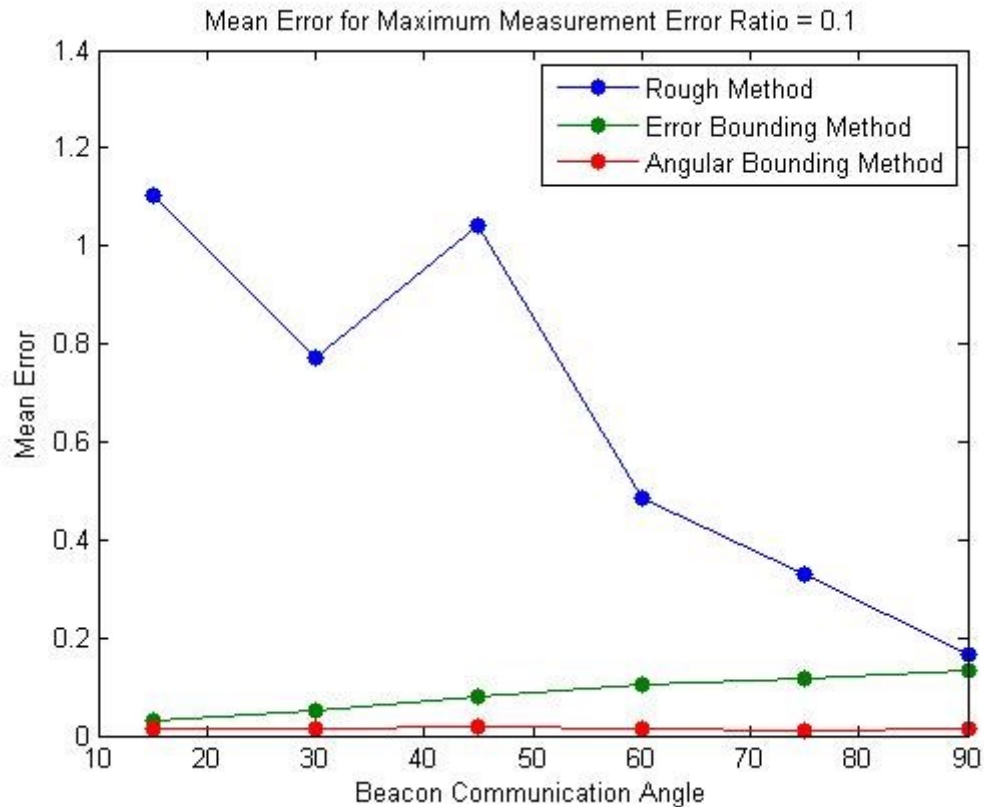


Figure 5.4-21 2-DMethods-Error Comparison for  $R_{\max} = 0.1$

The rough method mean error is at its peak at the beacon communication angle of 15 degree, but then it drops dramatically for the beacon communication angles of 15-30 degree while the error bounding method and the angular bounding method slightly increase. From the beacon communication angles of 30-50 degree, the mean error for the rough method rapidly increases and then significantly decreases reaching a mean error of about 0.5 at the communication angle of 60 degree while the error bounding method mean error continues to increase and the angular bounding method mean error increases and decreases very slightly.



In summary, the rough method's mean error fluctuates and does not essentially depend on the beacon communication angle if the angle is smaller than 45 degrees. It is only after that that the mean error becomes dependent on the beacon angle and it does so in an extreme manner in which the mean error decreases as the beacon angle increases and the same goes for the  $R_{max}$  since the mean error also decreases while the  $R_{max}$  decreases. On the other hand, the error bounding method is dependent on the beacon angle; more specifically, as the beacon angle increases the mean error rises slightly along with it. The angular bounding method is exactly the opposite because it almost always never depends on the angle of the beacon since its mean error basically stays the same as the beacon angle changes; this is all because the determined area for the sensor's possible location is extremely minimized as a result of the angle relationships [refer to Section 4.6].

## **Chapter Six: Conclusion**

The approaches, methods, and analysis presented herein provided a new direction and a set of methods for wireless sensor network (WSN) localization. A discussion of the background and current approaches and technologies localization efforts and the shortcomings and poor assumptions of many existing state-of-the-art methods was provided to illustrate the need for a better approach. Building upon these limitations and flaws, a new means of utilizing error-modeling to improve the precision in sensor localization was presented along with the necessary terminology, algorithms, and analyses to implement and verify the methods designed upon the research and understanding contributed by this work.

After careful mathematical analyses were performed on the information to be gathered from the wireless sensor network, structured mathematical models were developed based on fundamentals of algebra, trigonometry, probability, and statistics. From these models, several localization methods were developed to exploit the relationships found and statistical indications. These methods ranged from the simplest rough methods to the considerably more magnitude and error-bounding methods to the most complex angular-bounding methods. Each developed method utilized the insights and benefits provided by the previous to further refine the estimations of sensor positions, ultimately producing increasingly-improved estimations. The rough methods utilized basic Boolean truth-statements of where a sensor could and could not be located based on

physical facts and predetermined assumptions. From these rough methods, magnitude and error-bounding methods were developed to further utilize other parameters of the information-gathering system, such as communication range and error ratio range, in order to further bound the estimated sensor location. From these observations, in the two-dimensional and three-dimensional cases, properties of trigonometric relationships were applied to the locations and distances determined in the previous methods to produce further derived boundaries on the estimated sensor location. Many of these relationships were grounded upon observations of the physical movement and transmission processed involved with the information-gathering process to create a type of recursive, dynamic checklist of conditions to provide increasingly-smaller possible locations for estimation. It should be kept in mind that the goal of this area-shrinking methodology was one of consequential, probabilistic minimization. Because a sensor is a physical object with a fixed area (or volume in three dimensions), an estimate of its location should be formed within the smallest area of positive probability possible. Once this area is determined, probabilistic analyses can be performed to yield the most-likely sensor location to finalize an estimate. It is from this perspective that we developed our simulation software.

The simulation constructed in this work was divided into three sections. The first was the physical modeling and information-gathering unit that was responsible for transforming input parameters (broadcast angle, communication range, etc.) into estimation error measurements for each localization method. Given the broad range of control offered through the input parameters, the estimation error measurements were able to vary widely to properly characterize the localization methods. This unit was given

the capability of being controlled by the second section, which was that of the trial test bed. The second unit's primary responsibility was to automate the operation of the first unit's processes in order to supply varying parameter values and record average estimation error measurements over the course of many trials. The measurements taken were collected into large tables to make them available for later analyses and graphing. The third unit's responsibility was to perform predetermined, automated analyses of the tables generated by the second unit to provide interesting, graphical representations that would yield insights as to the operating characteristics and optimal parameter values for each method based on sets of limiting criteria. For example, lowering the distance estimation ratio might lead to better performance by one method and worse performance by another, which indicates their operating differences and the ways in which controlling parameters should be varied to yield ideal performance.

The resulting performance results gathered were able to meet the design criteria of the software. Many combinations of parameters and resulting performances were gathered, analyzed, and graphed in the previous chapter. These results are too widely-varied and detailed to mention in summary. They were able to indicate both expected and surprising application selections for localization method depending on desired modeling based on input parameters. Overall, the results indicated large, incremental improvements over the methods ranging from simple to complex. The results fully met the desired outcomes of the research and development criteria set forth for the work, though further areas of improvement and development are still possible.

As error analysis is fundamental to the methods that were designed and presented, any implementations built upon this work should benefit from the candid and open evaluations that have been provided. Solid and realistic assumptions, coupled with extensive simulation results, were used to prove the validity and performance of the methods herein that were built upon mathematical fundamentals and probabilistic models. Componentized, single-dimensional error quantities and radial error factors were discussed, analyzed, and utilized in-depth to iteratively improve the precision of localization efforts and provide a means of evaluation for most real-world scenarios based on the assumptions and needs for particular applications. We believe that there are many possibilities for the extension of these efforts into greater dimensions and more complex, concrete models. The approaches taken should provide a clear path to building upon different assumptions than those made here while maintaining the integrity and reliability of such efforts.

It is our belief that the methods of localization designed and tested within this work, based upon reasonably-realistic models and assumptions, show great promise in practical localization applications for real-world wireless sensor networks. With slight refinements of the geometric models utilized and appropriate tuning of the dependent parameters, each of the methods herein should provide reasonable localization outcomes with relatively-minimal power consumption compared with other localization methods. This was accomplished through exploitation of deep mathematical relationships on simple feedback information. The usage of such derived knowledge allows for shifting of the burden of localization (and therefore power consumption) from the wireless sensors

themselves to the final processing station. This satisfies the requisite requirements of accurate localization with minimal power usage, which is typical, primary goal of any localization system of quality.

## References

- [1] Makki, S. Kami, Xiang-Yang Li, Niki Pissinou, Shamila Makki, Masoumeh Karimi, and Kia Makki. *Sensor and Ad-Hoc Networks: Theoretical and Algorithmic Aspects*. Vol. 7. Springer, 2010.
- [2] Iyengar, S. Sitharama, and Richard R. Brooks, eds. *Distributed Sensor Networks: Sensor Networking and Applications*. CRC press, 2012.
- [3] Park, Chulsung, Jinfeng Liu, and Pai H. Chou. "Eco: an ultra-compact low-power wireless sensor node for real-time motion monitoring." *Information Processing in Sensor Networks*, 2005. IPSN 2005. Fourth International Symposium on. IEEE, 2005.
- [4] Dressler, Falko. *Self-organization in sensor and actor networks*. John Wiley & Sons, 2008.
- [5] Wang, Feng, and Jiangchuan Liu. "Networked wireless sensor data collection: Issues, challenges, and approaches." *Communications Surveys & Tutorials*, IEEE 13.4 (2011): 673-687.
- [6] Mao, Guoqiang, and Baris Fidan. *Localization Algorithms and Strategies for Wireless Sensor Networks: Monitoring and Surveillance Techniques for Target Tracking*. Information Science Reference, 2009.
- [7] Krishnamachari, Bhaskar. *Networking wireless sensors*. Cambridge University Press, 2005.
- [8] P. Taylor, S. Pandey, and P. Agrawal, "Journal of the Chinese Institute of Engineers A survey on localization techniques for wireless networks A SURVEY ON LOCALIZATION TECHNIQUES FOR," *Ultrasound*, no. 2012, pp. 37-41, 2011.
- [9] Pandey, Santosh, and Prathima Agrawal. "A survey on localization techniques for wireless networks." *Journal of the Chinese Institute of Engineers* 29.7 (2006): 1125-1148.
- [10] Bojkovic, Zoran, and Bojan Bakmaz. "A survey on wireless sensor networks deployment." *WSEAS Transactions on Communications* 7.12 (2008): 1172-1181.
- [11] Bharathidasan, Archana, and Vijay Anand Sai Ponduru. "Sensor networks: An overview." Department of Computer Science. University of California (2002).

- [12] Yick, Jennifer, Biswanath Mukherjee, and Dipak Ghosal. "Wireless sensor network survey." *Computer networks* 52.12 (2008): 2292-2330.
- [13] Bojkovic, Zoran, and Bojan Bakmaz. "A survey on wireless sensor networks deployment." *WSEAS Transactions on Communications* 7.12 (2008): 1172-1181.
- [14] Amundson, Isaac, and Xenofon D. Koutsoukos. "A survey on localization for mobile wireless sensor networks." *Mobile Entity Localization and Tracking in GPS-less Environments*. Springer Berlin Heidelberg, 2009. 235-254.
- [15] Demirkol, Ilker, Cem Ersoy, and Fatih Alagoz. "MAC protocols for wireless sensor networks: a survey." *Communications Magazine, IEEE* 44.4 (2006): 115-121.
- [16] V. Yadav, M. K. Mishra, A. K. Singh, and M. M. Gore, "LOCALIZATION SCHEME FOR THREE DIMENSIONAL WIRELESS SENSOR NETWORKS," *International Journal*, vol. 1, no. 1, pp. 60-72, 2009.
- [17] Giorgetti, Gianni, Sandeep KS Gupta, and Gianfranco Manes. "Localization using signal strength: to range or not to range?." *Proceedings of the first ACM international workshop on Mobile entity localization and tracking in GPS-less environments*. ACM, 2008.
- [18] Brito, Lina M., and Laura M. Rodríguez Peralta. "An analysis of localization problems and solutions in wireless sensor networks." *Tékhné-Revista de Estudos Politécnicos* 9 (2008): 146-172.
- [19] Mao, Guoqiang, Barış Fidan, and Brian Anderson. "Wireless sensor network localization techniques." *Computer networks* 51.10 (2007): 2529-2553.
- [20] Cheng, Xiuzhen, et al. "TPS: A time-based positioning scheme for outdoor wireless sensor networks." *INFOCOM 2004. Twenty-third Annual Joint Conference of the IEEE Computer and Communications Societies*. Vol. 4. IEEE, 2004.
- [21] Pal, Amitangshu. "Localization Algorithms in Wireless Sensor Networks: Current Approaches and Future Challenges." *Network Protocols & Algorithms* 2.1 (2010).
- [22] Lee, Sangho, et al. "Localization with a mobile beacon based on geometric constraints in wireless sensor networks." *Wireless Communications, IEEE Transactions on* 8.12 (2009): 5801-5805.



- [23] Xu, Jiuqiang, et al. "Distance Measurement Model Based on RSSI in WSN." *Wireless Sensor Network* 2.8 (2010): 606-611.
- [24] Giacomini, João C., et al. "Radio Channel Model of Wireless Sensor Networks Operating in 2.4 GHz ISM Band." *INFOCOMP Journal of Computer Science* 9.1 (2010): 98-106.
- [25] K. Liu and J. Xiong, "A Fine-grained Localization Scheme Using A Mobile Beacon Node for Wireless Sensor Networks," *Journal of Information Processing Systems*, vol. 6, no. 2, pp. 147-162, Jun. 2010.
- [26] Boushaba, Mustapha, Abdel Hafid, and Abderrahim Benslimane. "HA-A2L: angle to landmark-based high accuracy localization method in sensor networks." *Proceedings of the 2007 international conference on Wireless communications and mobile computing*. ACM, 2007.
- [27] Bao, Han, et al. "Mobile anchor assisted particle swarm optimization (PSO) based localization algorithms for wireless sensor networks." *Wireless Communications and Mobile Computing* 12.15 (2012): 1313-1325.
- [28] M. Kushwaha, "Sensor Node Localization Using Mobile Acoustic Beacons," Self, 2005.
- [29] G. Teng, K. Zheng, and G. Yu, "A Mobile-Beacon-Assisted Sensor Network Localization Based on RSS and Connectivity Observations," *International Journal of Distributed Sensor Networks*, vol. 2011, pp. 1-14, 2011.
- [30] Y.-J. Fu, T.-H. Lee, L.-huang Chang, and T.-P. Wang, "A Single Mobile Anchor Localization Scheme for Wireless Sensor Networks," *2011 IEEE International Conference on High Performance Computing and Communications*, pp. 946-950, Sep. 2011.
- [31] Blumenthal, Jan, Frank Reichenbach, and Dirk Timmermann. "Minimal transmission power vs. signal strength as distance estimation for localization in wireless sensor networks." *Sensor and Ad Hoc Communications and Networks, 2006. SECON'06. 2006 3rd Annual IEEE Communications Society on*. Vol. 3. IEEE, 2006.
- [32] Giacomini, João Carlos, and Flávio Henrique Vasconcelos. "Wireless sensor network as a measurement tool in precision agriculture." In *Proc. XVIII IMEKO World Congress-Metrology for a Sustainable Development*. 2006.

- [33] T. He, C. Huang, B. M. Blum, J. A. Stankovic, and T. Abdelzaher, "Range-Free Localization Schemes for Large Scale Sensor Networks 1," Main, pp. 81-95, 2003.
- [34] E. Guerrero et al., "ADAL : A Distributed Range-Free Localization Algorithm Based on a Mobile Beacon for Wireless Sensor Networks," Electronics.
- [35] C.-ho Ou, "A Localization Scheme for Wireless Sensor Networks," Sensors (Peterborough, NH), vol. 11, no. 7, pp. 1607-1616, 2011.
- [36] He, Tian, et al. "Range-free localization schemes for large scale sensor networks." Proceedings of the 9th annual international conference on Mobile computing and networking. ACM, 2003.
- [37] H. Chen, Q. Shi, P. Huang, H. V. Poor, and K. Sezaki, "Mobile Anchor Assisted Node Localization for Wireless Sensor Networks," Science, pp. 5-9.
- [38] K.-feng Ssu, C.-ho Ou, and H. C. Jiau, "Localization with Mobile Anchor Points in Wireless Sensor Networks," vol. 54, no. 3, pp. 1187-1197, 2005.
- [39] Langendoen, Koen, and Niels Reijers. "Distributed localization in wireless sensor networks: a quantitative comparison." Computer Networks 43.4 (2003): 499-518.
- [40] He, Tian, et al. "Range-free localization schemes for large scale sensor networks." Proceedings of the 9th annual international conference on Mobile computing and networking. ACM, 2003.
- [41] Y. Xu, Y. Ouyang, Z. Le, J. Ford, and F. Makedon, "Mobile Anchor-free Localization for Wireless Sensor Networks."
- [42] J. Park, S.-mok Yoo, and C.-sig Pyo, "Localization using Mobile Anchor Trajectory in Wireless Sensor Networks," no. September, pp. 21-23, 2011.
- [43] F. Geng and S. Xue, "Mobile beacon node path scheme in arbitrary region for wireless sensor networks," Proceedings of 2011 International Conference on Electronic & Mechanical Engineering and Information Technology, pp. 3429-3433, Aug. 2011.
- [44] Sichitiu, Mihail L., and Vaidyanathan Ramadurai. "Localization of wireless sensor networks with a mobile beacon." Mobile Ad-hoc and Sensor Systems, 2004 IEEE International Conference on. IEEE, 2004.

- [45] K. Kim and W. Lee, "MBAL : A Mobile Beacon-Assisted Localization Scheme for Wireless Sensor Networks," *Main*, pp. 57-62, 2007.
- [46] J. M. Bahi, A. Mostefaoui, R. E. Gros, and B. Cedex, "A Mobile Beacon Based Approach for Sensor Network Localization," *Communications*, no. 1, 2007.
- [47] Fang, Zhao, Luo Hai-yong, and Quan Lin. "A mobile beacon-assisted localization algorithm based on network-density clustering for wireless sensor networks." *Mobile Ad-hoc and Sensor Networks, 2009. MSN'09. 5th International Conference on*. IEEE, 2009.
- [48] S. Lee, S. Member, E. Kim, C. Kim, K. Kim, and S. Member, "Localization with a Mobile Beacon Based on Geometric Constraints in Wireless Sensor Networks," vol. 8, no. 12, pp. 5801-5805, 2009.
- [49] F. Caballero, L. Merino, I. Maza, and a. Ollero, "A particle filtering method for wireless sensor network localization with an aerial robot beacon," *2008 IEEE International Conference on Robotics and Automation*, pp. 596-601, May 2008.
- [50] B. Zhang, F. Yu, and Z. Zhang, "A High Energy Efficient Localization Algorithm for Wireless Sensor Networks Using Directional Antenna," *2009 11th IEEE International Conference on High Performance Computing and Communications*, pp. 230-236, 2009.
- [51] C.-ho Ou and K.-feng Ssu, "Sensor Position Determination with Flying Anchors in Three-Dimensional Wireless Sensor Networks," *IEEE Transactions on Mobile Computing*, vol. 7, no. 9, pp. 1084-1097, Sep. 2008.
- [52] H. Cui and Y. Wang, "Four-mobile-beacon assisted localization in three-dimensional wireless sensor networks," *COMPUTER AND ELECTRICAL ENGINEERING*, 2011.
- [53] Ou, Chia-Ho, and Kuo-Feng Ssu. "Sensor position determination with flying anchors in three-dimensional wireless sensor networks." *Mobile Computing, IEEE Transactions on* 7.9 (2008): 1084-1097.
- [54] H.-qing Cui, Y.-long Wang, J.-liang Lv, and Y.-ming Mao, "Three-Mobile-Beacon Assisted Weighted Centroid Localization Method in Wireless Sensor Networks," *Computer Communications*, 2011.
- [55] B. Xiao, H. Chen, and S. Zhou, "Distributed Localization Using a Moving Beacon in Wireless Sensor Networks," *IEEE Transactions on Parallel and Distributed Systems*, vol. 19, no. 5, pp. 587-600, May 2008.

- [56] Xiao, Sheng, Changfeng Xing, and Zhangsong Shi. "A new distributed node localization scheme using a mobile beacon." *Advances in Computation and Intelligence*. Springer Berlin Heidelberg, 2010. 140-147.
- [57] Z. Guo et al., "Perpendicular Intersection : Locating Wireless Sensors with Mobile Beacon," *Science and Technology*.
- [58] R. Stoleru, T. He, J. A. Stankovic, and D. Luebke, "A High-Accuracy, Low-Cost Localization System for Wireless Sensor Networks," *Event (London)*, 2005.
- [59] Zhang, Baoli, Fengqi Yu, and Zusheng Zhang. "A high energy efficient localization algorithm for wireless sensor networks using directional antenna." *High Performance Computing and Communications, 2009. HPCC'09. 11th IEEE International Conference on*. IEEE, 2009.
- [60] M. L. Sichitiu and V. Ramadurai, "Localization of wireless sensor networks with a mobile beacon," *2004 IEEE International Conference on Mobile Ad-hoc and Sensor Systems (IEEE Cat. No.04EX975)*, pp. 174-183, 2004.
- [61] Marks, Michał, and Ewa Niewiadomska-Szynkiewicz. "Multiobjective approach to localization in wireless sensor networks." *Journal of Telecommunications and Information Technology* 3 (2009): 59-67.
- [62] Tam, Vincent, King-Yip Cheng, and King-Shan Lui. "Using micro-genetic algorithms to improve localization in wireless sensor networks." *Journal of Communications* 1.4 (2006): 1-10.
- [63] Langendoen, Koen, and Niels Reijers. "Distributed localization in wireless sensor networks: a quantitative comparison." *Computer Networks* 43.4 (2003): 499-518.
- [64] Qiao, D., and G. K. H. Pang. "Localization in wireless sensor networks with gradient descent."
- [65] Doherty, Lance, and Laurent El Ghaoui. "Convex position estimation in wireless sensor networks." *INFOCOM 2001. Twentieth Annual Joint Conference of the IEEE Computer and Communications Societies. Proceedings. IEEE. Vol. 3*. IEEE, 2001.
- [66] Sivakumar, S., R. Venkatesan, and M. Karthiga. "Error Minimization in Localization of Wireless Sensor Networks using Genetic Algorithm." *International Journal of Computer Applications* 43 (2012).

- [67] Garg, Ravi, Avinash L. Varna, and Min Wu. "An efficient gradient descent approach to secure localization in resource constrained wireless sensor networks." *Information Forensics and Security, IEEE Transactions on* 7.2 (2012): 717-730.
- [68] Tarrio, Paula, Ana M. Bernardos, and Jose R. Casar. "An RSS localization method based on parametric channel models." *Sensor Technologies and Applications, 2007. SensorComm 2007. International Conference on*. IEEE, 2007.
- [69] M. Karagiannis, I. Chatzigiannakis, and J. Rolim, "Multilateration: methods for clustering intersection points for wireless sensor networks localization with distance estimation error," 2008
- [70] Baggio, Aline, and Koen Langendoen. "Monte Carlo localization for mobile wireless sensor networks." *Ad Hoc Networks* 6.5 (2008): 718-733.
- [71] Cota-Ruiz, Juan, et al. "A low-complexity geometric bilateration method for localization in wireless sensor networks and its comparison with least-squares methods." *Sensors* 12.1 (2012): 839-862.
- [72] Demirbas, Murat, and Youngwhan Song. "An RSSI-based scheme for sybil attack detection in wireless sensor networks." *Proceedings of the 2006 International Symposium on on World of Wireless, Mobile and Multimedia Networks*. IEEE Computer Society, 2006.
- [73] Yu, Ying, et al. "Sequence-based localization algorithm with improved correlation metric and dynamic centroid." *Science China Information Sciences* 54.11 (2011): 2349-2358.
- [74] Xu, Kaihua, Mi Chen, and Yuhua Liu. "A novel localization algorithm based on received signal strength indicator for wireless sensor networks." *Computer Science and Information Technology, 2008. ICCSIT'08. International Conference on*. IEEE, 2008.